IMPROVEMENT OF STRUCTURAL DESIGN OF PENSTOCK BIFURCATION BY STRESS ANALYSIS USING FINITE ELEMENT METHOD
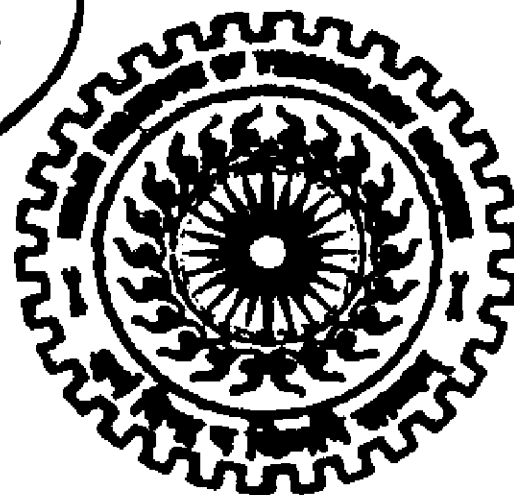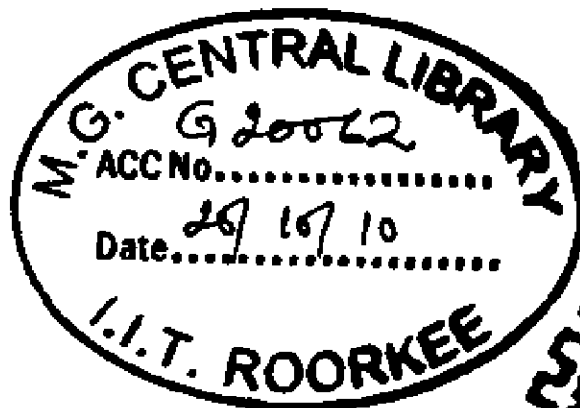
A DISSERTATION

Submitted in partial fulfillment of the requirements for the award of the degree
of

MASTER OF TECHNOLOGY

in

WATER RESOURCES DEVELOPMENT
(CIVIL)

By

SHYAMLI PASWAN

DEPARTMENT OF WATER RESOURCES DEVELOPMENT AND MANAGEMENT
INDIAN INSTITUTE OF TECHNOLOGY ROORKEE
ROORKEE -247 667 (INDIA)
MARCH, 2010

CANDIDATE'S DECLARATION

I hereby certify that work which is being presented in the dissertation entitled "IMPROVEMENT OF STRUCTURAL DESIGN OF PENSTOCK BIFURCATION BY STRESS ANALYSIS USING FINITE ELEMENT METHOD" is in partial fulfillment of the requirement for the award of the degree of master of technology and submitted to the Department of Water Resources Development and Management (WRD&M), Indian Institute of Technology, Roorkee. This is an authentic record of my own work carried out at CW&PRS, Pune, during the period from July, 2008 to March, 2010 under the supervision and guidance of Dr. R. P. Singh, Prof. WRD & M, IITR and Prof. Gopal Chauhan, Emeritus Fellow, WRD&M, IITR, Roorkee-247667, Uttarakhand, and Shri Rizwan Ali, Senior Research Officer, CW&PRS, Pune.

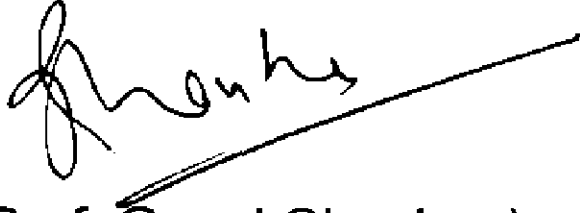The matter presented in this dissertation has not been submitted by me for the award of any other degree.
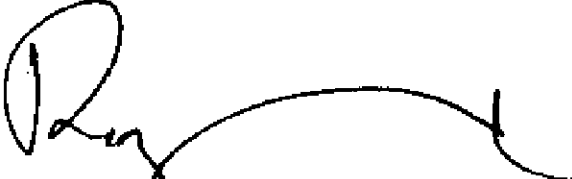
Dated :-12 March, 2010   [Shyamli Paswan]
WRD&M, IIT Roorkee   Enrolment No: 076017

CERTIFICATE

This is to certify that the above statement made by the candidate is correct to the best of my knowledge.

(Dr. R. P. Singh)   (Prof. Gopal Chauhan)
Prof. & Head   Emeritus Fellow
WRD & M, IITR,   WRD & M, IITR,
Roorkee – 247667   Roorkee - 247667
India   India

(Shri Rizwan Ali)
Senior Research Officer,
CWPRS, Pune- 411 024
India

i

ACKNOWLEDGEMENT

Place: WRD&M, IIT Roorkee   [Shyamli Paswan]

Date : March, 2010   Enrolment No. 076017
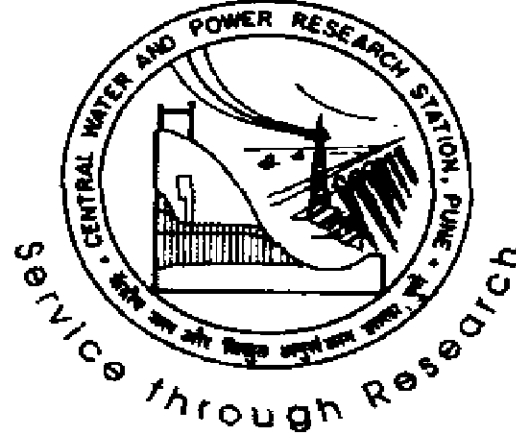
भारत सरकार
Government of India

जल संसाधन मंत्रालय
Ministry of Water Resources

केन्द्रीय जल और विद्युत अनुसंधान शाला
Central Water & Power Research Station
खडकवासला पुणे - 411 024
Khadakwasla , Pune – 411 024

CERTIFICATE

Certified that the dissertation titled "**IMPROVEMENT OF STRUCTURAL DESIGN OF PENSTOCK BIFURCATION BY STRESS ANALYSIS USING FINITE ELEMENT METHOD**", which is being submitted by Shri Shyamli Paswan in partial fulfillment of the requirements for the award of Degree of Master of Technology in Department of Water Resources Development and Management (WRD&M), Indian Institute of Technology, Roorkee, is a record of student's own work carried out by him at CW&PRS, Pune, under my supervision and guidance. The matter included in this dissertation has not been submitted for the award of any other Degree.

(Rizwan Ali)
Senior Research Officer

LIST OF SYMBOLS

A, A_n	:	area of single pipe and n number of pipe respectively
α	:	variables angle
β	:	angle of bifurcation
B	:	Total width of sickle plate
b	:	Width of sickle plate at any section
C_1	:	annual cost due to investment for a pipe of diameter D
C_2	:	value of energy that can be produced at the same diameter
D, d	:	diameters of main pipe and branch pipe respectively
$d\alpha$	:	elemental angle
$\{\delta\}^e$	:	nodal displacement vector
dH	:	elemental force due to circumferential and axial stress in horizontal direction
dH_1	:	elemental force due to circumferential stress
dH_2	:	elemental force due to axial stress
dl	:	elemental length
dV	:	elemental force due to circumferential and axial stress in in vertical direction
dy, dz, dr,	:	elemental distances
$\varepsilon_A, \varepsilon_B, \varepsilon_X$	:	measured strains along three directions at any rosette strain gauge location.
E_m	:	modulus of elasticity of model material
E_p	:	modulus of elasticity of prototype material
f	:	head loss coefficient /friction coefficient
ϕ	:	angle of reducer
$\{F\}^e$	:	nodal force vector

F	:	connecting point
g	:	acceleration due to gravity
H	:	head of water
h_f	:	head loss radial stress
H_F	:	total force in horizontal
$[K]^e$	:	element stiffness matrix
K_1	:	annual cost of penstock per kg elemental area
K_2	:	value of one kWh at generator terminals in the same units
1	:	normal length
L,	:	length of penstock
M	:	total moment
M_H	:	moment in horizontal direction
M_V	:	moment in vertical
[N]	:	components in general functions of position
n	:	number of penstocks /also roughness coefficient
O	:	origin of coordinate
Ø	:	joint efficiency of longitudinal joints
p	:	hydrostatic pressure
p_m	:	pressure in model
p_p	:	pressure in prototype
Q	:	discharge of water through pipe/penstock
R	:	resultant force
R	:	hydraulic radius
R_1, r	:	radius of penstocks
s	:	Thickness of shell
S	:	Thickness of sickle plate
s or t_p	:	Shell thickness /thickness of pipe

t, t_n	:	thickness of single pipe and n number of pipes respectively
U^e	:	polynomial function
V	:	total force in vertical direction
v, v_n	:	velocity of water through single pipe and n number of pipes respectively
x, y, z	:	Coordinate points
γ	:	angle of resultant
$\varepsilon_1, \varepsilon_2$	:	principal strains
ε_m	:	strain in model
ε_p	:	strain in prototype
μ	:	Poisson' ratio of steel
σ_y	:	allowable stress in steel kg/cm^2
σ_1, σ_2	:	principal stresses
σ_r	:	Stress acting biaxially

LIST OF FIGURES

LIST OF PHOTOGRAPHS

LIST OF TABLES

ABSTRACT

The present study is concerned with the improvement of structural design of penstock bifurcation. The Penstock bifurcation is most complicated structural part of a water conductor system in a hydroelectric electric project. Due to its complex geometry, it is very difficult for carrying out structural analysis by analytical method. Also analytical method does not give exact solution because of complex geometry formation by combination of cylindrical shell / conical shell and internally reinforced sickle plate. In this study the structural design of symmetric penstock bifurcation has been carried out by conventional design approach. The design has been validated by conducting structural model studies by fabricating geometrically similar physical model and by applying strain gauge technology. The design of penstock bifurcation has also been compared by mathematical model studies using Finite Element Method. Finally hydrostatic test has been conducted on full scale prototype. After comparing results of various studies it was found that design of penstock bifurcation by conventional methods is very approximate because of oversimplification of behaviour of various structural components. The conventional design does not consider the limitation of weld efficiency. Also physical model studies gives better idea of design deficiency by conventional approach but it also does not take into account weld defects and is also time consuming. Further stress analysis has been carried out by conducting mathematical model studies by applying Finite Element Technique. Upon comparing various studies it was found that mathematical model studies give better pattern of stress results but it also results some approximations as compared to actual behaviour of penstock bifurcation. The design can be improved very fast by mathematical studies by making changes in the size various stiffeners. After conducting the hydrostatic test it was found that Mathematical model studies gives best results as compared to other studies. The nature or patterns of stresses at various locations fairly match in various studies. In the present study it was found that during hydrostatic test the prototype can withstand only 50 kg / cm^2 internal pressure as compared to actual design pressure of the order of 70 kg / cm^2. Finally it was concluded that further refinement is necessary in the design of penstock bifurcations. The mathematical model studies should be carried out for design improvement. The hydrostatic test on prototype should be carried out to assess weld efficiency and actual pressure resisting capacity.

CONTENTS

INTRODUCTION

1.1 GENERAL

India is a very vast country and its population is about 125 crore. The energy required for the country is in huge amount. Though the initial cost of hydro electric plant is more but the running and maintenance cost is very less in comparison to thermal plant. Also, the production of hydro electric power is environmental friendly. That is why not only central and state government and organizations like NHPC, NTPC, THDC, SJVN etc but also other private and semi private companies are taking interest in production of hydro electric power.

In a hydroelectric project, a water conductor system is the main part, which consists of a headrace tunnel, surge shaft, **pressure shaft / penstocks**, tailrace tunnel etc. Penstock is a very important component and pivotal structures especially in medium head, high head and pumped storage scheme plants for water diversion and flow regulation to generate power. It is a pressure conduit, which controls water flow and delivers water from reservoir / surge tank / forebay on a canal or river pond to the power generating unit i.e. turbine of the hydroelectric plant[1,2]. It constitutes major expense in total hydro project budget. Penstocks should be as hydraulically efficient as practical to conserve available head and structurally safe to prevent failure, which would results in loss of life and property [6, 16].

The hydrostatic test of Varahi penstock bifurcation was conducted at Varahi H E project site inside the tunnel during the last week of March 2007. Stress analysis is carried out to the same penstock bifurcation by finite element method for dissertation and also by analytical method. The results are compared with hydrostatic test results and physical model studies.

Scope of study

1.2 OBJECTIVES

The objectives of this study are as follows:

 (i) Determination of stresses in an internally reinforced penstock
   bifurcation using finite element method and analytical method.

(ii) Comparison of stresses evaluated by FEM with hydrostatic test, physical model study.

1.3 DISSERTATION ORGANIZATION

This dissertation is organized into 6 chapters. The brief description of each chapter is as follows:

Chapter 1   Introduction

This chapter briefly gives the overview of application and importance of water conducting system in hydroelectric plant and objectives of the study.

Chapter 2   Penstocks

In this chapter following topics have been covered briefly:
(i)   Definitions and basic concepts of penstocks and its branching
(ii)   Needs and consideration for branching
(iii)   Types of branching
(iv)   Structural components of penstock branching
(v)   Number of penstocks
(vi)   Economic diameter of penstock

Chapter 3   Design of Penstock Bifurcation

For computing the stresses at the sickle plate by analytical method has been covered in this chapter.

Chapter 4   Verification of Design of Penstock Bifurcation by Different Methods for Computation of Stress in

Different methods for computation of stress in penstock bifurcation are discussed in this chapter. These methods are Finite Element Method, Physical Model Study, Ultrasonic Examination, Radiographic Test, Magnetic Particle Method and Hydrostatic Test. This chapter also covers plotting of counters of different stresses like maximum principal stress,

minimum principal stress and shear stress at different locations on penstock bifurcation by finite element analysis. Besides this the chapter covers the procedures of physical model study and hydrostatic test and their results

Chapter 5   Analysis of Results and Discussion

This chapter includes analysis of result of analytical method, physical model study, hydrostatic test on prototype and FEM studies followed by discussion of the results

Chapter 6   Conclusions and Recommendations

This chapter includes conclusions, based on analysis of the results obtained and recommendations based on the study.

References

This section lists various publications refereed in the study

PENSTOCKS

2.1 GENERAL

The development of the Hydro Electric Engineering during the present century has stimulated intensive and continuous study of the problems evolved in the design and construction of penstock for supplying water to turbine for power generation. As, the requirement of electric power is increasing day by day due to fast increasing in population of the country, the installation of hydroelectric power stations are required in large number and of greater capacity. But the availability of water throughout the year is not same. In rainy season availability of water is sufficient and can run continuously a big capacity turbine where as in winter and summer seasons it not possible to fulfill the need of water for large capacity turbine. So, for running the hydroelectric power station efficiently throughout the year, it better to install a number of turbines/units of smaller capacity than a large one. To feed each turbine/unit separately is uneconomical than the branching a large single penstock near the power generating unit [11].

A penstock branch connection is a complicated structure, usually having external reinforcement such as several stiffening beams to resist the loads applied by internal pressure water, and other having internal tension members called tie rods or internal reinforcement like sickle plate or both as per consideration and requirement of design. The purpose of the tie rods is to assist the stiffening beams in carrying the applied loads [3].

In order to analyze the branch connection, many simplifications and approximations are considered such as the localized effect of structural discontinuities, restraints of the stiffening beams methods of support and dead load of the filled pipe have been neglected [16.41].

Structural analysis of the pipe branch connection consists in general of four parts:

a. Determination of the part of the structure which resists the unbalanced load.

b. Determination of the load imposed on the resisting members.

c. Analysis of the loaded structure.

d. Interpretation of the findings of the analysis.

The parts of the branch connection resisting the unbalanced pressure load are assumed to consist of the external stiffening beams, the internal tie rods, and the portion of the pipe shell adjacent to the stiffener acting integrally as an effective flange.

The stiffener beams are assumed to carry the vertical component of the membrane girth.. This load varies linearly from zero at the top centerline of the pipe to a maximum at the horizontal centerline of the pipe.

The intersecting beams and tie rods are analyzed as a statically indeterminate structure by the virtual work method utilizing the conditions of continuity at the junctions of the beams and rods to determine the moments and shear at the ends of the individual beams and rods.

Interpretation of the stresses obtained in any structure is done by appraisal of the general acceptability of the assumptions made in the methods of structural action, the applied loading and the accuracy of the analysis. For the conditions given, the methods presented here in are considered to represent the best currently available solution for determination of stresses in wye branches.

2.2   NEEDS AND CONSIDERATIONS FOR BRANCHING OF PENSTOCKS

Branching of penstock is necessitated when more than one turbine machine in a multiunit powerhouse of hydroelectric power plant is to be fed by a single header penstock. It is better to carry the water through a main header penstock and branch it into a number of pipes using bifurcation / trifurcation near the power unit to feed each unit as per its requirement. By doing so, maximum economy can be achieved. On account of inherent economy, adopting minimum no of header penstock for power development and then, branching the same near the power house is obvious. The economy of both such alternatives shall depend as on individual installation, but generally speaking with long headers alternatives with branching shall be better. It is better than isolated penstock to conduct water through a main header penstock and branch it into a number of small penstock using bifurcation / trifurcation near to the power house to feed each unit as per generation requirement.

A final decision can only be taken on the matter after comparing the results of design. However the requisite of good branching are [6, 18]:

    i.   Hydraulic loss under all operating conditions is the minimum.

ii. The boundary geometry of the transition should be streamlined so that there are no local pockets of low pressure, and should ensure favorable flow conditions

iii. The reinforcement provided (splitter, girders, tie rods etc.) should ensure that the stress concentration is within reasonable limits and bending stresses is eliminated, leaving only tensile stresses.

iv. Variation under all operation conditions should be within limits.

v. It should be economical and convenient to fabricate locally and transport.

Especially in case of the medium and low head plants, a saving of even a small head which is otherwise lost at the branching due to its poor hydraulic design, may affect the economy in the annual power production. This may be important in estimating the economics of the project as a whole. In view of the high Reynolds number usually encountered in prototype penstocks, the energy loss at the penstock branching is essentially due to form drag. Hence streamlining the boundary geometry at the junction and keeping the deflection angle to a minimum will contribute significantly to reduction of energy loss at the pipe junction. From structural point of view, an ideal design should tend to subject the reinforcement to the tensile stresses only with practically no bending stresses. The tensile stresses should further be distributed as uniformly as possible and be nearly equal to the tensile stresses in the adjacent shell section.

2.3 TYPES OF BRANCHING

Geometrically, there are several types of branching possible, such as bifurcation, trifurcation, manifolds, double wyes arrangement etc. However, in practical application, generally a bifurcation is employed [1,24].

2.3.1 Penstock Bifurcation / Wye branching

The wye branching is the one in which the main pipe diverges into two branch pipes In the wye branching the following categories are available:

a) Wyes with sharp transition
b) Wyes with conical transition
c) Wyes with tie rods
d) Wyes with sickle

A) Symmetrical bifurcation/ Wyes

In a symmetrical branch, angles of bifurcation are equal i.e. angle a = angle b. When branches have similar diameter, the branch is known as equibranch is shown in Fig. 2.1
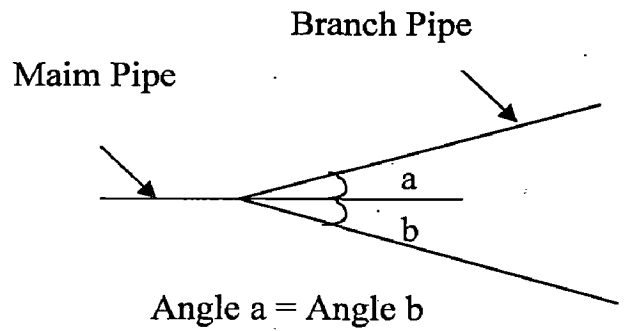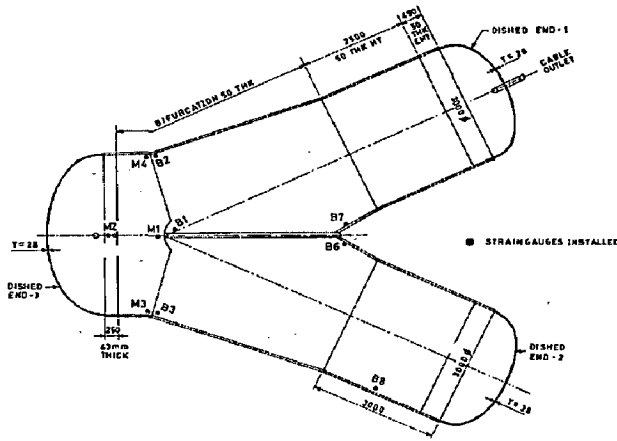
Fig. 2.1: Symmetrical Bifurcation

B) Unsymmetrical bifurcation

In unsymmetrical bifurcation the angle of bifurcation are not equal i.e. angle a ≠ angle b. Unsymmetrical bifurcation is shown in Fig.2.2
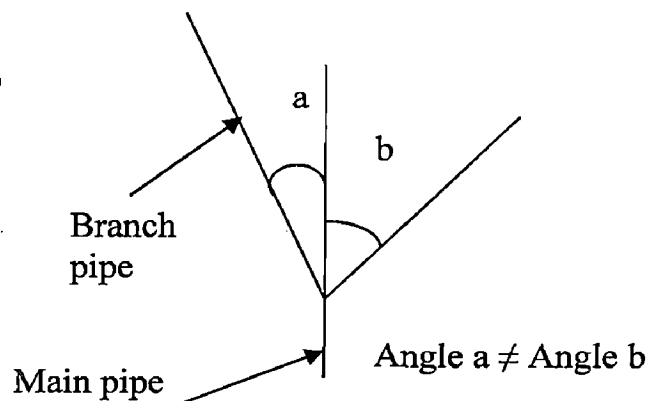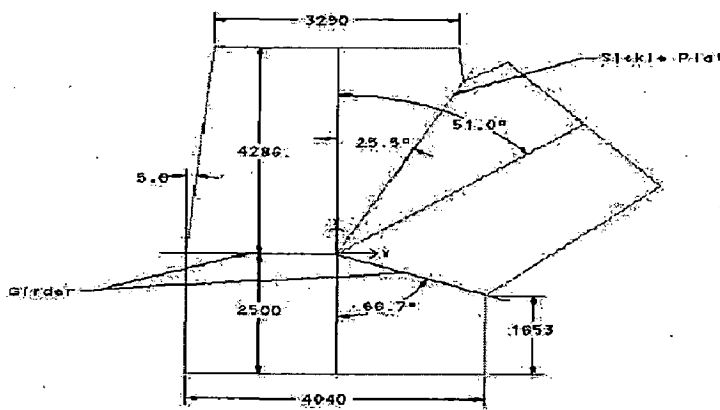
Fig. 2.2: Unsymmetrical Bifurcation

2.3.2 Trifurcation

A trifurcation is one of such branching components which trifurcates the header penstock so as to feed three power units, i.e. in this branching the main pipe directly trifurcated is shown in Fig. 2.3.

Fig. 2.3: Trifurcation

2.3.3 Manifold and Double wyes arrangement

This is such type of branching in which pipes are branches in the same direction in succession from a straight pipe

Fig. 2.4: Manifolds

2.4 Structural Components of Branching [6,15]

➤ Header pipe (Cylindrical shell)

➤ Branch pipe (Cylindrical shell)

➤ Transition pipe (Conical shell)

➤ Splitter / sickle plate

➤ Tie rod

➤ Horse shoe ring girder (Ring beam)

Photo 2.1 shows structural components of branching of a penstock.
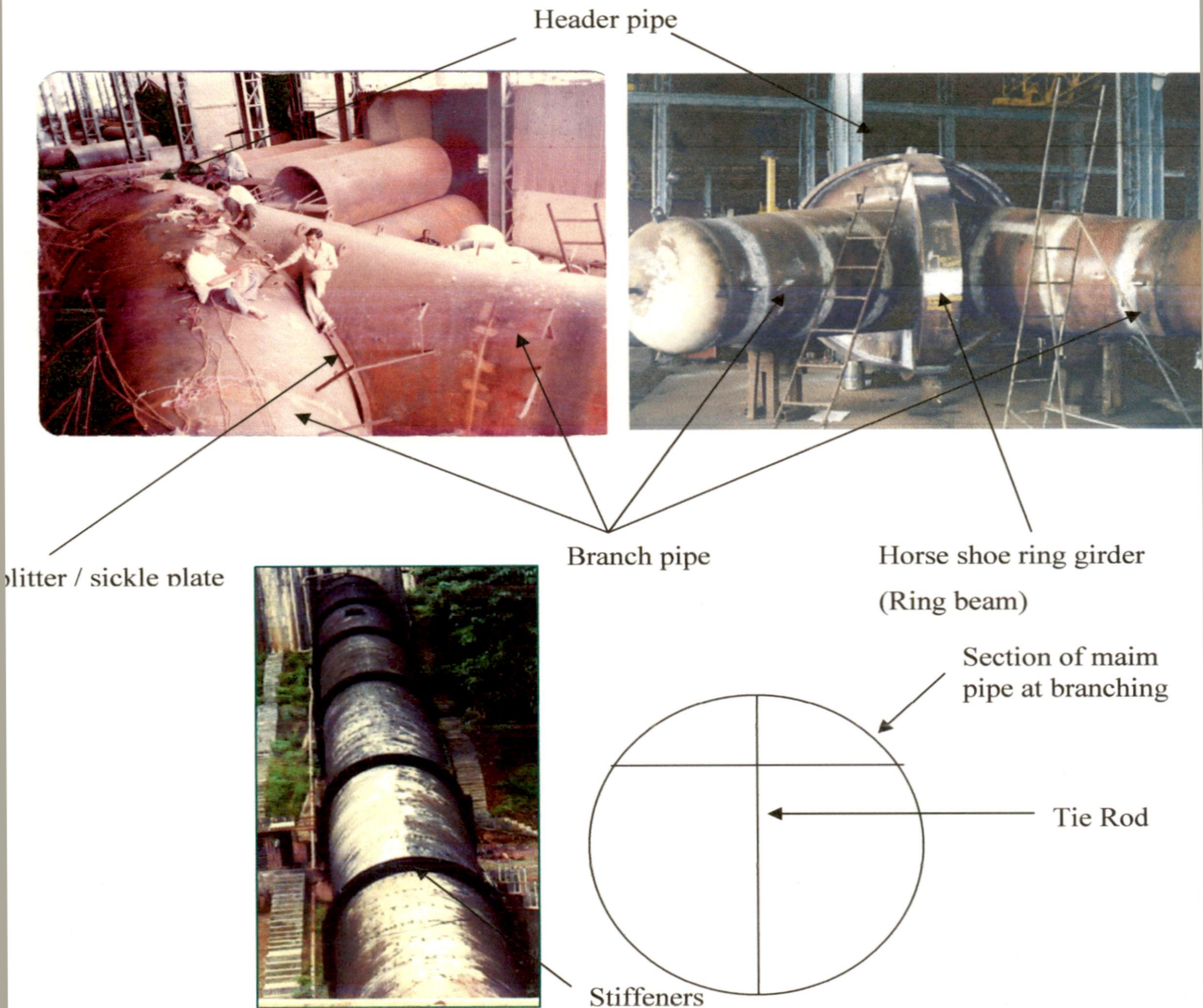
Photo.2.1: Structural Components of Branching

2.5   NUMBER OF PENSTOCKS

One penstock may be provided for each machine or one penstock may feed to more than one machine or all the machines in a power station. In case one penstock serves more than one unit at the tail end a suitable branching arrangement will have to be adopted. The choice of number of penstock in a hydro-power development will depend upon overall economy, manufacture and branching feasibilities. Various factors affecting the choice are size, transport limitation and economy etc.

? Large size will need greater thickness, since total on the conduit section varies directly as the diameter. In case of light bend development excessive thick plates or special types of steel may be needed for very large size penstocks, which may entail difficulties in procurement and also in fabrication. Maximum wall thickness for steel penstocks is kept 60 mm for welded construction and 40 mm for riveted construction.

Transport limitations: Available transport facilities may limit the size of penstock. However for sizeable works such difficulties may be overcome by transport of the pipes in segment and then joining at site.

One penstock for each unit affords a more convenient arrangement and better operational convenience. Damage in one penstock will affect only one unit.

In case of multi units serving penstock, branching arrangement creates complication in design and also in operation. Stress pattern in Y-pieces and other branching arrangements is quite complex and uncertain and not amenable to structural analysis. When one of the machines fed by a penstock is closed resulting differential in loads and operating conditions further complicate the stress pattern.

From pure economical consideration, bigger the size, less the overall cost. If the same discharge is passed through a number of penstocks (n), cost will be greater as compared to single penstock whether it may be in terms of cost of steel or increased friction head loss. If the head loss is kept same, velocity will have to be reduced in ratio of $1:n^{1/6}$ and weight of steel required for pipe alone will be $n^{1/5}$ times. In case of velocity is kept same, head loss will increase to $n^{1/2}$. The weight of steel required for joints, couplings and fittings will add to difference in weight of steel indicated above. In case of isolated penstocks, cost of civil works involved as in supports and anchors etc. will more.

Recent trend is in favour of single penstock with branching with limitations. However in such an arrangement, there will be significant losses at manifolds which should be taken in to account.

Numbers of penstocks to be adopted for any installation should be decided on the basis of through analysis of merits and demerits and economics of different feasible alternatives. Total head losses and water hammer which also depends upon the size of conduit, have a bearing on turbine governing and that should also be taken into consideration. If the length of pressure conduit is not long and spacing of units is wide adoption of individual penstock for each unit may be more economical.

For high capacity units in case of low head development, discharge itself for each machine may be so large as may need quite a big penstock and mere consideration of size may rule out multiunit serving penstocks.

In case of high head development adoption of multi units serving penstock in upper stretches and branching lower down where increase in head so warrants may also be considered.

Mathematical comparative study for one or 'n' number of penstock for discharge (Q) and head (H) remaining same [11,20].

(a) If velocity is kept same i.e. $v = v_n$

$$v = \frac{Q}{A} = \frac{Q}{\frac{\pi D^2}{4}}$$ Velocity for one single penstock

$$v_n \quad \frac{Q}{n A_n} = \frac{Q}{\frac{n \pi d^2}{4}}$$ Velocity for 'n' number of penstocks

As,

$$v = v_n$$

$$or, \quad \frac{Q}{A} = \frac{Q}{n A_n}$$

$$or, \quad \frac{Q}{\frac{\pi D^2}{4}} = \frac{Q}{\frac{n \pi d}{4}}$$

$$or, \quad n \frac{\pi d^2}{4} = \frac{\pi D^2}{4}$$

$$or \quad d = \frac{D}{\sqrt{n}}$$

If t and t_n are the respective thick ness in the two cases, then

$$t = \frac{0.1 H D}{2\sigma} \qquad \text{and} \qquad t_n = \frac{0.1 H d}{2\sigma}$$

$$\therefore \; t_n = \frac{0.1 \, HD}{2\sigma\sqrt{n}} = \frac{t}{\sqrt{n}}$$

Volume of steel per unit length in 'n' number of conduits (penstocks)

$$= \pi \, d \, t_n \times n$$

$$= \frac{\pi D}{\sqrt{n}} \times \frac{t}{\sqrt{n}} \times n = \pi D t$$

which is the same as for a single penstock.

(b)   Head loss is kept same in two cases:

Head loss for one single penstock $= \dfrac{4 f l v^2}{2 g D}$

Head loss for 'n' number of penstock $= \dfrac{4 f l v_n^{\,2}}{2 g d} = \dfrac{4 f l v^2}{2 g \dfrac{D}{\sqrt{n}}} = \sqrt{n} \, \dfrac{4 f l v^2}{2 g D}$

If head loss is kept the same, head loss is proportional to $\dfrac{v^2}{D}$ or $\dfrac{Q^3}{A^2 D}$ or $\dfrac{Q^2}{D^5}$

$$\therefore \; h_f = a_1 \frac{Q^2}{D^5} = a_1 \frac{Q^2}{n^2 D^5}$$

$$d = \frac{D}{n^{2/5}}$$

Wall thickness is proportional to the diameter under a given head with the same permissible stress

$$t = a_2 \, D \qquad \text{and} \qquad t_n = a_2 \, d$$

12

$$\text{then,} \quad t_n = \frac{t}{n^{2/5}}$$

Volume of steel per unit length in 'n' number of penstock

$$= \pi\, d\, t_n \times n = \frac{\pi D}{n^{2/5}} \times \frac{t}{n^{2/5}} \times n$$

$$\pi D t \times n^{1/5}$$

Velocity of flow v_n $\dfrac{Q}{n\pi\dfrac{d^2}{4}} = \dfrac{Q}{\dfrac{n\pi D^2}{n^{4/5}\,4}} = \dfrac{v}{n^{1/5}}$

Where,

    v = velocity of flow in one single penstock

    v_n = velocity of flow in 'n' number of penstock

    Q = discharge through one single penstock

    Q_n = total discharge through 'n' number of penstock

    D = diameter of one single penstock

    d = diameter of each 'n' number of penstock

    A = Area of one single penstock

    A_n = Area of each 'n' number of penstock

    n = number of penstock

    t = thickness of one single penstock

    t_n = thickness of 'n' number of penstock

    h_f = head loss

    f = head loss coefficient

    l = length of penstock

2.6 ECONOMIC DIAMETER OF PENSTOCK

Different diameters may be considered for a penstock required to carry a given discharge Q. Although the weight and thus the first cost of the penstock increases with increasing diameter the output in electrical energy is also increased owing to the reduction in frictional head loss. The economic diameter for a penstock required to carry a discharge Q is the one at which annual costs due to greater investment do not

13

exceed the annual value of resulting increment energy. Mathematically this criterion may be expressed by the relation

$$\frac{dC_1}{dD} \leq \frac{dC_2}{dD}$$

Where, C_1 is the annual cost due to investment for a pipe of diameter D and C_2 is the value of energy that can be produced at the same diameter.

Shell thickness, $t = \dfrac{0.1 H D}{2\sigma}$

Where, H = design head at any section

Weight of the penstock section of unit length say 1 meter, adding 20 % additional allowance neglecting joint efficiency

$$= 1.2 \times 7850 \, \pi \, D \, b$$

$$= \frac{1.2 \times 7850 \pi \times 0.1 H \times D^2}{2\sigma}$$

$$= \frac{1480 \; HD^2}{\sigma}$$

Weight of L meters will be

$$= \frac{1480 \; HD^2 \, L}{\sigma}$$

If annual operating charges including depreciation and maintenance is taken proportional to first cost

$$C_1 = K_1 \frac{1480 H D^2 L}{\sigma}$$

$$\frac{dC_1}{dD} = 2 \times 1480 K_1 \frac{H \, L}{\sigma} D^2$$

Considering the influence of the change in diameter on the annual energy output and its value,

Fractional head loss

$$= \frac{f \, L \, v^2}{2 \, g \, D}$$

$$= \frac{f \, L Q^2}{2g \, \frac{(\pi D^2)^2}{4^2} D}$$

$$= \frac{f \, L Q^2}{12.1 \times D^5}$$

With a head H and discharge Q, power potential is $9.81 \times Q \times H$ kW

Taking the overall efficiency as 80 % power potential corresponding to frictional loss will be

$$9.81 \times 80 \, percent \, of \left(\frac{f \, L Q^2}{12.1 \times D^5} \right) Q \text{ kW}$$

If t is the annual duration of operation in hours, the energy generated will be

$$\frac{9.81 \times 0.80}{12.1} \times \left(\frac{f \, L Q^3 t}{D^5} \right) \text{ kWh}$$

$$= 0.65 \, \frac{f \, L Q^3}{D^5} t \text{ kWh}$$

If K_2 is the value of energy at generator terminals

$$C_2 = 0.65 \times \frac{f \, L Q^3 t}{D^5} \times K_2$$

$$\frac{dC_2}{dD} = -6 \times 0.65 \times \frac{f \, L Q^3 t}{D^6} \times K_2$$

$$\therefore 2 \times 1480 \, \frac{K_1 H D L}{\sigma} \le 3.25 \times \frac{f \, L Q^3 t}{D^6} \times K_2$$

15

$$or, \quad D^7 \leq \frac{3.25}{2 \times 1480} \times \frac{f \sigma K_2}{K_1} \times \frac{Q^3}{H} t$$

$$or, \quad D \leq \left(\frac{1}{1100} \times \frac{f \sigma K_2}{K_1} \times \frac{Q^3}{H} t \right)^{1/7} \quad \text{in meters.}$$

Where

Q = discharge in cumecs

H design head in meters

σ = allowable stress in steel kg/cm^2

K_1 = annual cost of penstock per kg

K_2 = value of one kWh at generator terminals in the same units

t = annual duration of operation in hours

f = friction coefficient, value of which may be taken as 0.02 for preliminary estimates.

2.7 HYDRAULIC HEAD LOSSES IN PENSTOCK

Hydraulics losses in penstock reduce the effective head in proportional to the length of the penstock and approximately as the square of the water velocity. The various head losses which occur between the reservoir and the turbine are as follows[1,6,26,34,36]:

2.7.1 Head loss at Trash rack

The losses through trash rack at the intake vary according to the velocity of flow are expressed as.

$$h_t = k_t \frac{v^2}{2g} \quad ,$$

where,

h_t =trash rack head loss,

k_t =loss coefficient,

v=actual velocity through trash rack,

g= acceleration due to gravity

Velocity of flow	Losses
1.0 feet / second	0.1
1.5 feet / second	0.3
2.0 feet / second	0.5

2.7.2 Head loss at Intake Entrance

The magnitude of entrance losses depends upon the shape of the intake opening. A properly proportioned circular bell mouth entrance is most efficient. The most desirable entrance curve is determined experimentally from the shape formed by the contraction of a jet (vena contracta) flowing through a sharp edge orifice. For bell mouth shape losses are given by

$$h_e = k_e \frac{v^2}{2g}$$

Where,

h_e = head loss at entrance,

k_e = loss coefficient at entrance,

v = velocity at entrance, and   g = acceleration due to gravity

Shape	Head losses
Circular bell mouth entrance	0.05 to 0.10 of the velocity head
Square bell mouth entrance	0.02 of the velocity head

2.7.3 Friction losses

Head losses in pipe because of friction vary considerably, depending upon velocity of flows, viscosity of fluid and condition of the inside surface of the pipe. It is estimated by following formulae:

2.7.3.1 Darcy-Waisbach formula

$$h_f = \frac{fLv^2}{2gD}$$

Where,

h_f = friction head loss in m

f = loss coefficient depending upon type, condition of pipe and Reynolds
   number.

L = length of pipe in m,

V = velocity through pipe in m/sec, and

D = diameter of pipe

17

2.7.3.2 Scobey formula

(Derived from experiments on numerous steel pipe installation)

$$H_F = K_S \frac{V^{1.9}}{D^{1.1}}$$

Where,

H_F = head loss due to friction in feet per 1000 feet of pipe

= loss coefficient, determined experimentally,

V = velocity of flow in feet/second

D = diameter pf pipe in feet.

2.7.4 Bend losses

Bend losses vary according to the shape of the bend, deflection angle, ratio of radius of bend to diameter of pipe and the condition of inside surface. It may be calculated as;

$$h_b = k_b \frac{v^2}{2g}$$

h_b = head loss due to bend,

k_b = bend loss coefficient

v = velocity in pipe

g = acceleration due to gravity

2.7.5 Loss due to Expansion and Contraction:

Head loss due to gradual expansion h_{ex} may be estimated from formula:

$$h_{ex} = \frac{k_{ex}(V_1 - V_2)^2}{2g}$$

Where,

h_{ex} = head loss due to gradual expansion

k_{ex} = loss coefficient depending upon the cone of angle

V_1 = velocity at upstream end in m / sec

V_2 = velocity at downstream end in m / sec

2.7.6 Losses in Penstock Branches and wyes pieces:

The hydraulic losses at wyes depends the following factors:

1) Angle of bifurcation (i.e. angle of deflection of the branch)

2) Ratio of cross sectional area (Ratio of discharge in branch pipe to the discharge in main pipe)

3) Types and shape of bifurcation (cylindrical or conical)

Various types of wyes and branches generally adopted are as follows and head loss coefficient for branches with sharp rounded and conical transitions (or at pipe junction with dividing flow) is given the graph of Fig. 2.5.

1) Wyes / branches with sharp transition

2) Wyes / branches with conical transition

3) Wyes / branches with round corners
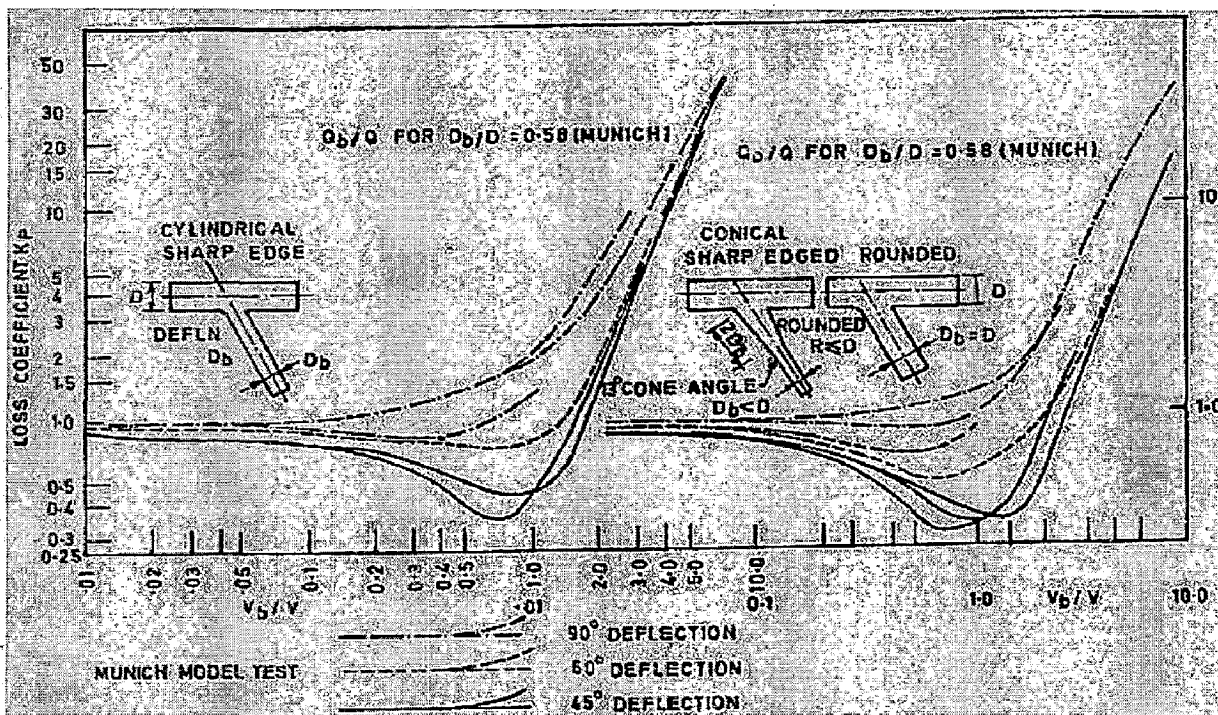
Fig. 2.5: Head Loss Coefficient for Branches with Sharp Rounded and Conical Transitions (or At Pipe Junction with Dividing Flow)

Wyes losses for the first Wye Piece at 0.3 $v^2/2g$

and for the second Wye Piece at 0.4 $v^2/2g$

19

2.7.7 Effect of Water Hammer

Water hammer is a phenomenon of pressure change in a closed pipe when flowing water in a pipe is decelerated or accelerated by closing or opening a valve or changing the velocity of water rapidly in some other manner. The phenomenon is accompanied by series of positive or negative pressure wave which travel back and forth in the pipe system until they are damped out by friction.

Rapid opening and closing of turbine gates produces a pressure wave in the penstocks called water hammer. The intensity of this pressure wave is proportional to the speed of propagation of the pressure wave produced velocity of flow destroyed. The maximum increase in head for closers in time less than 2L/a second,

$$\Delta H = \frac{av}{g}$$

ΔH = maximum in crease in head

a = velocity of pressure wave

v = velocity of flow destroyed

g = acceleration due to gravity

L=length of penstock from forebay to turbine gates
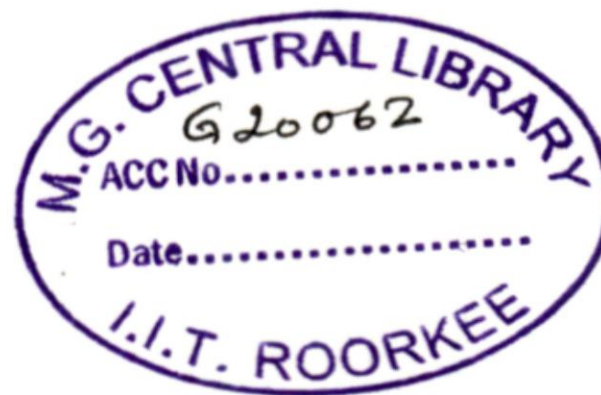
It is necessary to consider the reflection of wave from the branch pipe and dead ends in order to determine the pressure rise due to velocity changes. Penstock must be safeguard against surge, accidental or otherwise. Surge of instantaneous type may develop through resonance caused by rhythmic gate movements or when the governor relief or stop valve is improperly adjusted.

DESIGN OF PENSTOCK BIFURCATION BY ANALYTICAL APPROACH

3.1 GENERAL

The branching of penstock considerably alters hydraulic and structural behavior of penstock in the vicinity of the wye. In fact the penstock wyes are highly complicated structures and are not amenable to exact theoretical analysis. Detailed model tests regarding their hydraulic performance and structural behaviour are often desirable. Basic criteria for designing penstock wye are the hydraulic efficiency and structural safety commensurate with job requirements. Hydraulic efficiency requires least head loss or streamed lined flow where as structural safety calls for provision of reinforcement.

The study of design of penstock bifurcation is mainly divided into two parts first hydraulic study which governs head losses and second one is structural study in which stresses developed in structure is brought down within the permissible limit. Determination of stresses and losses of head in view of the choice of a penstock branch connection is very complicated structure, The penstock bifurcation usually having several stiffening beams to resist the loads due to internal pressure of water. Internal tension members called tie rods or external horse shoe ring girder /yoke or internal reinforcement like sickle plate forms a very complicated structure. The purpose of the tie rods is to assist the stiffening beams in carrying the applied loads [37].

The structural and hydraulic behaviour of penstock wyes are quit complex. A good design of penstock wyes warrants [6, 20, 25, 33].

   i)   Minimum hydraulic losses
   ii)   Streamlining of the boundary geometry of the transition
   iii) Limitation of stress concentration in the reinforcement provided at the junction of the wyes
   iv)   Limitation of stress variation under all the operating conditions
   v)   Economy in fabrication testing and easy transport

These aspects are discussed in subsequent paragraphs under the heading of hydraulic design and structural design.

3.2 HYDRAULIC DESIGN

Requirement of minimum hydraulic loss and streamlining calls for a good hydraulic design to achieve minimum losses of energy in carrying out water from reservoir to power house. The velocity of flow should remain in economical velocity range of 3.0 to 6.0 m/sec. The bifurcation of large penstock, since, generally involves additional loss of head, change in flow pattern and pressure distribution at the splitter causing the deviation / division of flow and pressure fluctuation leading to the vibration of the structure.

A preliminary hydraulic design involves the fixation of dimension and geometric shape of the wyes-branches which include the following:

i)   Diameter of branch penstock

ii)   Angle of branching

iii)   Transitions

The principal on which the hydraulic design is based, are briefed as below

3.2.1 Diameter of Branch Penstock

Whenever a header penstock is to be branched into two or more penstock the equation of determining the diameter of branch penstock arises. This can be achieved through fundamental condition of equivalent discharge by selecting diameter either for [20,35]

i)   Identical flow velocities

ii)   Identical head losses

3.2.1.1 Identical Flow Velocities

In this case, if the total discharge is to be divided into a number of branch penstocks, the condition is that the identical flow velocity exists to determine the diameter of each penstock.

If   Q   = Discharge in header pipe

    Q_n = Number of branch penstocks

    Q/n   = Discharge through branch penstock

n   = Number of branches

For identical velocity, velocity in header pipe is equated to velocity in branch pipe, i.e.

$$\frac{Q}{\frac{\pi D^2}{4}} = \frac{Q_n}{\frac{\pi D_n^2}{4}}$$

Where D and D_n are the diameter of header and branch pipe respectively

$$D_n = D\sqrt{\frac{Q_n}{Q}} = \frac{D}{\sqrt{n}}$$

For wyes branch, $D_n = \frac{D}{\sqrt{2}}$

3.2.1.2 Identical Head Losses

In this case head loss in header penstock is equated to the head loss of all branch pipe per unit length. Let h_f be the total head loss in metres of water, is equal to

$$h_f = \frac{f L}{D}\frac{v^2}{2g} \quad \text{and} \quad v^2 = \frac{2.h_f . g D}{f L}$$

Discharge, $Q = A v$

$$Q^2 = A^2 v^2$$

$$= \frac{\pi^2 D^4}{16}\frac{2 h_f g D}{f L}$$

$$= \frac{\pi^2 2g h_f D^5}{16 f L}$$

i.e. $\frac{Q^2}{D^5} = constan. h_f$

$$h_f = \frac{Q^2}{D^5} cons\tan t$$

Now, equating head losses in header penstock to that of branch penstock,

$$\frac{Q^2}{D^5} \cdot cons \tan t = \frac{\left(\frac{Q}{n}\right)^2}{D_n^{\ 5}} \cdot cons \tan t$$

$$so, \quad D_n^{\ 5} = \frac{Q^2 D^5}{Q^2 n^2} = \frac{D^5}{n^2}$$

$$or, \quad D_n = \frac{D}{\sqrt[5]{n^2}} = \frac{D}{n^{0.4}}$$

For a penstock bifurcation,

$$D_n = \frac{D}{2^{0.4}} = \frac{D}{1.32}$$

3.2.2   Angle of Branching

The branch outlet and wyes are usually designed in such a way that the header and the branches are in the same plane. The use of frustum of cone with convergence of 6° to 8°, reduces the branch loss to approximately one-third that of a cylindrical branch. The hydraulic efficiency increases as the deflection angle of branching decreases. Generally the deflection angle varies between 30° to 75°. Smaller angle of deflection (less than 45°) causes difficulty in reinforcing branch outlet and wyes and greater deflection angle effect more losses.

3.2.3   Transitions

Transition is section of conduit which connect one prismatic portion to another by a reducing the cross section. Transition is provided to avoid high energy loss in reduction of area by an abrupt junction of branch and header and so this gives gradual reduction in cross sections to make the flow path steamed-lined.

The transitions can be achieved on the following principles:

    i)   Transitions and bends are made about the centre line of the mass flow.

    ii)   Conical pieces with flare angle 6° to 8° introduced to connect the main with the branch.

    iii)   By providing elliptical shaped entranced.

As per U.S.B.R, conical pieces of favourable flare angle i.e. angle of reducer 6° to 8°to connect main with branches fixes up the transition length without much difficulties. If the transition length is increased, velocity gradient will decrease resulting less energy loss. But the greater length of transition will mean greater friction loss together with increased cost of the structures. Hence an optimum length of transition should be fixed to give minimum loss of energy in the transition and this is only possible by model studies. Before final design, detail investigation are carried out on hydraulic scale model to observe the head loss, change in flow pattern, pressure distribution at the splitter causing division of flow, pressure fluctuation leading to vibration of structure, cavitations effect etc.

Last but not the least, aspect of hydraulic design is the geometric shape of the branching transitions. Transitions are the section of penstock wyes which connect one prismatic portion to another by gradual change in cross section. A gradual change in cross section or in other words streamlining the flow path reduces the hydraulic loss. Cylindrical branch connections should therefore be avoided where hydraulic efficiency is important. Generally conical connection with side wall angle of six to eight degree is used to reduce the hydraulic losses to about one third of those resulting from cylindrical connections. Provision of perforated curve plate at critical locations inside the wyes where eddied are expected to be formed also helps in streamlining the flow, so that the hydraulically losses are minimized.

3.3   STRUCTURAL DESIGN

The junction of a branch with head is inherently is a point of weakness. The absence of the metal in the opening cut in the header penstock for connecting it to the branch penstock results in to inadequate constraint against the internal pressure. Since openings reduce the strength of the penstock pipe at the opening it becomes necessary to reinforce the area around the opening. The provision of reinforcement should be thought of not as a mere addition of certain area of metal out as being in form of ring clamp, or sickle to prevent radial movement of the hole cut in the penstock.

Structural design of penstock pipe lines requires that members be so designed as to ensure smooth flow and minimum losses. Stress distribution in all the members should be uniform as possible without any excessive concentration at some points. The stress developed in all the members should only be tensile in nature without any bending stresses. Model test may indicate overall behavior of the structure. The

25

structural design of wyes branch requires uniform stress distribution in all the members. The preliminary structural design consists of thickness of shell and dimensions of reinforcement, which are required to be provided for preventing radial movement of the unreinforced area of the branch and to make stress distribution uniform and within allowable limits. The preliminary structural design consists of

i)   Thickness of shell
ii)   Dimensions of reinforcement
      a)   External reinforcement
      b)   Internal reinforcement

3.3.1   Shell Thickness

Thickness of shell for majority of pipelines is usually small as compared to the diameter. According to thin walled vessel theory, circumferential hoop stresses is applicable for calculating the thickness of the shell. Determination of shell thickness is simple and based on hoop stress consideration as in thin wall cylinder theory. This formula holds good for up to the diameter thickness ratio of 20 [39].

$$\text{Shell thickness, } t_p = \frac{pD}{2\phi\sigma} = \frac{0.1HD}{2\phi\sigma}$$

D = Diameter in mm

H = Design pressure head in m

σ = Permissible hoop stress in shell in Kg/cm^2

$\emptyset$ = Joint efficiency of longitudinal joints (0.85 to 0.95 for welded joints depending on percentage radiographic test []

The nominal corrosion allowance 1.5 mm [1]

Also, by consideration of likely vacuum pressure which may be due to water hammer, wave oscillation, the shell thickness should not be less than 1/100 of the diameter.

3.3.2   Dimensions of Reinforcement

Depending on the type of reinforcement, there are broadly two types of wyes, namely:
      a)   Externally reinforced bifurcation
      b)   Internally reinforced bifurcation

3.3.2.1 External Reinforcement

In this type reinforcement is provided completely externally and consists of ribs and girders. The basic design for the external reinforcement was stablished by J.S.Blair, U.K. for one and two plate.

When externally reinforced is used in condition with tie rods and ring girder, analysis become statically indeterminate. In such cases the deflections of reinforcing girders at the junctions with the tie rods or ring girder are computed and equated to the elongations or deflections of the tie rods or ring girder. In externally reinforced wye branch the unbalanced force is resisted by providing a curved ring girder /horse shoe ring girder/ring beam (Yoke girder) along the junction of two branches and a circular girder at the junction of main header and branches.

The reinforcement is provided in the form of curved plate girder or ribs, mounted externally along the intersection of the branch and main penstock depending upon the number of curved plates used for reinforcing as shown in photo 3.1. The external reinforcement falls in to three categories [1, 37, 41].

    a)   Single plate reinforcement

    b)   Two plate reinforcement

    c)   Three plate reinforcement
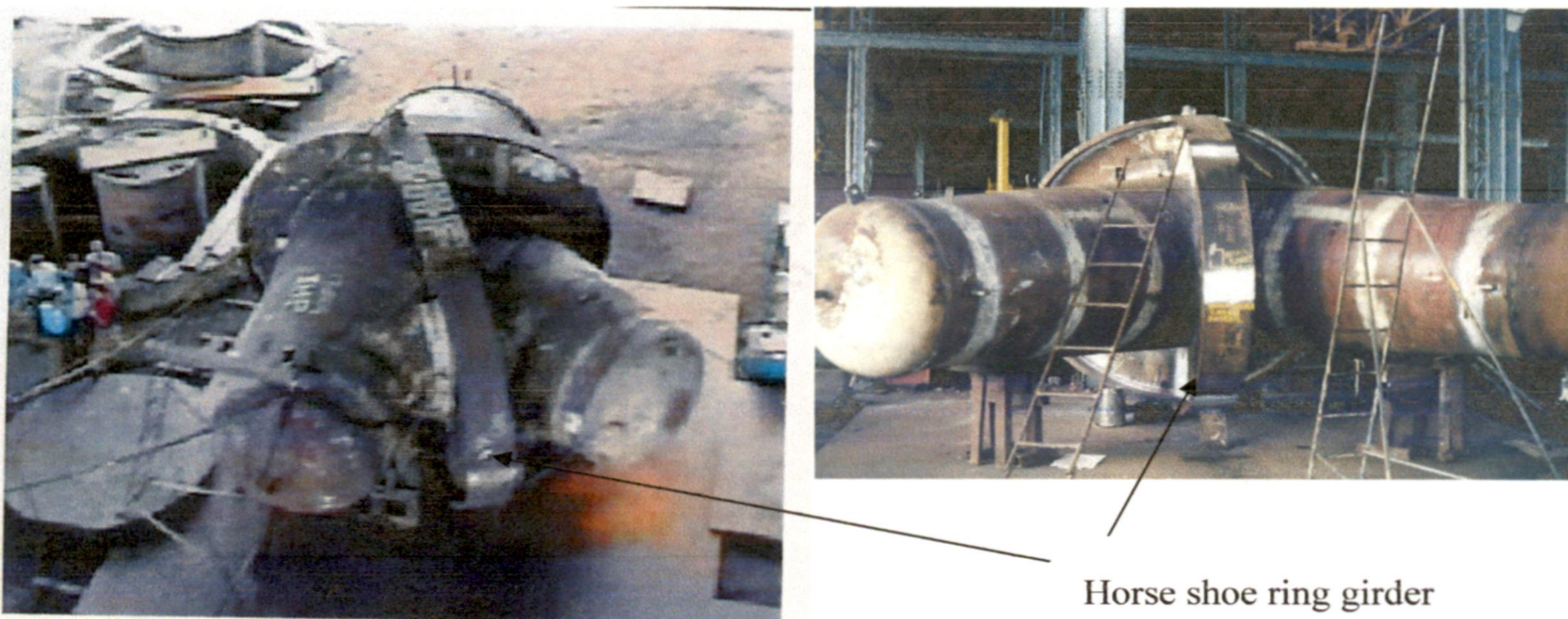
Horse shoe ring girder (Ring beam)/ Yoke girder

Photo 3.1: View of Externally Reinforced Bifurcati

3.3.2.2 Internal Reinforcement

In an internally reinforced wye branch, an internal splitter plate is provided to resist the unbalanced force by tension. This type of wye is developed by Escher Wyes and generally consists of crescent shaped rib inside the branch pipe and is designed in such way that the rib is directly subjected to tension and has the same the magnitude as the stress in shell section of pipes adjacent to it. The photo 3.2 and Fig. 3.1 show the clear cut visualization of penstock bifurcation. The stress analysis of internal reinforcement for wyes is shown in Fig. 3.2 and Fig.3.3 is statically determinate, and the bending and direct stresses can be computed without much difficulty for any section. Increase in the bending stress due to the small radius of the curvature at the throat of reinforcement may be evaluated by applying a correction factor to the bending formula for straight beams and stress analysis is done. Alternative stress analysis of internal reinforcement provided in the plane of intersection of the wye junction is based on the assumption that the reinforcement is subjected to only normal stresses. This assumption is reasonable. In fact, radial width of internal reinforcement is provided to cater for the requirement of its symmetry about the resultant. Thus, the stress analysis of internal reinforcement involves determination of magnitude, direction and position of the resultant at various points along the intersection of wye so that adequate radial width of reinforcement is provided symmetrically about the resultant at every point.
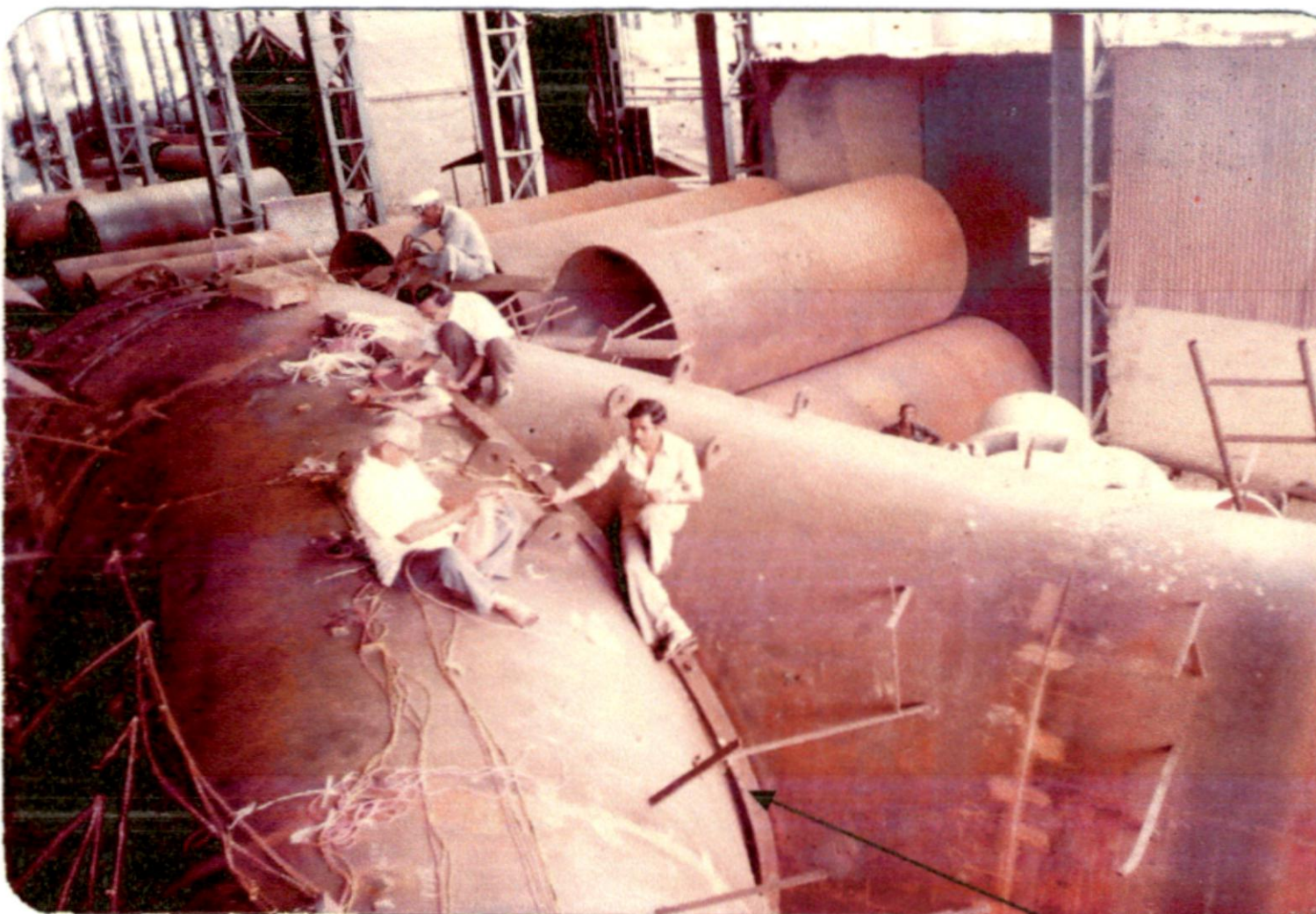
Splitter / sickle

Photo 3.2: View of Internally Reinforced Bifurcation

Internal sickle Plate
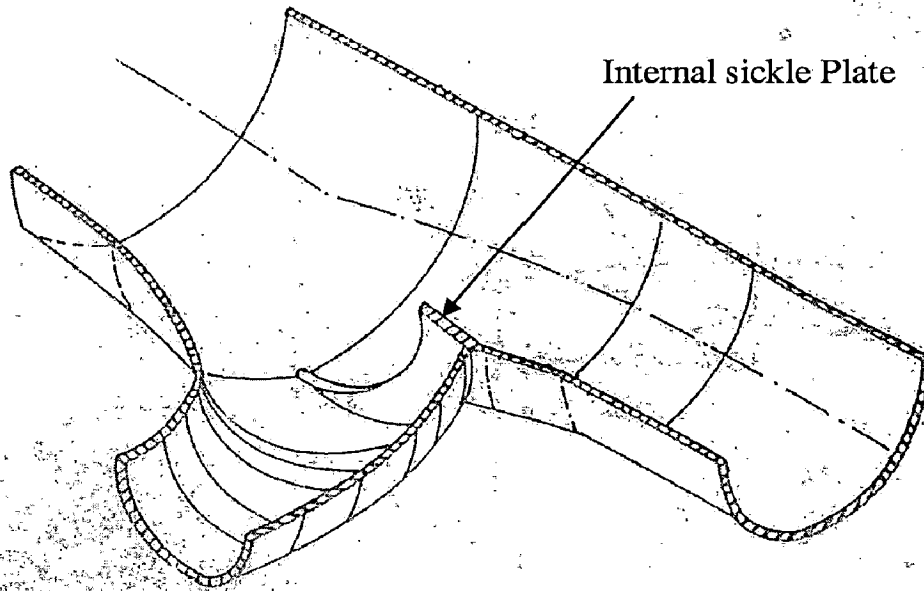
Fig. 3.1: Internal Reinforcement as Sickle Plate

Stress analysis is illustrated in subsequent sub-paragraph for the case of symmetrical wyes and to fulfill the requirement of thesis. In view of the fact that the penstock wye chosen for the study is internally reinforced the structural design has been presented for the internal reinforcement only. However, considering the size, structural efficiency, hydraulic efficiency, and embedment in concrete internally reinforced bifurcation generally favoured [14,20,35].

Stress analysis of internal reinforcement for wyes calls for considering the geometry of the wye and the relevant forces, which are shown in Fig.3.2 and Fig.3.3 Where, 2β = angle of intersection of wye / deflection angle of wye

R_1 = Radius of the main pipe *or* r = Variable radius of the splitter section of pipe

Splitter section of elliptical form is found by the intersection of a cylinder or a cone by a plane. r and $a = r/\sin\beta$ are the semi minor and semi major axis of the ellipse respectively. Let F be any point on the intersection of the curve and the lining joining it to the centre makes an angle α with centre 'O', the coordinate of the points are

$$x = r\frac{\sin\alpha}{\sin\beta} \qquad\qquad y = r\cos\alpha$$

$z = r \cot\beta \, \sin\alpha$

so that,

$dz = r \cot\beta \cdot \cos\alpha \, d\alpha$

The pipe walls transmit forces at the point of intersection from both sides on to the reinforcement or strengthening collar, which lies in the plane of intersection of 'AB', and on account of symmetry the resultant of these forces must always fall in the plane of intersection. If the walls of pipe are assumed to be thin membranes having no resistance against bending so that they inflict only tractive and shearing force on the strengthening collar, when subjected to internal pressure 'p' then the forces per unit length in cylindrical membrane are:

    i) In circumferential direction, $p. r$

    ii) In axial direction, $(1/2)\, p. r$

Where, p = Internal pressure
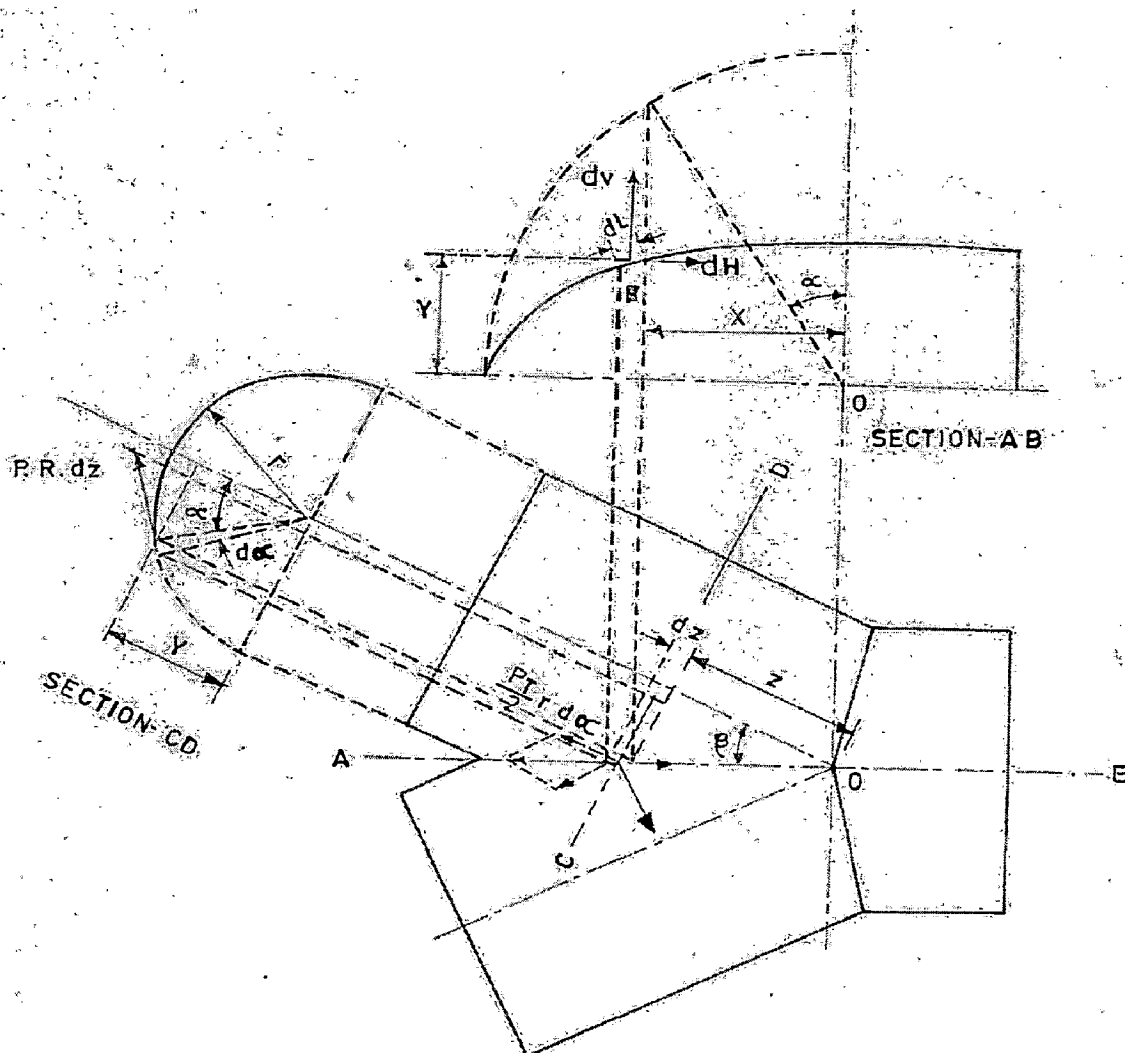
Fig. 3.2: Plan of a Cylindrical Symmetrical Pipe Branch (To Assist the Calculation of the Forces Transmitted From Pipe Wall to the Strengthening Ribs)
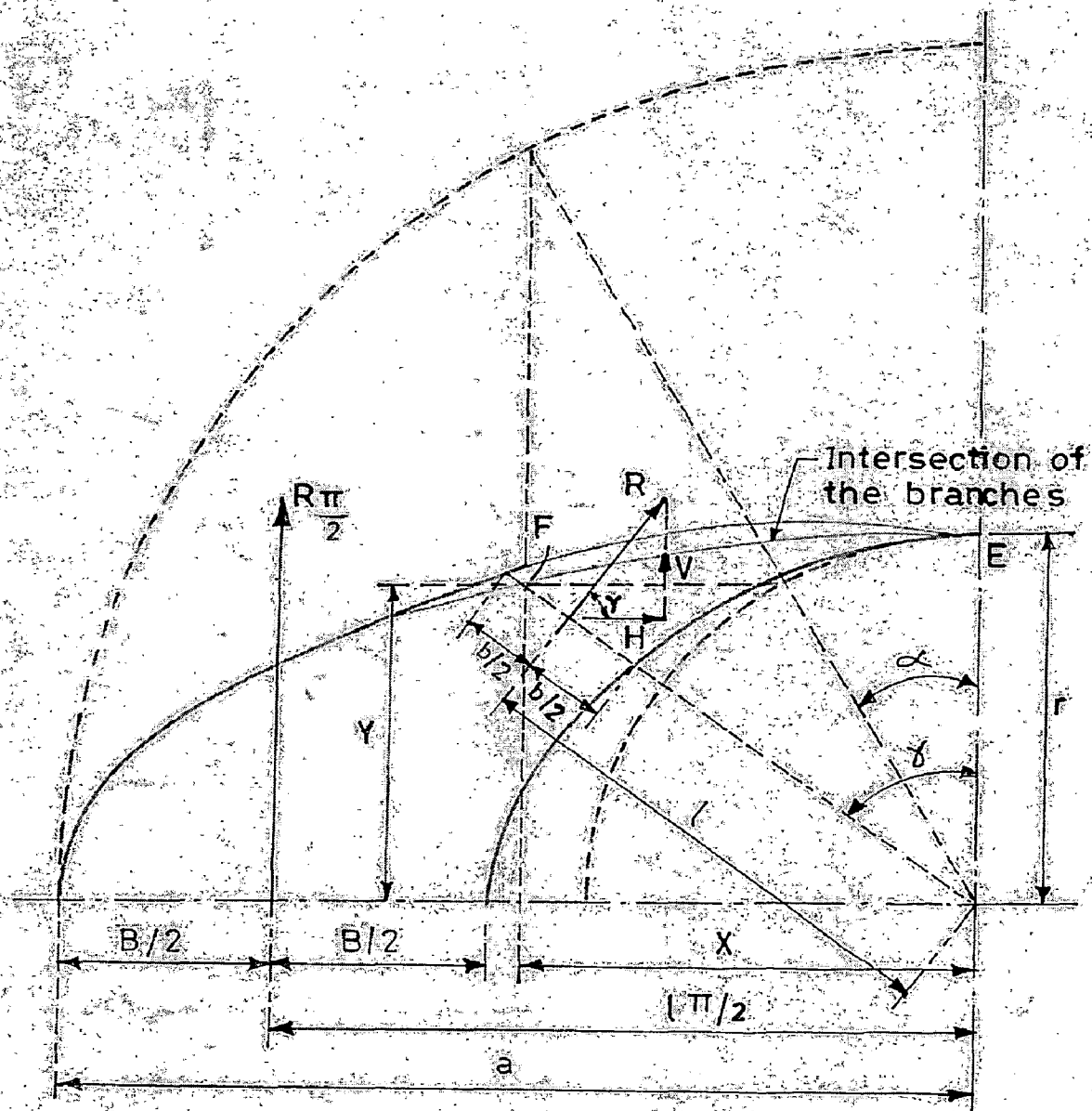
Fig. 3.3: Half of the Sickle-Shaped Strengthening Rib of Fig. 3.2 with Resulting Forces

Considering an element of length dl of the line of intersection, the forces inflicted on the strengthening rib from one side are:

(a) as a result of circumferential stress

$$p . r . dz = p . r^2 \cot \beta \cos \alpha \ d\alpha$$

(b) as a result of axial stress

$$(1/2)\ (p.\ r.)\ dr = (1/2)\ p.\ r^2\ d\alpha$$

Where, dr and $d\alpha$, are shown in the figure

These forces resolved in horizontally and vertically directions, produce for both parts of

the pipe together, the force differential, we get

$$dH_1 = (p\ r^2\ cot\beta\ cos\alpha\ d\alpha\ )\ (\ cos90°\text{-}\beta\ )$$

$$= (p\ r^2\ cot\beta\ cos\alpha\ d\alpha\ )\ (\ sin\beta\ cos\alpha\ )$$

$$= p\ r^2\ cos\beta\ cos2\alpha\ d\alpha \qquad \text{(due to circumferential stress)}$$

$$dH_2 = (p\ r^2/2\ )\ d\alpha\ cos\beta \qquad \text{(due to axial stress)}$$

$$\sum dH = (pr^2/2\ )\ cos\beta\ (\ cos^2\alpha - 1/2\ )\ d\alpha$$

$$= (pr^2/2\ )\ cos\beta\ (2cos^2\alpha - 1)\ d\alpha$$

Total dH from both side, in horizontal direction=$2 \times \sum dH$

i.e. $dH = p\ r^2\ cos\beta\ (2cos^2\alpha\text{-}1)\ d\alpha \qquad\qquad \longrightarrow\ \text{+ve}$

Total dv from both sides $= 2 \times$ (dv due to circumferential stress)

i.e. $dv = 2\ p\ r^2\ cot\beta\ cos\alpha\ sin\alpha\ d\alpha \qquad\qquad \uparrow\ \text{+ve}$

Integrating with limit of 0 to α, yields

Vertical force, $\qquad V = p\ r^2\ cot\beta\ sin^2\alpha \qquad\qquad$ and

Horizontal force, $\qquad H = p\ r^2\ cos\beta\ sin\alpha\ cos\alpha$

Therefore resultant R of all the forces which act in the elliptical arc EF on the

strengthening collar, Then:

$$R = \sqrt{V^2 + H^2}$$

$$R = p\,r^2\ cot\beta\ sin\alpha\sqrt{sin^2\alpha + cos^2\alpha sin^2\beta}$$

and the angle of resultant 'R' to the X-axis at any place is given by

$$tan\gamma = \frac{V}{H} = \frac{tan\alpha}{sin\beta} = \frac{x}{y}$$

The resultant is at right angle to the line of connecting point 'F' with the origin of coordinates 'O'

When $\alpha = \pi/2$ (i.e. at crown)

(R) $_{\pi/2} = p\, r^2 \cot \beta = $ (V) $_{\pi/2}$ and

(H) $_{\pi/2} = 0$ and $\gamma = 90°$

In order to determine the position of the resultants at various points, it is required to find out all the moments with reference to point 'O'.

Moment due to vertical force is

$$M_V = \int_0^\alpha x.dV = \frac{2p^3 \cot \beta}{3 \sin \beta} \sin^3 \alpha,$$

Moment due to horizontal force is

$$M_H = \int_0^\alpha y.dH = pr^3 \cos \beta \sin \alpha (1 - \frac{2}{3} \sin^2 \alpha)$$

Therefore, total moment $= M = M_V + M_H = p\, r^3 \cos \beta \sin \alpha\, (1 + 2/3\, \sin^2\alpha\, \cot^2 \beta)$

Normal distance l at which the resultant is acting from O is

$$l = \frac{M}{R} = r.\sin \beta \frac{1 + (2/3) \cot^2 \beta \, \sin^2 \alpha}{\sqrt{\sin^2 \alpha + \cos^2 \alpha \sin^2 \beta}}$$

Thus, all the elements are known which are required for determining the magnitude, direction and position of the resultant for any cross section characterized by angle α.

When $\alpha = 0$, (l)$_0 = r$; and at the crown i.e.

When $\alpha = \pi/2$, (l) $_{\pi/2} = r .\sin \beta \{ 1 + (2/3\,) \cot^2 \beta \}$

If the strengthening rib is of equal (uniform) thickness made from steel sheet, then half the width of the sickle at crown i.e. at $\alpha = \pi/2$ is obtained by

$$\frac{B}{2} = a - (l)_{\pi/2} \qquad \text{where, } a = \frac{r}{\sin \beta} \quad = \text{the major axis of ellipse}$$

Substituting the value of 'a' and l$_{\pi/2}$ the full width of sickle plate at crown works out to be

$\therefore$ B = 2/3 .r . cos β cot β (putting the value of a $l_{\pi/2}$ in the above equation)

The width of sickle at any section is obtained on applying in the above principle,

$$\frac{b}{R} = \left\{\frac{b}{R}\right\}_{\pi/2}$$

Or, $b = B \dfrac{R}{(R)_{\pi/2}}$

Substituting values of B, R and $R_{\pi/2}$

$$b = \frac{2}{3} r.\cot\beta.\cos\beta.\sin\alpha\left[\sqrt{\sin^2\alpha + \cos^2\alpha.\sin^2\beta}\right]$$

In order to determine the thickness of the sickle, it is assumed that the stresses in the sickle plate should be the same as those in the pipe walls. The comparable stresses are based on the hypothesis of Misses-Huber which are taken as the means for determining the danger of rupture and are calculated with the aid of following formula for a cylinder pipe of wall thickness 's' which is closed at both ends and therefore stressed bi-axially are given by

$$\sigma_r = \frac{p.r}{s}\sqrt{0.75}$$

The sickle plate of thickness 'S' is subjected only to tensile stresses along one axis. The tensile stress at the crown section is

$$(\sigma)_{\pi/2} = \frac{\sqrt{R_{\pi/2}}}{B.S}$$

$$= \frac{p\,r2}{2/3} \frac{\cot\beta}{r.\cos\beta\cot\beta.s}$$

$$= \frac{2}{3} \frac{p.r}{\cos\beta.s}$$

By equating the two stresses, the wall thickness of the sickle plate 'S' in term of wall thickness of the pipe 's' is given by following simple relation

$$S = s \frac{\sqrt{3}}{\cos \beta}$$

$$= s \frac{\sqrt{3}}{\cos 25°}$$

$$= 1.911. s \cong 2. s$$

2×50 mm=100 mm, where s= 50 mm (thickness of pipe)

Thus the wye is completely analysed by determining the forces, direction and position fixing up the dimension of reinforcement. However simplifying assumptions are involved in the stress analysis. The assumption that the pipe is closed at both ends and is subjected to biaxial stresses is not an exact proposition. Likewise, the assumption that the stresses in splitter and shell are same is also not correct for high thickness of splitter when rigidity conditions prevail near the junction and more stresses are induced in the shell of the pipe near splitter. Nevertheless, this type of stress analysis with internal reinforcement is simple accurate and more reliable than the one with external reinforcement where the material is badly utilized.

Verification of analytical solution of the structural design is performed by mathematical model study using Finite Element Method, physical model study and hydrostatic test on prototype by determining the distribution of stresses in the splitter plate and shell. The stresses guide the designer to find the dependency of the stresses on shell thickness or splitter thickness etc.

3.4   SALIENT FEATURE OF PENSTOCK BIFURCATION

3.4.1   Dimension

Diameter of header pipe, D_1 = 4000 mm

Diameter of branch pipe, D_2 = 3000 mm

Thickness of shell pipe, t_p = 50 mm

Thickness of sickle plate, ts   = 100 mm

Angle of bifurcation, β = 25°   and symmetrical with central line

Reducer angle $\emptyset$ = 6°   for sub branches

Joint efficiency ϕ = 0.95 (Joint efficiency of longitudinal joints)

3.4.2   Properties of Steel Used

Type of steel   ASTM A-537 Class II

UTS	5625-7031 kg/cm^2
Minimum UTS	6525 kg/cm^2
Yield Stress of Steel	4219 kg/cm^2
Modulus of elasticity (E)	2.1 × 10^6 kg/cm^2
Poisson' ratio (μ)	0.3
HOOP STRESS LIMIT	50% of minimum UTS =2812.5 kg/cm^2
	50% of yield stress = 2110 kg/cm^2
	60% of yield stress = 2531.4 kg/cm^2
	75% of yield stress = 3164.3 kg/cm^2
Rock participation	50% (assumption as per of designer & authority)

3.4.3 Hydraulic Properties

| Static head | 47.3 kg/cm^2 |
| Total design pressure | 55.73 kg/cm^2 |

Note: Static head for calculation is taken 50 kg/cm^2 to compare the result with hydrostatic test and physical model test.

Fig. 3.4: Plan of Penstock Bifurcation

Fig. 3.5: Section of Sickle Plate

3.5 CALCULATIONS

3.5.1 Calculation for Shell Thickness

Shell thickness, $t_p = \dfrac{pD}{2\phi\sigma} = \dfrac{0.1HD}{2\phi\sigma}$

$$t_p = \frac{0.1 \times 500 \times 4000}{2 \times 1.0 \times 2100} = 47.62 \text{ mm} + 1.5 \text{ mm (Corrosion allowance)}$$

$$= 49.12 \text{ (say 50 mm)}$$

When taking σ_y = 50% of minimum yield stress

3.5.2 Calculation for Sickle Plate

The pipes are slightly conical type with variable radius 'r' which has been expressed in term of R_1, the radius of main pipe at the point of bifurcation as below

$$r = \frac{R_1}{1 + c \sin \alpha} \qquad\qquad (5.1)$$

Where, $c = \tan \emptyset . \cot \beta$

And coordinate of intersection,

37

$$x = r\frac{\sin\alpha}{\sin\beta} \tag{5.2}$$

$$y = r\cos\alpha \tag{5.3}$$

$$\psi = \sin\beta\left(\frac{1+\frac{2}{3}\cot^2\beta\,\sin^2\alpha}{\sqrt{\sin^2\beta+\cos^2\beta\,\sin^2\alpha}}\right) \tag{5.4}$$

$$\xi = \frac{1}{3}\cos\beta.\cot\beta.\sin\alpha \times \sqrt{\sin^2\alpha+\cos^2\beta.\sin^2\alpha} \tag{5.5}$$

$$A = \psi.\,r \tag{5.6}$$

$$b = \xi\,(2\,r) \tag{5.7}$$

Here,

$$x_i = r\frac{\sin\alpha}{\sin\beta} \tag{5.2a}$$

$$y_i = r\cos\alpha \tag{5.3a}$$

Here, $R_1 = 2000$ mm

$\beta = 25°$

$\emptyset = 6°$

$\alpha = 0°$ to $90°$ (variable angle)

r = variable radius

R_1 = the radius of main pipe at the point of bifurcation

b = width of sickle plate at any section corresponding to coordinates x_i, y_i

Calculation of geometric parameter of sickle plate r, ψ, ξ, A are shown in table 5.1

Table 3.1: Calculation of Geometric Parameter of Sickle Plate r, ψ, ξ, A

α (deg)	r	ψ	A	ξ	b	x_i	y_i	θ (deg)
0	2000	1.0000	2000.00	0.0000	0.0000	0.00	2000.00	0°
5	1961	1.0059	1972.98	0.0243	95.2344	404.51	1954.00	11°41'45"
10	1925	1.0238	1970.41	0.0507	195.2928	790.82	1895.43	22°38'50"
15	1890	1.0539	1991.66	0.0810	306.3216	1157.32	1825.37	32°22'32"
20	1857	1.0956	2034.28	0.1161	431.2844	1502.73	1744.87	40°44'09"
25	1826	1.1467	2093.97	0.1562	570.3276	1826.06	1654.97	47°48'49"
30	1797	1.2048	2165.56	0.2007	721.5633	2126.54	1556.62	53°47'45"
35	1771	1.2671	2244.08	0.2490	881.8095	2403.65	1450.75	58°53'11"
40	1747	1.3311	2325.23	0.2997	1047.1472	2656.98	1338.21	63°16'03"
45	1725	1.3945	2405.54	0.3517	1213.3068	2886.30	1219.80	67°05'25"
50	1706	1.4555	2482.32	0.4034	1375.9356	3091.45	1096.29	70°28'28"
55	1688	1.5125	2553.50	0.4534	1530.7881	3272.37	968.36	73°33'55"
60	1673	1.5642	2617.53	0.5002	1673.8655	3429.04	836.68	76°17'16"
65	1661	1.6097	2673.25	0.5424	1801.5234	3561.48	701.86	78°51'05"
70	1650	1.6479	2719.81	0.5788	1910.5539	3669.74	564.48	81°15'19"
75	1642	1.6784	2756.59	0.6083	1998.2513	3753.87	425.09	83°32'22"
80	1637	1.7005	2783.14	0.6301	2062.4617	3813.92	284.21	85°44'18"
85	1633	1.7139	2799.18	0.6434	2101.6209	3849.93	142.35	87°52'57"
90	1632	1.7183	2804.55	0.6479	2114.7799	3861.94	0.00	90°

Also,

$$x = r \frac{\sin \alpha}{\sin \beta}$$

$$y = r \cos \alpha$$

$$z = r \cot \beta \sin \alpha$$

$$dz = r \cot \beta \cos \alpha \; d\alpha$$

The forces per unit length in cylindrical membrane in circumferential direction = p.r and in axial direction = ½ p.r, then considering an elemental length 'dl' of the line of intersection, the forces inflicted on the strengthening rib from one side are

(a) Result of circumferential stress = p.r.dz = $p.r^2.\cot\beta.\cos\alpha.d\alpha$ (5.8)

(b) Result of axial stress = (1/2). P.r.dr = (1/2). $P.r^2.d\alpha$ (5.9)

Vertical forces, V = $p.r^2.\cot\beta. \sin^2\alpha$ (5.10)

Horizontal forces, H = $p.r^2.\cot\beta. \sin\alpha . \cos\alpha$ (5.11)

Resultant forces, R = $\sqrt{(V^2+H^2)} = p.r^2.\cot\beta \sin\alpha \sqrt{(\sin2\beta +\cos^2\beta.\sin^2\alpha)}$ (5.12)

when $\alpha = \pi/2$, i.e. at crown, $R_{\pi/2}/2 = V_{\pi/2}/2 = p.r^2.\cot\beta$ and $H_{\pi/2}/2 = 0$

Moment due to vertical force, $M_V = \int_0^\alpha x.dV = \dfrac{2p^3 \cot\beta}{3\sin\beta} \sin^3 \alpha$ (5.13)

Moment due to horizontal force, $M_H = \int_0^\alpha y.dH = p r^3 \cos\beta \sin\alpha(1-\dfrac{2}{3}\sin^2\alpha)$ (5.14)

Total moment, $M = M_V + M_H = p r^3 \cos\beta \sin\alpha \, (1 + 2/3 \sin^2\alpha \, \cot^2 \beta)$ (5.15)

$$l = \dfrac{M}{R} = r.\sin\beta \dfrac{1+(2/3)\cot^2 \beta \, \sin^2 \alpha}{\sqrt{\sin^2 \alpha + \cos^2 \alpha \, \sin^2 \beta}} \qquad (5.16)$$

l = Normal distance at which the resultant is acting from O.

is given by $\tan\gamma = \dfrac{V}{H} = \dfrac{\tan\alpha}{\sin\beta} = \dfrac{x}{y}$ (5.17)

γ = angle of resultant 'R' to the X-axis at any place

σ_c = resultant of circumferential stress along the junction of shell and sickle plate vary from $4289.01 kg/cm^2$ at $0°$ to 378.81 or up to 0 kg/cm^2 at $90°$

σ_a = resultant of circumferential stress along the junction of shell and sickle plate vary from 1570.80 kg/cm^2 at $90°$ to 87.28 or up to 0 kg/cm^2 at $0°$

Vertical forces,   V = vary from $4289.01 kg/cm^2$ at $90°$ to 378.81 or up to 0 kg/cm^2 at $0°$

Horizontal forces, H = vary from 906.31 kg/cm^2 at $45°$ to 157.38 or up to 0 kg/cm^2 at $0°$ or $90°$

Resultant forces, R = vary from 0.0 kg/cm^2 at $0°$ to 4298. 01 kg/cm^2 at $90°$

Total moment, M = vary from 0.0 kg-cm at $0°$ to **147399.72** kg-cm at $90°$

Normal distance at which the resultant is acting from point 'O', l and angle of resultant 'R' to the X-axis at any place, γ.

The above calculations are shown in the Table 3.2.

Table 3.2: Calculation of Stresses and Forces and Positions σ_c, σ_a, V, H, R and l, defined as above

α (deg)	R_1	r	σ_c	σ_a	V	H	R	γ	M_V	M_H	M_V+M_H	$l= M/R$
0	2000	2000	4289.01	0.00	0.00	0.00	0.00	0°	0	0	0	0
5	2000	1961	4272.69	87.27	32.58	157.38	160.72	11°41'45"	89.59	3143.60	3233.18	2011.74
10	2000	1925	4223.85	174.53	129.33	309.98	335.87	22°38'50"	708.53	6168.60	6877.13	2047.54
15	2000	1890	4142.87	261.80	287.31	453.15	536.56	32°22'32"	2346.05	8963.77	11309.82	2107.84
20	2000	1857	4030.35	349.07	501.72	582.56	768.83	40°44'09"	5413.81	11432.08	16845.89	2191.10
25	2000	1826	3887.17	436.33	766.04	694.27	1033.85	47°48'49"	10213.93	13496.62	23710.54	2293.43
30	2000	1797	3714.39	523.60	1072.25	784.89	1328.82	53°47'45"	16914.45	15105.13	32019.58	2409.62
35	2000	1771	3513.35	610.87	1411.04	851.65	1648.14	58°53'11"	25534.17	16232.91	41767.08	2534.20
40	2000	1747	3285.58	698.13	1772.12	892.54	1984.19	63°16'03"	35937.71	16883.84	52821.55	2662.12
45	2000	1725	3032.79	785.40	2144.51	906.31	2328.15	67°05'25"	47841.30	17089.50	64930.80	2788.94
50	2000	1706	2756.92	872.66	2516.90	892.54	2670.47	70°28'28"	60828.88	16906.47	77735.35	2910.93
55	2000	1688	2460.08	959.93	2877.97	851.65	3001.34	73°33'55"	74377.48	16411.88	90789.36	3024.96
60	2000	1673	2144.51	1047.20	3216.76	784.89	3311.13	76°17'16"	87890.07	15697.71	103587.78	3128.47
65	2000	1661	1812.62	1134.46	3522.97	694.27	3590.73	78°51'05"	100733.76	14864.08	115597.84	3219.34
70	2000	1650	1466.93	1221.73	3787.29	582.56	3831.84	81°15'19"	112280.77	14011.99	126292.76	3295.88
75	2000	1642	1110.08	1309.00	4001.70	453.15	4027.28	83°32'22"	121949.29	13236.15	135185.43	3356.74
80	2000	1637	744.78	1396.26	4159.68	309.98	4171.22	85°44'18"	129241.59	12618.21	141859.80	3400.92
85	2000	1633	373.81	1483.53	4256.43	157.38	4259.34	87°52'57"	133776.74	12221.01	145997.74	3427.71
90	2000	1632	0.00	1570.80	4289.01	0.00	4289.01	90°	135315.62	12084.10	147399.72	3436.68

VARIFICATION OF DESIGN OF PENSTOCK BIFURCATION BY DIFFERENT METHODS

4.1 GENERAL

There are many methods for computation of stresses in penstock bifurcation. Since the penstock bifurcation is very complicated structure, its analytical analysis by conventional method is not sufficient. For its structural stability and reliability, the design must be checked / verified by other available methods such as

1. Finite Element Method
2. Photoelastic Techniques
3. Physical Model Studies using Strain Gauge Technology
4. Hydrostatic Test on Prototype using Strain Gauge Technology

In the present study, following three methods have been adopted for verification of structural design of present penstock bifurcation.

1. Finite Element Method
2. Physical Model Studies using Strain Gauge Technology
3. Hydrostatic Test on Prototype using Strain Gauge Technology

4.2 FINITE ELEMENT METHOD

Finite element method is a numerical analysis technique for obtaining approximate solutions to a wide variety of engineering problems like analyzing structures, which permit the calculations of stresses and deflections. The most distinctive feature of the finite element method that it separates from others in the division of a given domain into a set of simple sub domains called elements. The finite element procedure produces many simultaneous algebraic equations, which are generated and solved on a digital computer. Results are rarely exact. However, processing more equations minimizes errors and results in general are accurate enough from engineering point of view [32,42].

Using such elements the structural idealization is obtained merely by dividing the original continuum into segments, all the material properties of the original system, is retained in the individual elements. Instead of solving the problem for entire body in one operation, the

solutions are formulated at each constituent unit and combined to obtain the solution for the original structure.

4.2.1   Brief Description of Finite Element Method

4.2.1.1   Discritization of Continuum

The continuum is the physical body structure, or solid being analyzed. Discritization may be described as the process in which the given body is subdivided into an equivalent system of finite elements. One must decide what number size, and arrangements of finite elements will give an effective representation of the given continuum for the particular problem considered. Continuum is simply zoned into small regions by imaginary planes in 3D bodies and by imaginary lines in 2D bodies. As general guidelines it can be said that where stress or strain gradients are expected to be comparatively flat i.e. the variation is not rapid, the mesh can be coarse to reduce the computation, where as zones in which stress or strain gradients are expected to be steep a finer mesh is considered to get more accurate results. Theoretically speaking to get an exact solution the number of nodal points is infinite. So trade off has to be made between computation effort and corresponding accuracy. It may be noted that the continuum is simply zoned into small regions of constant span.

4.2.1.2 Selection of Proper Interpolation or Displacement Model

In finite element method we approximate a solution to a complicated problem by subdividing the region of interest into finite number of elements and representing the solution within each element by a relatively simple function of polynomials for ease of computation. The degree of the polynomial chosen depends on the number of nodes assigned to the elements.

For the triangular element the linear polynomial

$$\emptyset = a_1 + a_2x + a_3y \qquad (4.1)$$

is appropriate

Where, a_1, a_2, a_3 are constants which can be expressed in terms of $\emptyset$ at these nodes.

For the four nodded quadrilateral the bilinear function

$$\emptyset = a_1 + a_2x + a_3y + a_4xy \qquad (4.2)$$

is appropriate

Eight-node quadrilateral has eight a_i in its polynomial expansion and can represent a parabolic function.

Equation (4.1) & (4.2) are interpolations of function $\emptyset$ in terms of the position (x, y) within an element. If mesh of element is not too coarse and if $\emptyset_1$ happened to be exact, and then $\emptyset$ would be a good approximation.

4.2.1.3 Convergence Requirements

In any acceptable numerical formulation, the numerical solution must coverage or tends to the exact solution of the problem. For this the criteria is as below.

    a) Displacement model must be continuous within the element and the displacements must be compatible within the adjacent elements.

The first part is automatically satisfied if displacement functions are polynomials. The second part implies that the adjacent elements must deform without causing openings, overlaps or discontinuities between them. This can be satisfied if displacements along the side of an element depend only upon displacements of the nodes occurring on that side. Since the displacements of nodes on common boundary will be same, displacement for boundary line for both elements will be identical.

    b) The displacement model must include rigid body displacement of the element.

Basically this condition states that there should exist such combinations of values of coefficients in displacement function that cause all points in the elements to experience the same displacement.

    c) The displacement model must include the constant strain states of elements.

This means that there should exist such combinations of values of the coefficients in the displacement function that cause all points on the element to experience the same strain. The necessity of this requirement can be understood if we imagine that the continuum is divided into infinitesimally small elements. In such a case the strains in each element approach constant values all over the element. The terms a_3 and a_6 in the following equations provide for uniform strain in x and y directions.

$$u(x) = a_1 + a_2x + a_3y$$

$$v(y) = a_4 + a_5x + a_6y$$

$$(4.3)$$

The elements, which meet first criterion, are called compatible or conforming. The elements, which meet second and third criteria, are called complete. For plain strain and plain stress and 3 D elasticity. the three conditions mentioned above are easily satisfied by linear polynomials.

4.2.1.4 Nodal Degree of Freedom

The nodal displacements, rotations and / or strains necessary to specify completely the deformation of finite elements are called degrees of freedom (DOF) of elements.

4.2.1.5 Element Stiffness Matrix

The equilibrium equation derived from principle of minimum potential energy between nodal loads and nodal displacements is expressed as

$$\{F\}^e = [K]^e \{\delta\}^e$$

Where
$$\{F\}^e = \text{nodal force vector}$$
$$\{\delta\}^e = \text{nodal displacement vector}$$
$$[K]^e = \text{element stiffness matrix}$$

The stiffness matrix consists of the coefficients of equilibrium equations derived from material and geometric properties of the element. The elements of stiffness matrix are the influence coefficient. Stiffness of a structure is an influence coefficient that gives the force at one point on a structure associated with a unit displacement at the same or a different point.

Local material properties as stated above are one of the factions, which determine stiffness matrix. For an elastic isotopic body, Modulus of Elasticity (E) and Poisson's ratio (v) define the local material properties. The stiffness matrix is essentially symmetric matrix, which follows from the principle of stationery potential energy, that "In an elastic structure work done by internal forces is equal in magnitude to the change in strain energy". And also from Maxwell Betti reciprocal theorem which states that : " If two set of loads $\{F\}_1$ and $\{F\}_2$ act on

a structure, work done by the first set in acting through displacements caused by the second set is equal to the work done by second set in action through displacements caused by first set.

4.2.1.6 Nodal Forces and Loads

Generally when subdividing a structure we select nodal locations that coincide with the locations of the concentrated external forces. In case of distributed loading over the body such as water pressure on dam or the gravity forces the loads acting over an element are distributed to the nodes of that element by principle of minimum potential energy. If the body forces are due to gravity only then they are equally distributed among the three nodes of a triangular element

4.2.1.7 Assembly of Algebraic Equations for the Overall Discretised Continuum

This process includes the assembly of overall or global stiffness matrix for the entire body from individual stiffness matrices of the elements and the overall or global force or load vectors. In general the basis for an assembly method is that the nodal interconnections require the displacement at a node to be the same for all elements adjacent to that node. The overall equilibrium relations between global stiffness matrix [K], the total load vector {F} and the nodal displacement vector for entire body {δ } is expressed by a set of simultaneous equations.

$$[K] \{\delta\} = \{F\}$$

The global stiffness matrix [K] will be banded and also symmetric of n x n where, n = total number of nodal points in the entire body. The steps involved in generation of global stiffness are:

i) All elements of global stiffness matrix [K] are assumed to be equal to zero

ii) Individual element stiffness matrices [K] are determined successively

iii) The element K_{ij} of element stiffness matrix are directed to the address of element K_{ij} of global stiffness matrix which means

$$K_{ij} = \Sigma K_{ij}$$

Similarly nodal load $\{F_i\}^e$ at a ' i' node of an element ' e' is directed to the address of $\{F_i\}$ total load vector i.e.

$$\{F_i\} = \Sigma\{F_i\}^e$$

4.2.1.8 Boundary Conditions

A problem in solid mechanics is not completely specified unless boundary conditions are prescribed. Boundary conditions arise from the fact that at certain points or near the edges the displacements are prescribed. The physical significance of this is that a loaded body or a structure is free to experience unlimited rigid body motion unless some supports or kinematics constraints are imposed that will ensure the equilibrium of the loads. These constraints are called boundary conditions. There are two basic types of boundary conditions, geometric and natural. One of the principal advantages of Finite Element Method is, we need to specify only geometric boundary conditions, and the natural boundary conditions are implicitly satisfied in the solution procedure as long as we employ a suitable valid variational principle. In other numerical methods, solutions are to be obtained by trial and error method to satisfy boundary conditions whereas in Finite Element Method boundary conditions are inserted prior to solving algebraic equations and the solution is obtained directly without requiring any trial.

4.2.1.9 Solution for the Unknown Displacements

The algebraic equations [K] {δ} = {F} formed are solved for unknown displacements {δ} wherein [K] and {F} are already determined. The equations can be solved either by iterative of elimination procedure. Once the nodal displacements are found, then element stains or stresses can be easily found from generalized Hooke's law for a linear isotropic material.

The assumption in displacements function, the stresses or strains are constant at all points over the element, may cause discontinuities at the boundaries of adjacent elements. To avoid this sometimes it is assumed the values of stresses and strains obtained are for the centers of gravity of the elements and linear variation is assumed to calculate them at other points in the body.

4.2.2 SUMMARY OF PROCEDURE

The principal computational steps of linear static stress analysis by Finite Element method are now listed.

i) **Input and Initialization:** Input the number of nodes and elements, nodal coordinates, structure node numbers of each element, material properties, temperature changes, mechanical loads and boundary conditions. Reserve storage space for structure arrays [K]and {F}. Initialize [K] and {F} to null arrays. If array ID is used to manage boundary conditions, initialize ID and then convert it to a table equation numbers.

ii) **Compute Element Properties:** For each element compute element property matrix [K] and {F} element load vector.

iii) **Assemble the Structure:** Add [k] into [K] and {f} into {F}. Go back to step 2, repeat steps 2 and 3 until all elements are assembled. Add external loads {P} to {f} Impose displacement boundary conditions (if not imposed implicitly during assembly by use of array ID).

iv) **Solve the equations:** $[K]\{\delta\} = \{F\}$ for $\{\delta\}$

v) **Stress Calculation:** For each element extract nodal DOF of element $\{\delta\}^e$ from nodal D O F of structure $\{\delta\}$. Compute mechanical strains, if any and convert resultant strains to stresses.

4.2.3 STRESS ANALYSIS OF PENSTOCK BIFURCATION BY FINITE ELEMENT METHOD

A mathematical model was prepared by finite element method by taking 4000 mm diameter of header pipe and 3000 mm diameter of branch pipes both having thickness of 50 mm and with internal sickle plate of 100 mm thickness. The angle of bifurcation is 25° and angle of reducer is 6°. General purpose Finite Element software I-DEAS is used for the stress analysis of penstock bifurcation [29]. The typical mathematical model is having a large number of nodes 19738 and 58294 solid linear tetrahedron elements. The solid model and its discretisation for finite element analysis are shown Fig. 4.1 and Fig. 4.2. The Internal hydrostatic pressure of the order of 50 kg/cm^2 and suitable boundary conditions are applied on the model is shown Fig. 4.3 and Fig. 4.4. The Cylindrical / conical part of penstock bifurcation model is restricted to elongate in the direction of pipe length (i.e. in the direction of streamline) and allowed to expand in diametrical direction, where as the sickle part is allowed to expand /elongate in all direction. Rotational movement is totally restricted on the model. A total internal pressure of 50 kg/cm^2 (i. e. 0.5 kg/mm^2) is applied on the model is shown in Fig. 4.3. Fig. 4.5 shows the boundary conditions and applied hydrostatic pressure applied on the model.
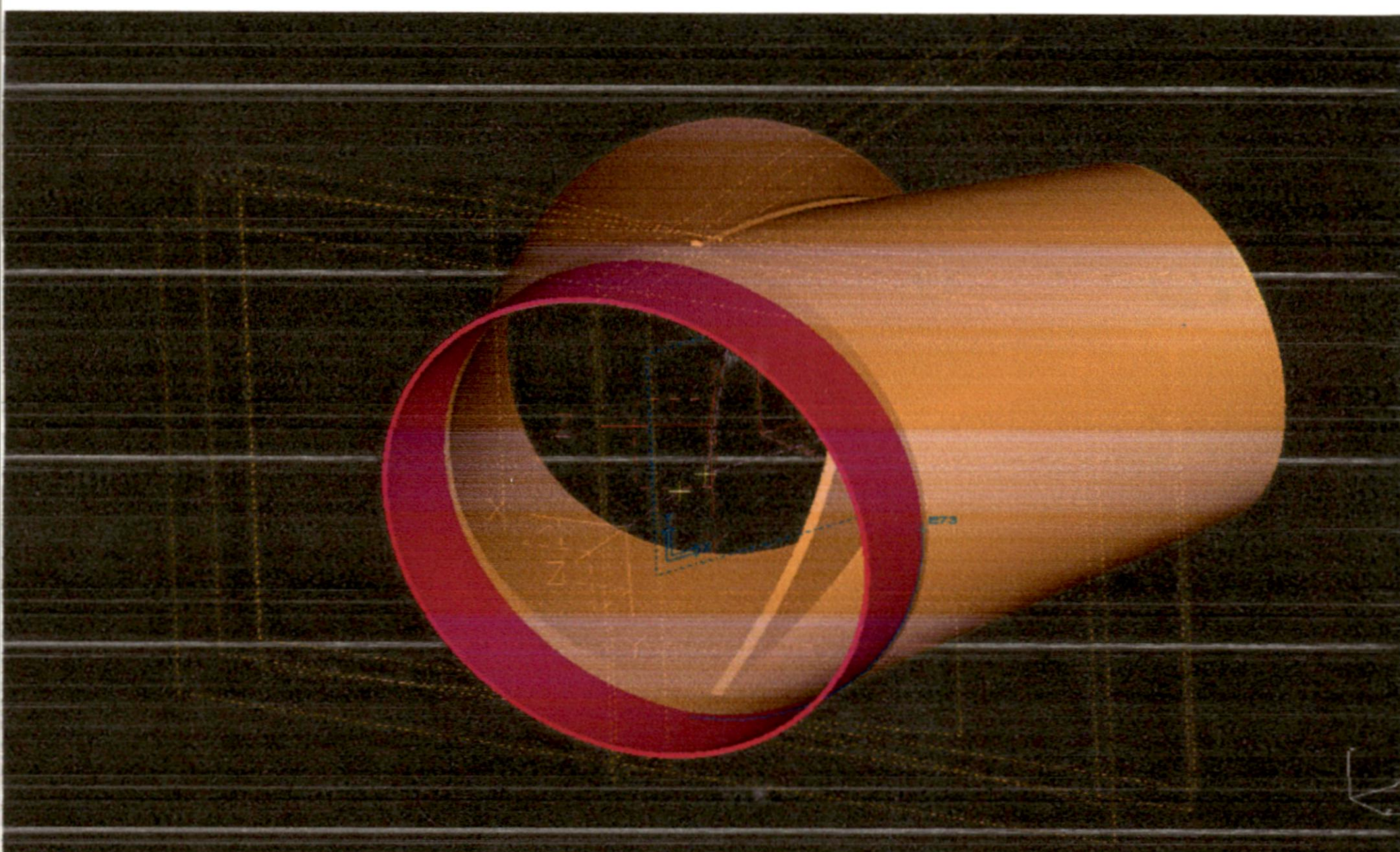
Fig. 4.1: General View of Penstock Bifurcation
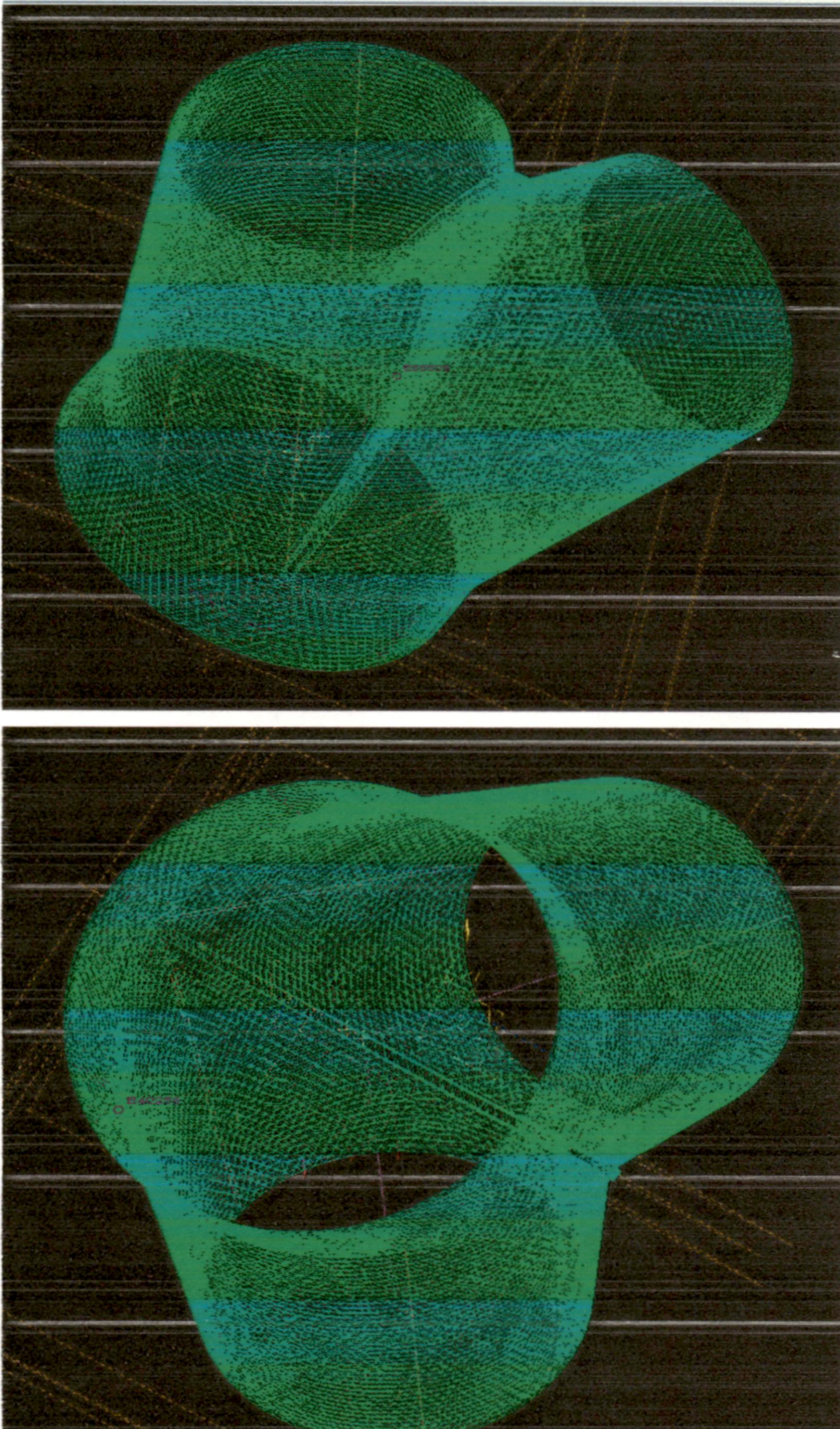
Fig. 4.2: Different Views of Mathematical Model of Penstock Bifurcation using Finite Element Method
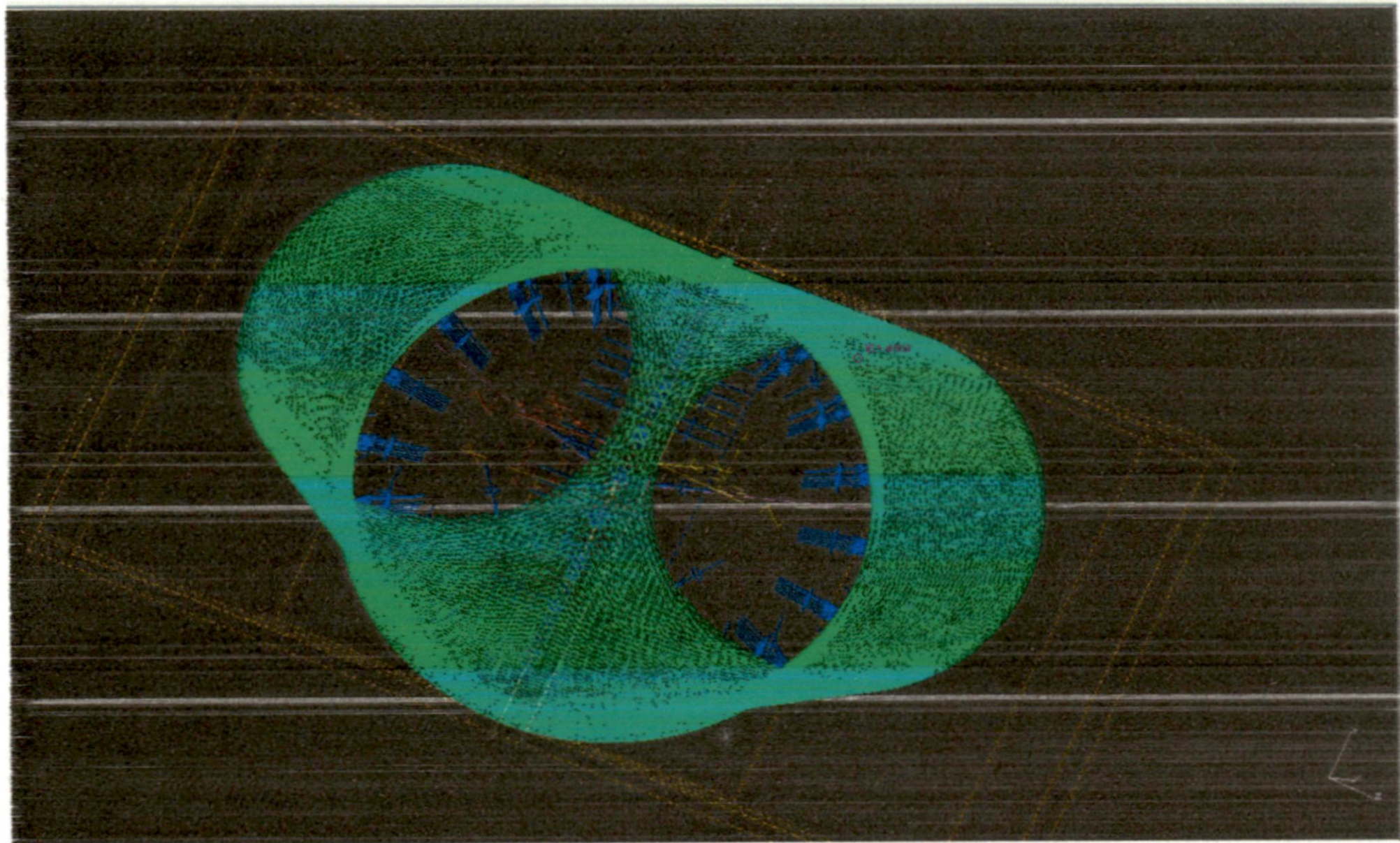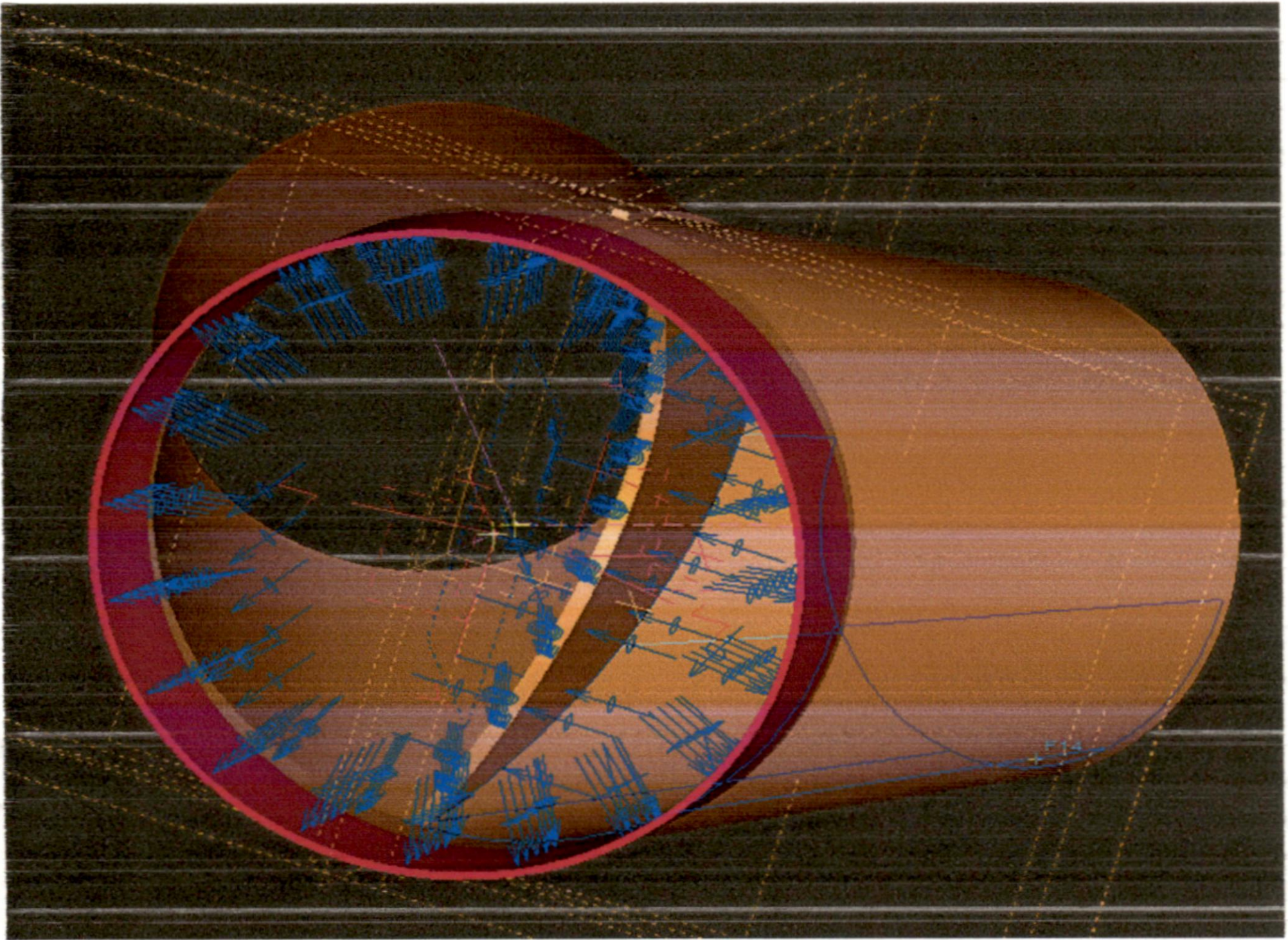
Fig. 4.3: Internal Hydrostatic Pressure acting on Penstock Bifurcation Model
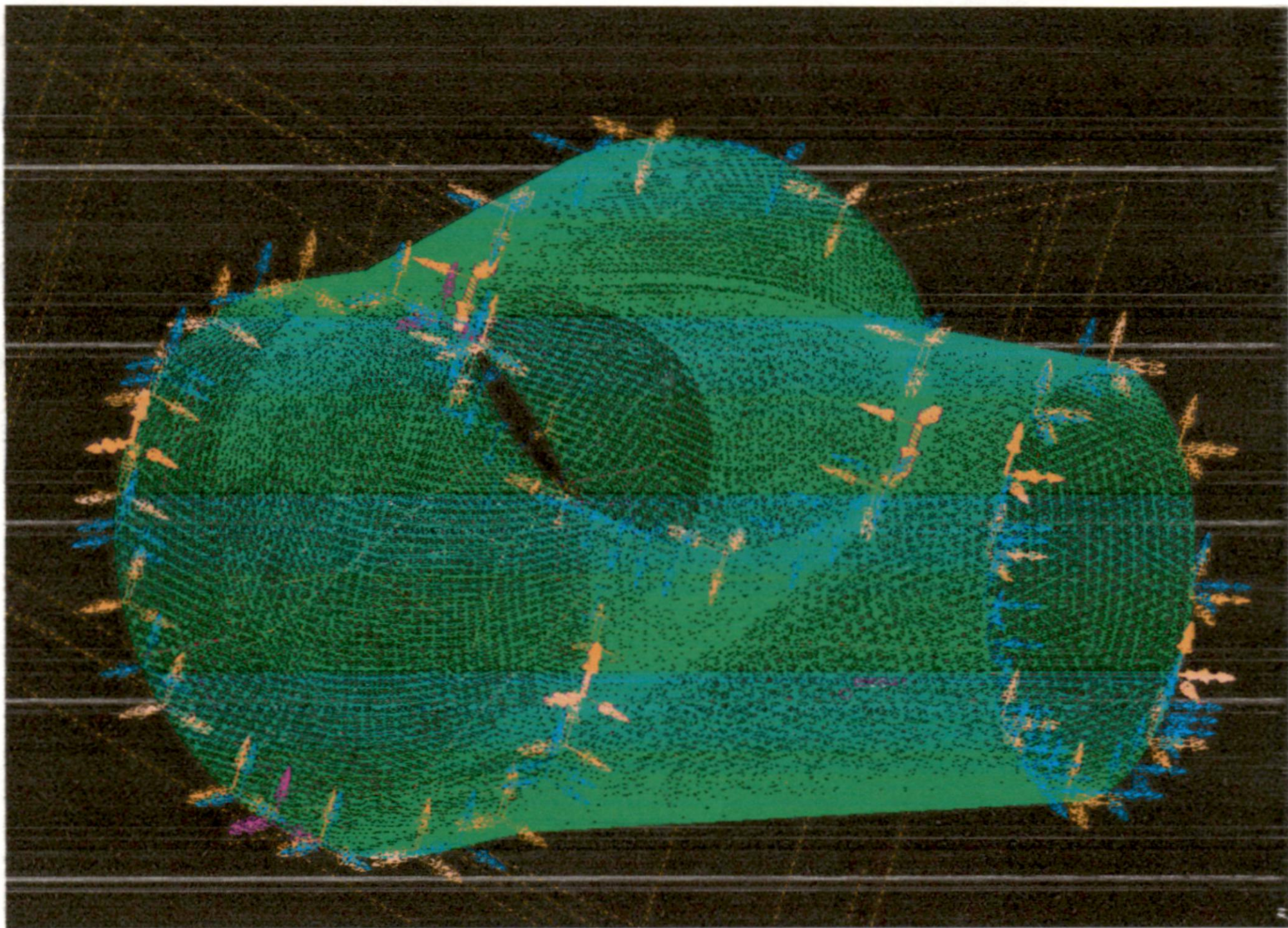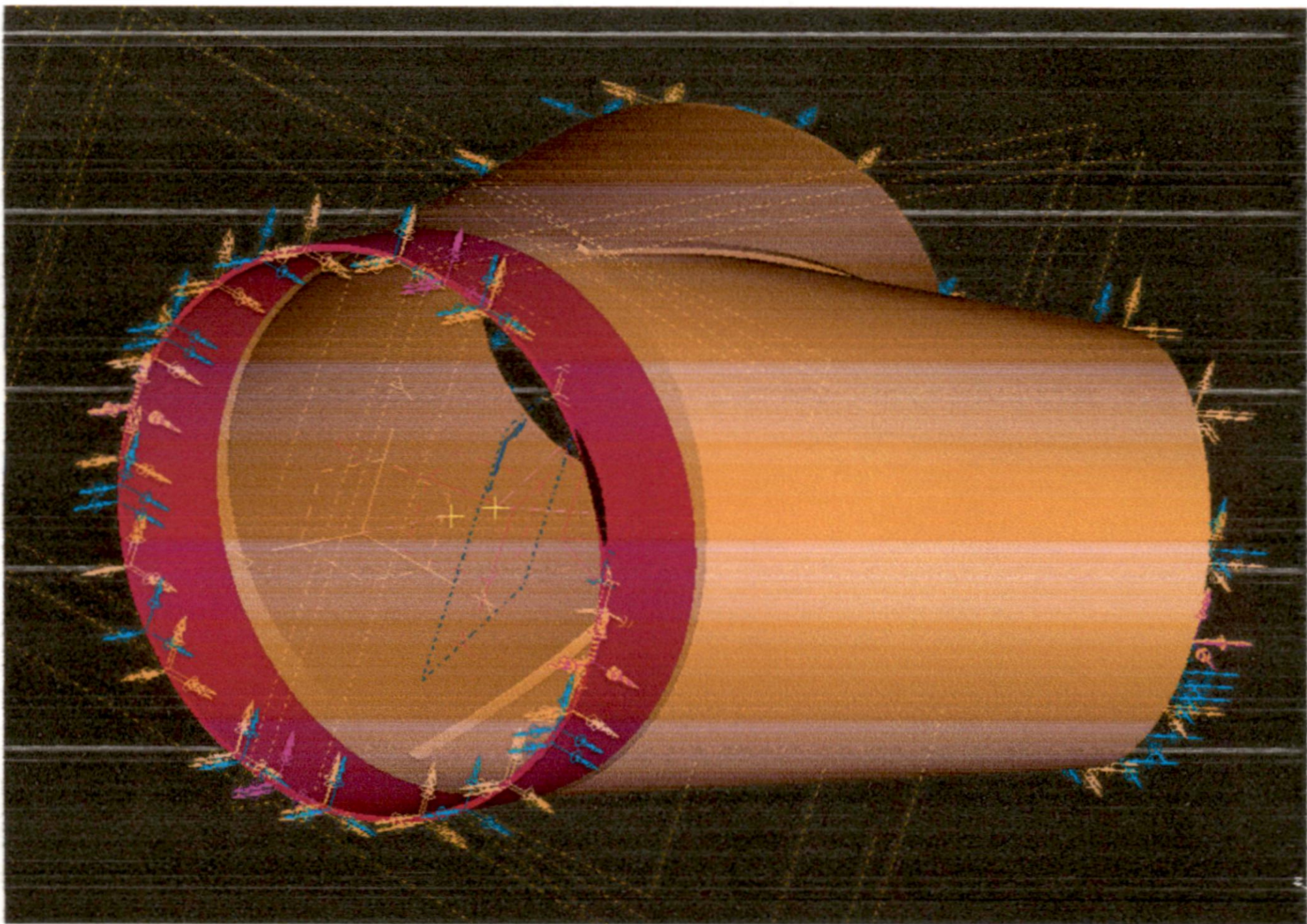
Fig. 4.4: Boundary Conditions applied on Penstock Bifurcation Model
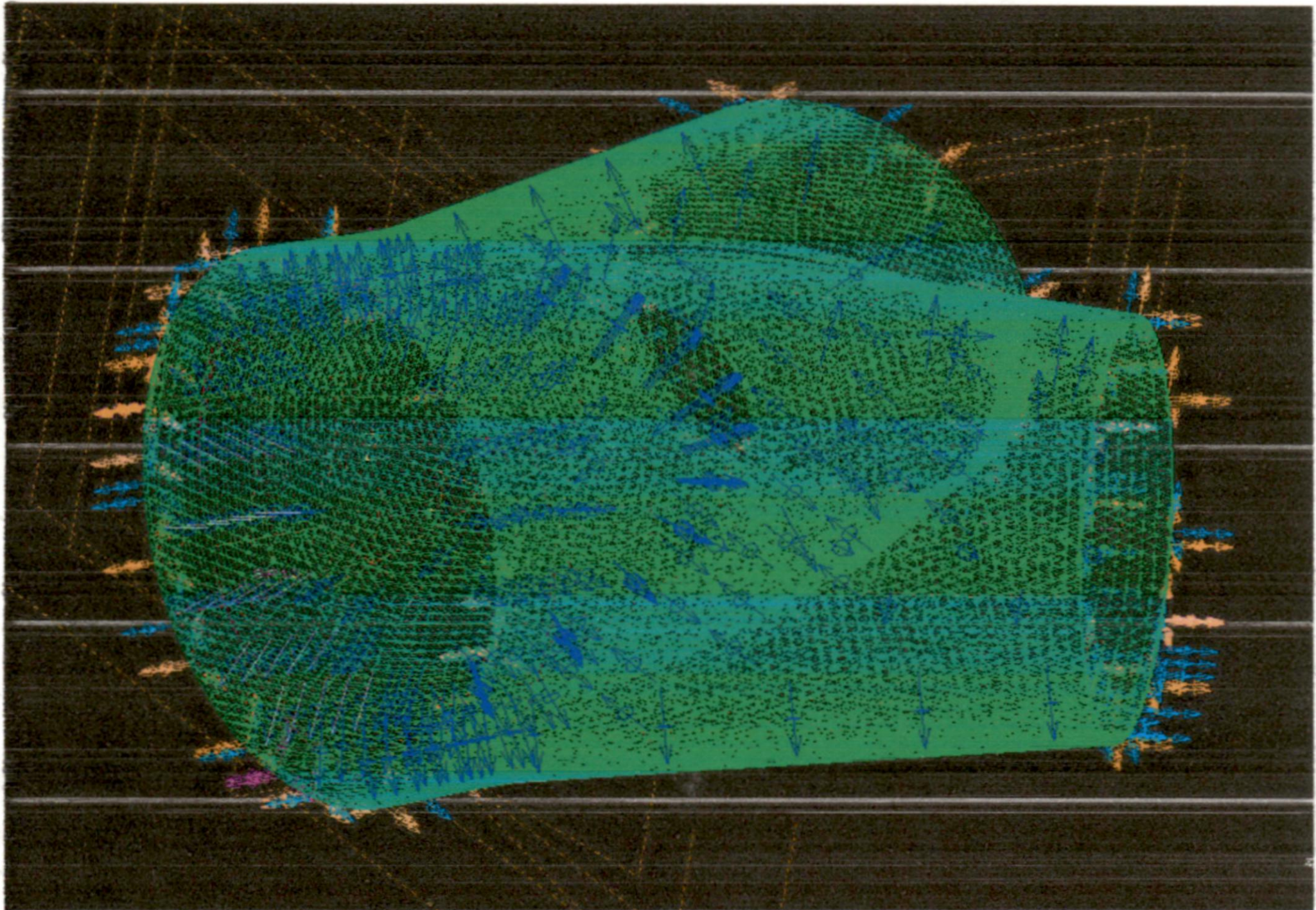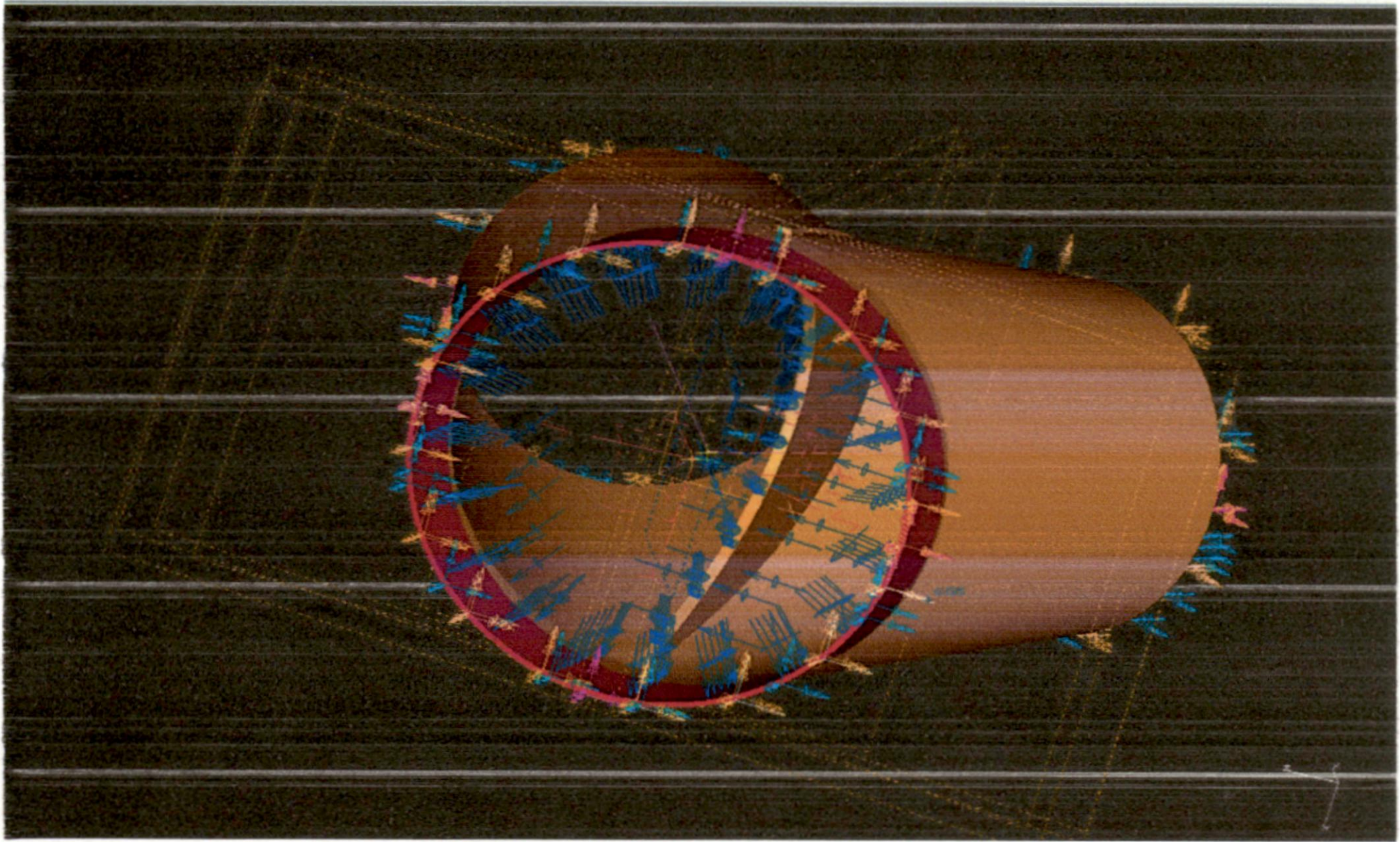
Fig. 4.5: Boundary Conditions as well as Internal Pressure applied on Penstock Bifurcation Model

4.2.4 RESULT OF FINITE ELEMENT ANALYSIS

The stresses evaluated in penstock bifurcation by the finite element method using I-DEAS software are within the permissible limits and varying from a maximum stress of order of 3780 kg/cm^2 to 998 kg/cm^2. The stress found in the header pipe are varying from 3250 kg/cm^2 to 590 kg/cm^2 .whereas the stresses found in front-middle face along central line of sickle plate facing water flow are of higher of 3840 kg/cm^2 to 729.4 kg/cm^2.

The maximum stress in the sickle plate is of order of 3840 kg/cm^2 whereas the maximum stresses at the bend of the penstock near the junction of cylindrical and conical part (i.e. junction of main pipe and branch pipe) of wye is of order of 3250 kg/cm^2.

The contours of maximum principal stresses in penstock are shown in the Fig. 4.6 and its value varies from 3780 kg/cm^2 to 99.8 kg/cm^2. The contour of maximum principal stresses in header pipe vary from 3250 kg/cm^2 to 590 kg/cm^2 is shown in Fig. 4.7 where as in sickle plate, the maximum principal stresses varies from 3840 kg/cm^2 to 72.94 kg/cm^2 as shown in Fig. 4.8. The contour of minimum principal stresses in penstock part is shown in Fig. 4.9 and from varies 505 kg/cm^2 to -1008 kg/cm^2 and also in sickle plate, it varies from 607 kg/cm^2 to -1380 kg/cm^2 as shown in Fig.4.10. The shear stress found in penstock is of order of 1900 kg/cm^2 to 49.9 kg/cm^2 and in sickle plate, it varies from 2090 kg/cm^2 to 114 kg/cm^2 are is shown Fig. 4.11a, 4.11b, and Fig. 4.12 respectively.

The maximum principal stresses, the minimum principal stresses and shear stresses at some critical parts / locations are elaborated in Fig.4.12, Fig.4.13 and Fig.4.14 respectively and their stress values at some selected nodes having higher order are shown in tabular form in Table 4.1, Table 4.2 and Table 4.3 respectively.
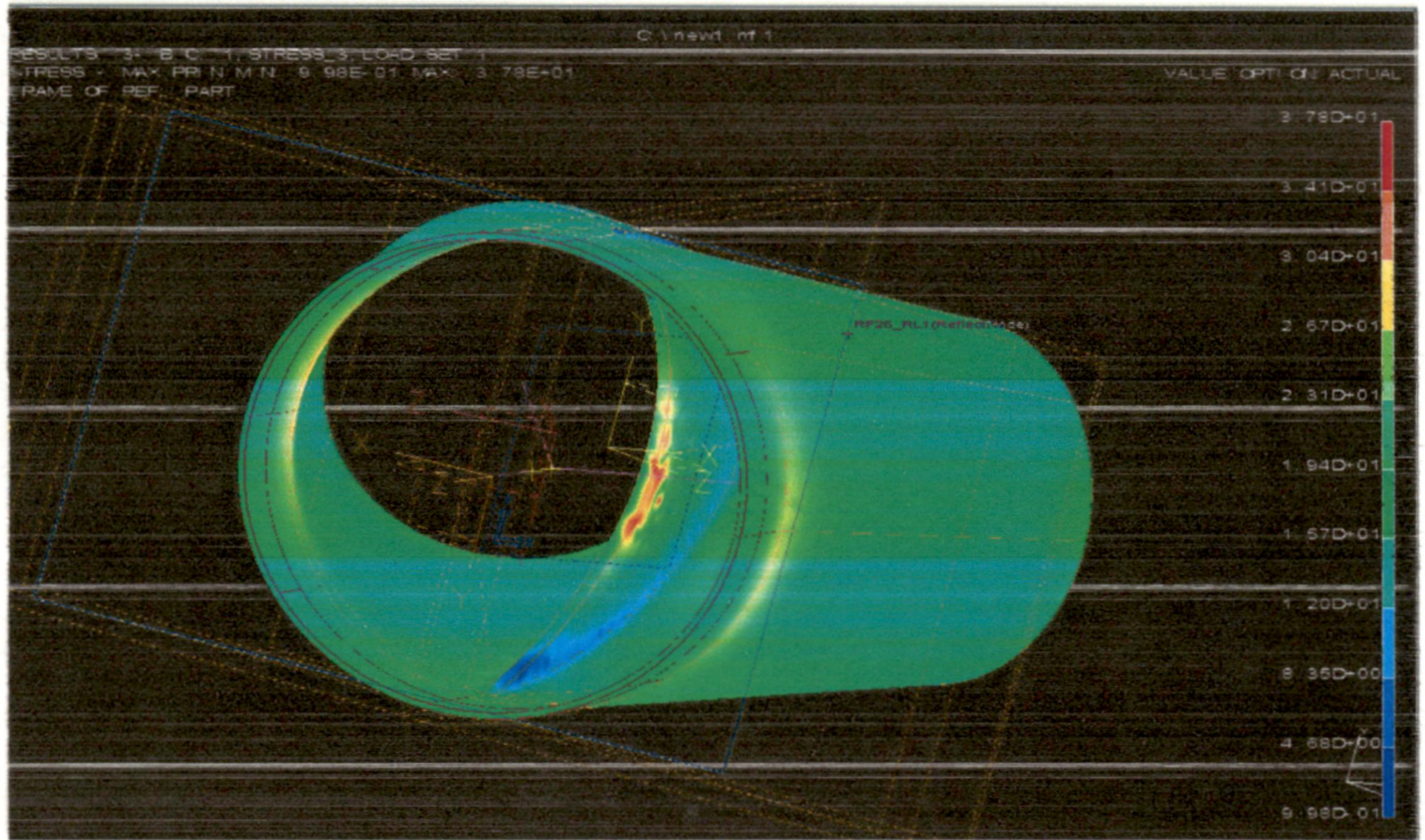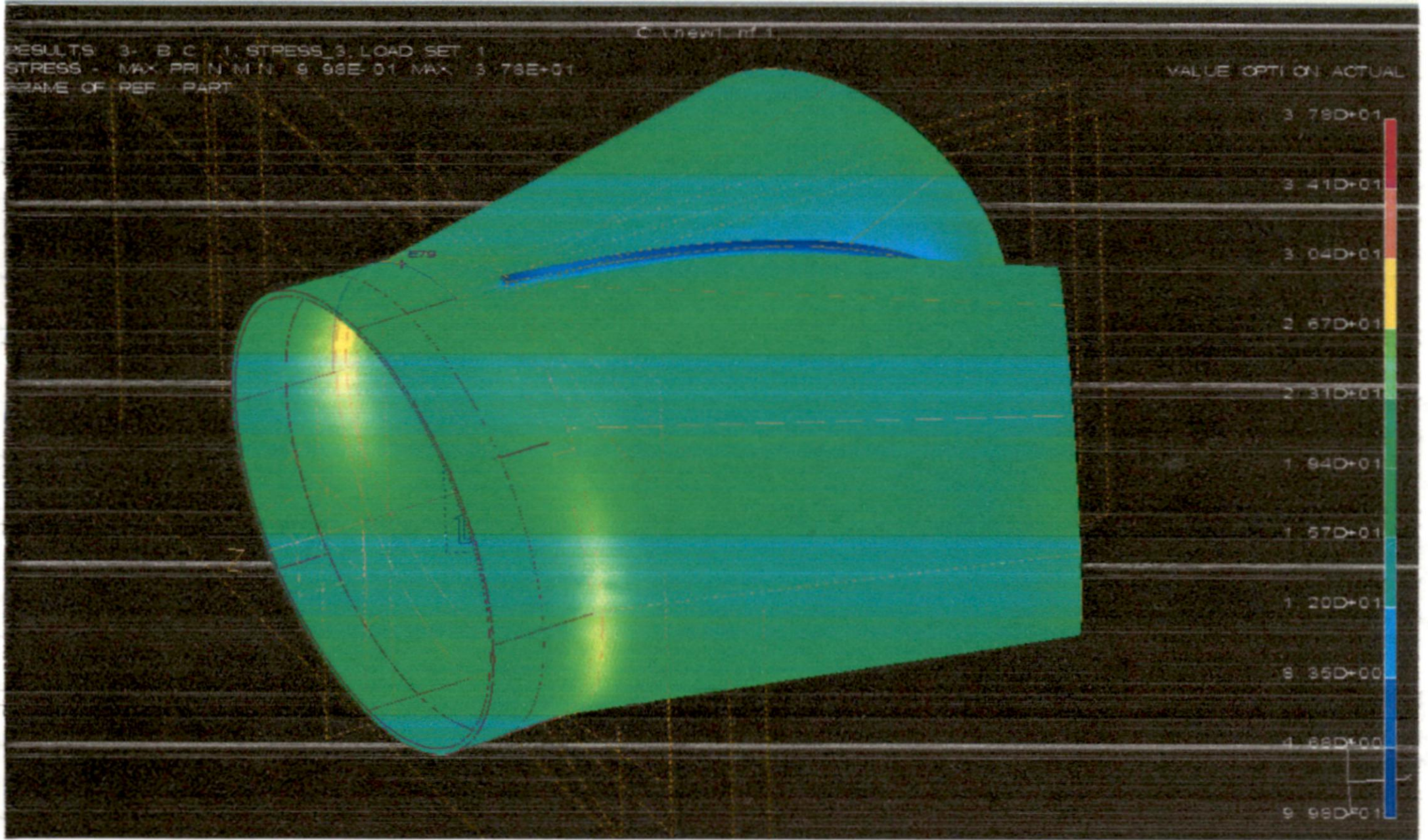
Fig. 4.6: Contours of Maximum Principal Stresses on Penstock Bifurcation Model
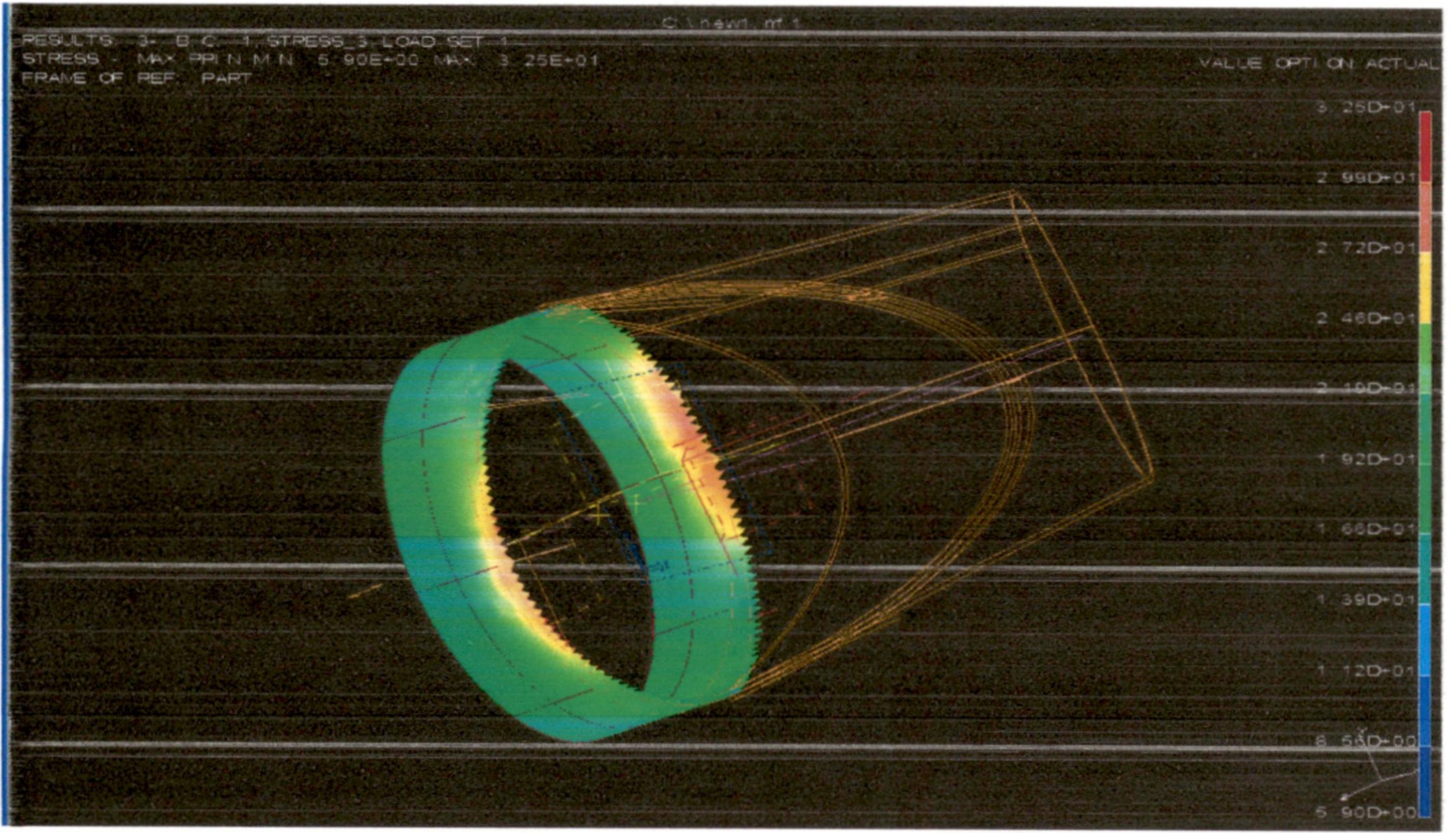
Fig. 4.7: Contours of Maximum Principal Stresses on Header Pipe
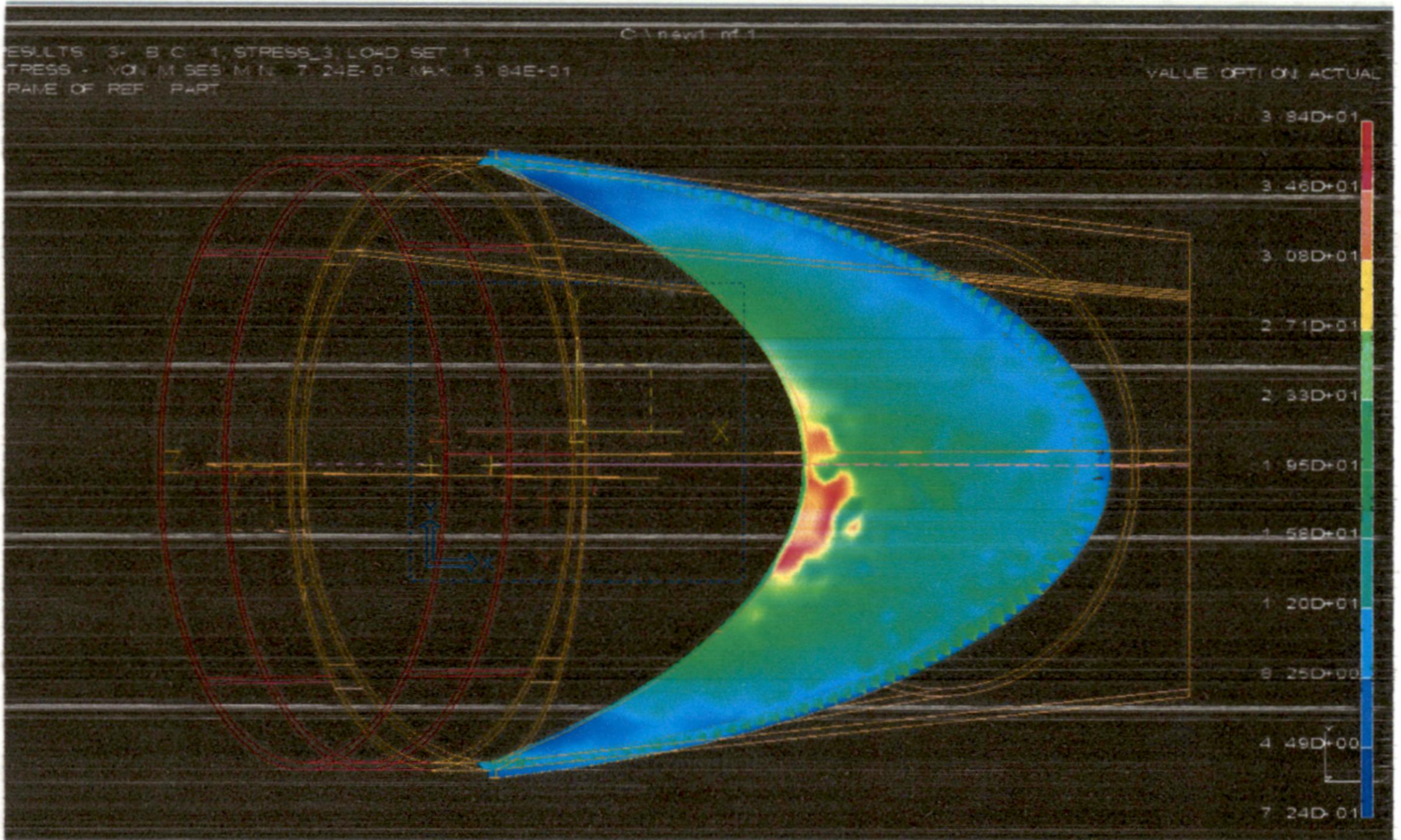
Fig. 4.8: Contours of Maximum Principal Stresses on Sickle Plate
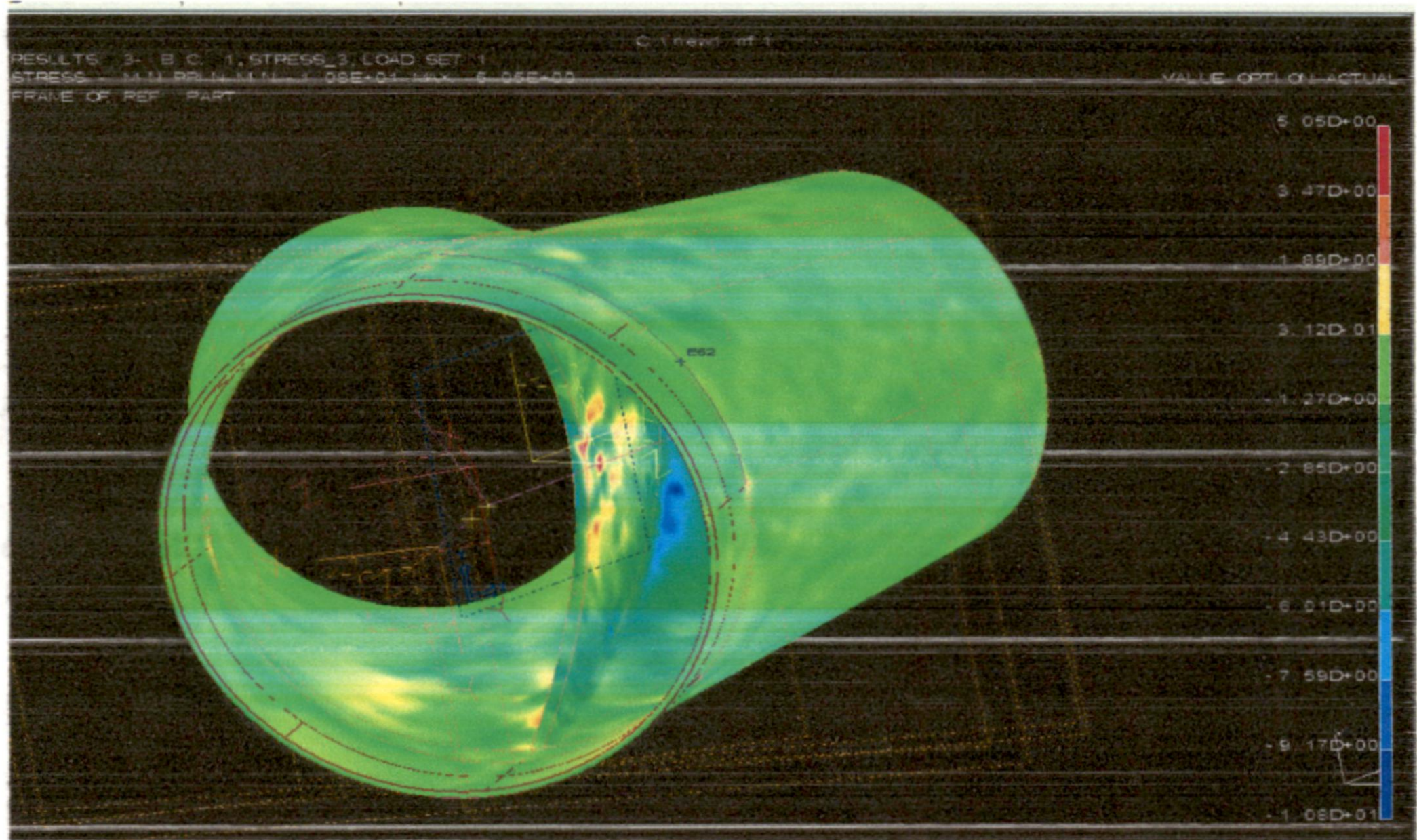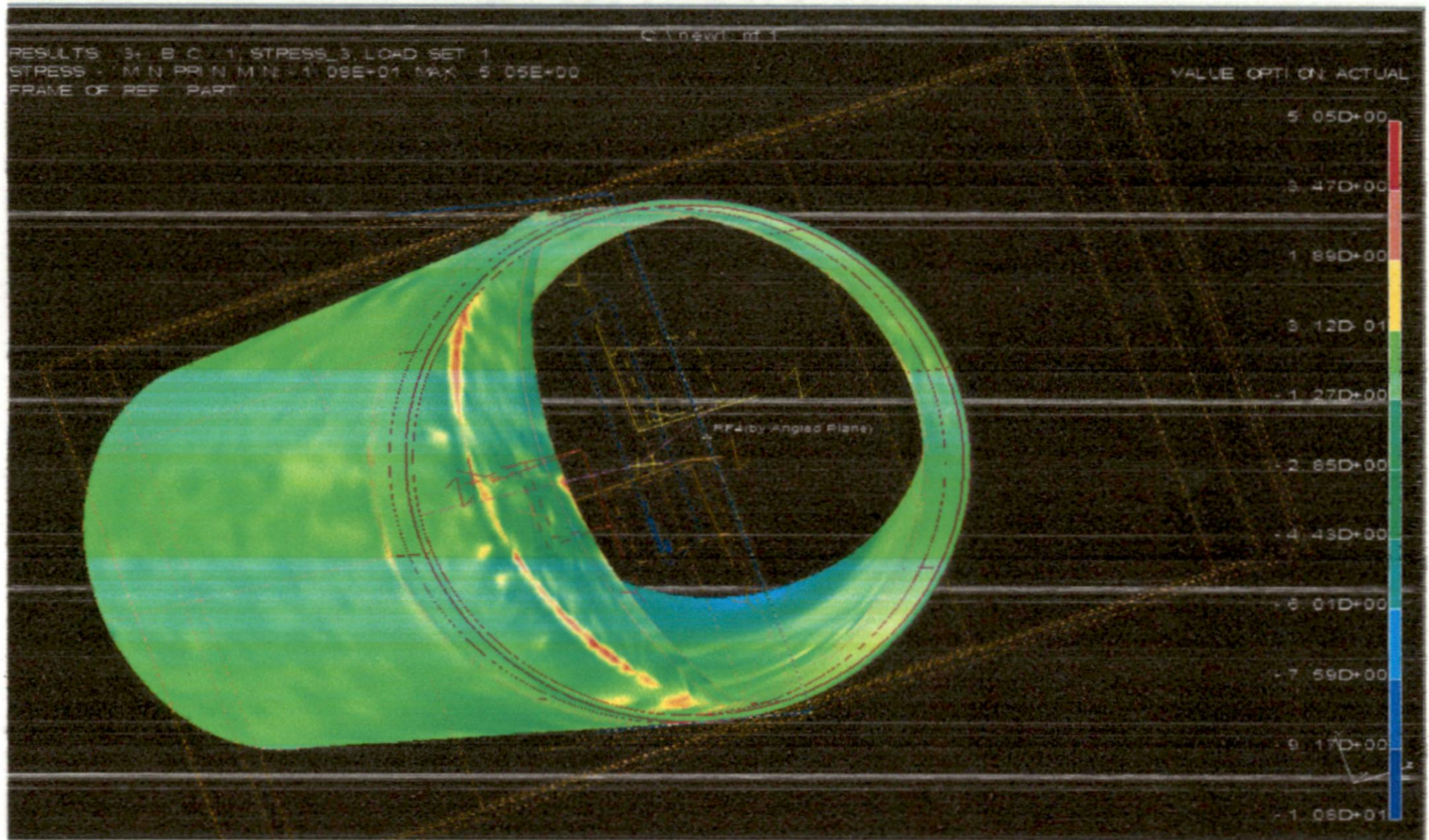
Fig. 4.9: Contours of Minimum Principal Stresses on Penstock Bifurcation
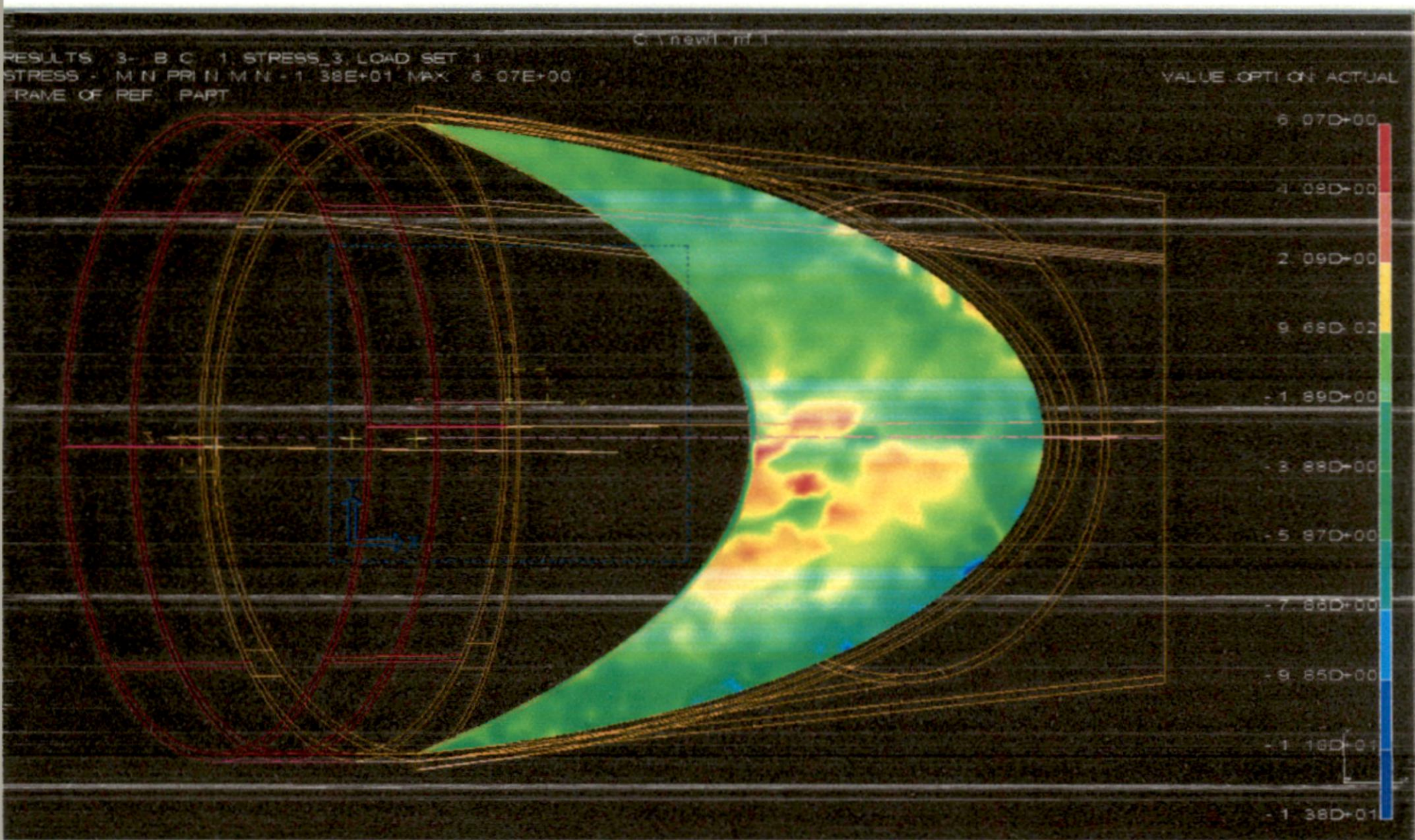
Fig. 4.10: Contours of Minimum Principal Stresses on Sickle Plate
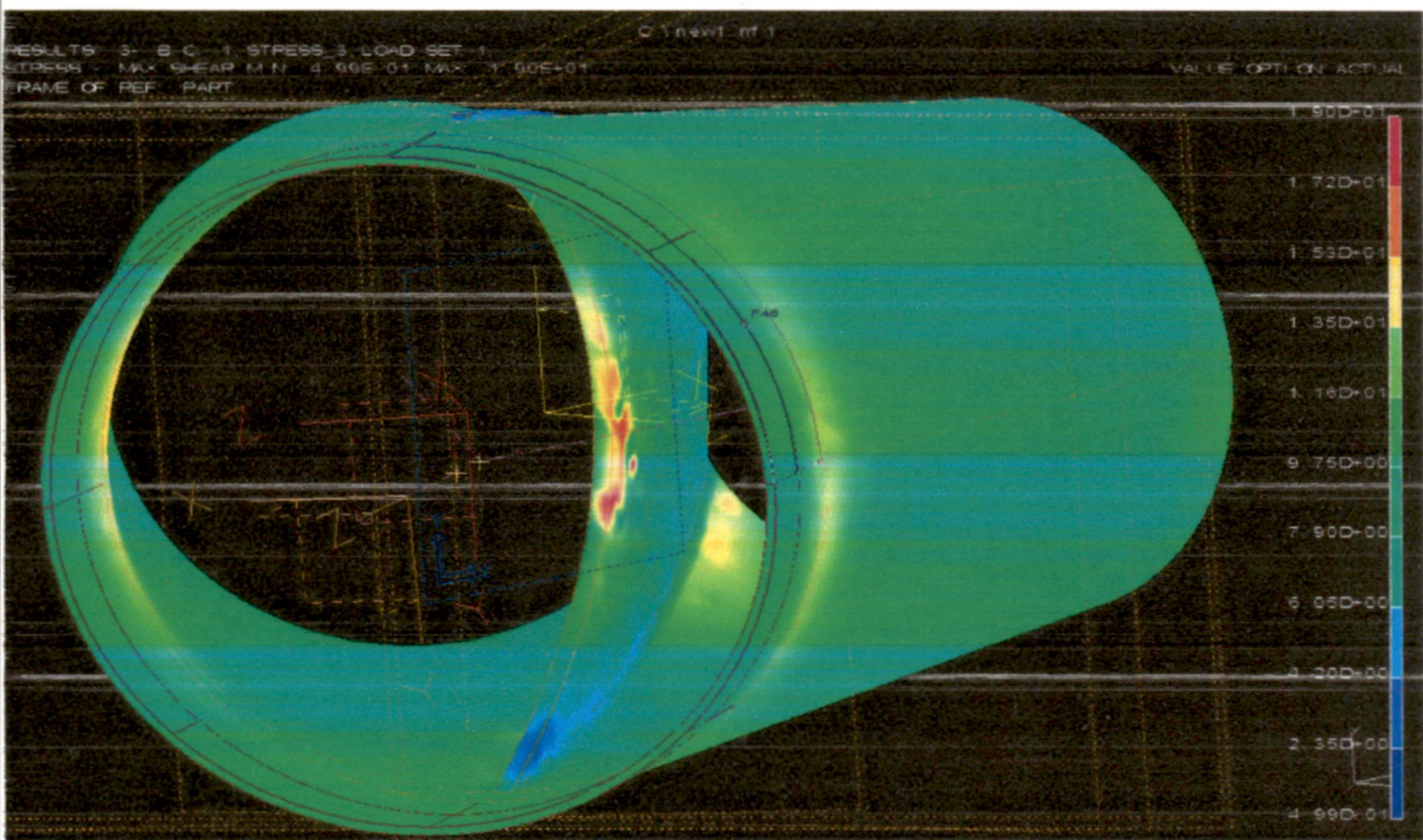
Fig. 4.11a: Contours of Shear Stresses on Penstock Bifurcation Model
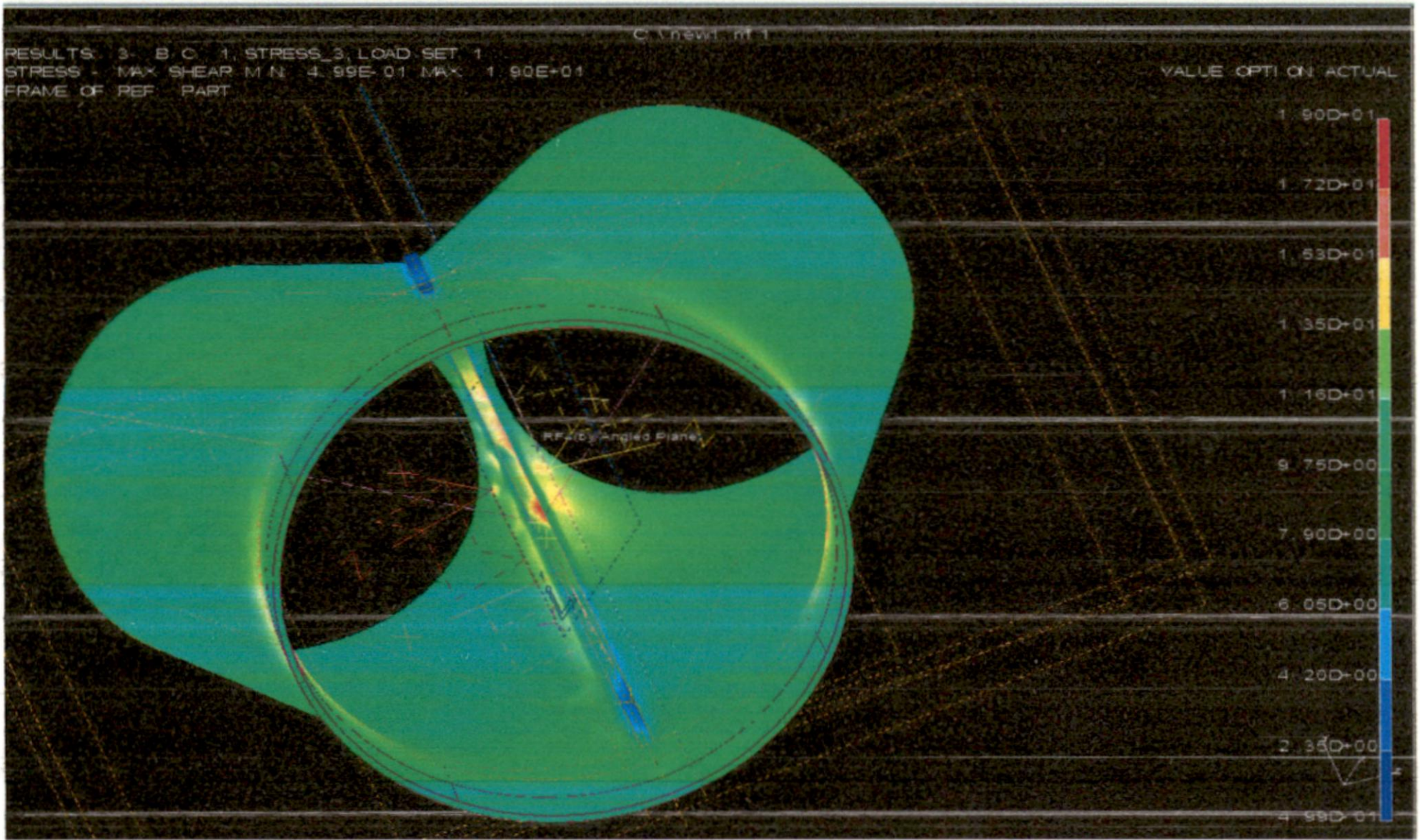
Fig. 4.11b: Contours of Shear Stresses on Penstock Bifurcation Model
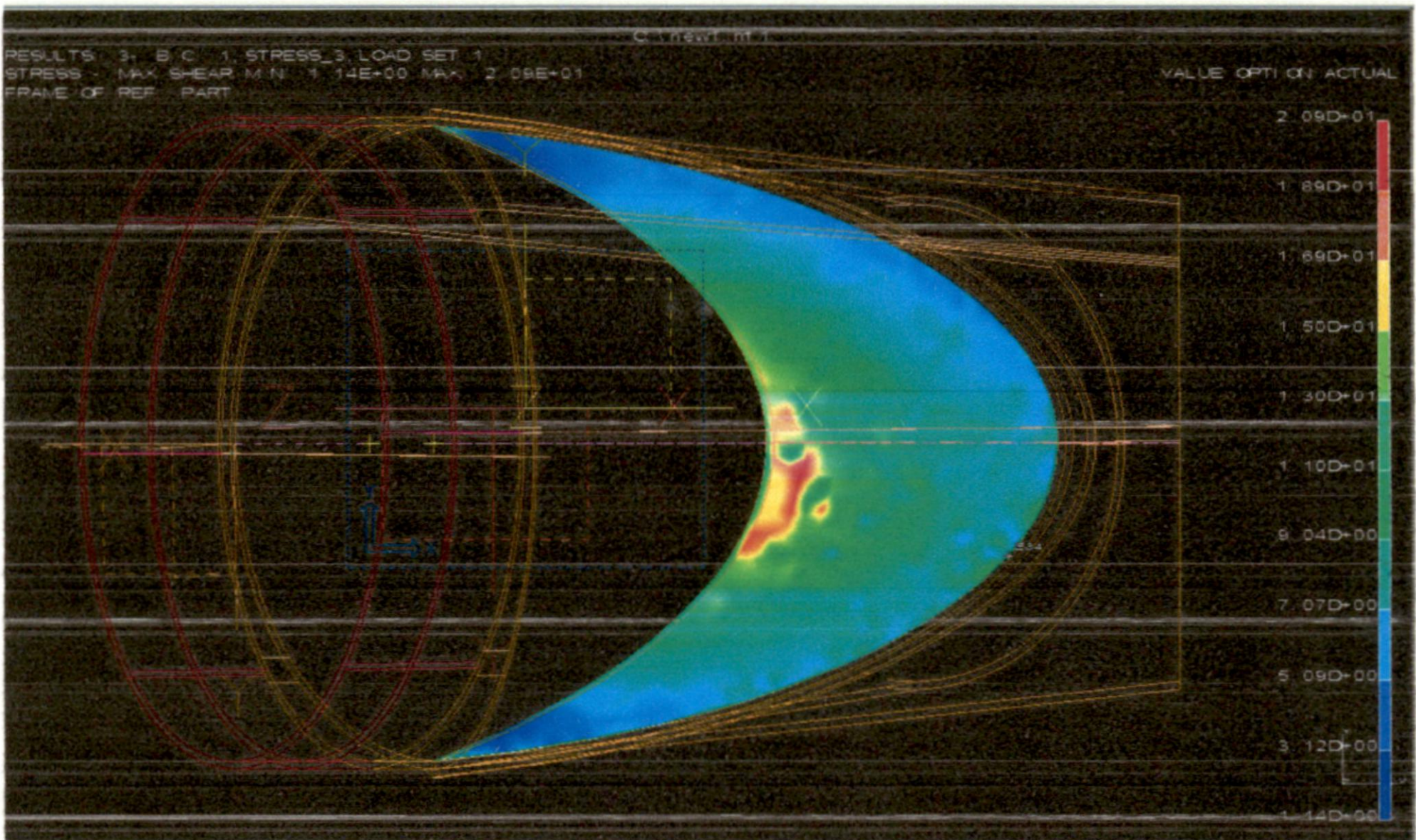
Fig. 4.12: Contours of Shear Stresses on Sickle Plate

Fig. 4.13: Maximum Principal Stresses showing Higher Order Values at the Selected Position at Bend-1

The maximum principal stresses at bend-1 showing higher order values are given in Table 4.1 is as below:

Table 4.1: Maximum Principal Stresses at Bend-1

S. No.	Node No.	Stress Kg/cm²	S. No.	Node No.	Stress Kg/cm²	S. No.	Node No.	Stress Kg/cm²
1	887	2882.37	41	8831	2827.94	81	10071	2765.90
2	885	2920.27	42	9975	2732.08	82	10194	2815.32
3	1019	2737.10	43	9448	2721.58	83	8842	2589.59
4	883	2942.33	44	9446	2806.15	84	8841	2626.15
5	8866	2714.39	45	8863	2800.41	85	8873	2448.77
6	8865	2733.15	46	1023	2780.56	86	9485	2533.32
7	881	2947.75	47	9963	2732.27	87	8872	2451.01
8	8864	2751.28	48	881	2947.75	88	9483	2568.19
9	879	2953.80	49	8864	2751.28	89	9952	2351.01
10	887	2882.37	50	881	2947.75	90	9947	2375.72
11	889	2848.20	51	8864	2751.28	91	9948	2250.11
12	891	2825.81	52	1023	2780.56	92	9944	2270.92
13	8869	2614.98	53	8865	2733.15	93	901	2509.96
14	8868	2634.40	54	883	2942.33	94	1012	2466.74
15	8867	2684.87	55	8865	2733.15	95	899	2594.11
16	885	2920.27	56	8866	2714.39	96	10728	2524.33
17	1020	2786.18	57	8835	2835.65	97	1013	2523.16

18	8869	2614.98	58	9447	2605.97	98	10834	2420.04
19	3369	2678.54	59	9451	2706.53	99	10726	2592.03
20	1017	2656.32	60	9468	2729.74	100	8875	2343.47
21	8870	2575.85	61	9466	2708.81	101	10831	2477.85
22	8838	2773.13	62	10015	2534.85	102	8874	2376.34
23	9932	2454.52	63	9467	2677.13	103	9467	2677.13
24	8839	2745.90	64	10017	2491.56	104	9466	2708.81
25	893	2790.25	65	9467	2677.13	105	9464	2578.97
26	1016	2640.98	66	10013	2363.95	106	10015	2534.85
27	8870	2575.85	67	10020	2236.18	107	9463	2601.91
28	8832	2849.98	68	9463	2601.91	108	10013	2363.95
29	8863	2800.41	69	9955	2505.91	109	9469	2472.95
30	875	2867.57	70	8675	2684.16	110	10020	2236.18
31	1025	2814.35	71	10193	2752.68	111	9408	2556.07
32	37	2856.43	72	10065	2784.65	112	9427	2416.20
33	10068	2873.32	73	10072	2738.80	113	9430	2425.03
34	10069	2812.08	74	10064	2749.46	114	9965	2246.97
35	10067	2842.38	75	10073	2723.32	115	9992	2235.65
36	10195	2817.88	76	10286	2575.60	116	9991	2120.03
37	10291	2696.60	77	20413	2457.51	117	8941	2520.40
38	19934	2679.59	78	19974	2589.75	118	9410	2519.87
39	8940	2691.59	79	20407	2403.89	119	8970	2386.04
40	8971	2571.87	80	10066	2812.06	120	8942	2414.99
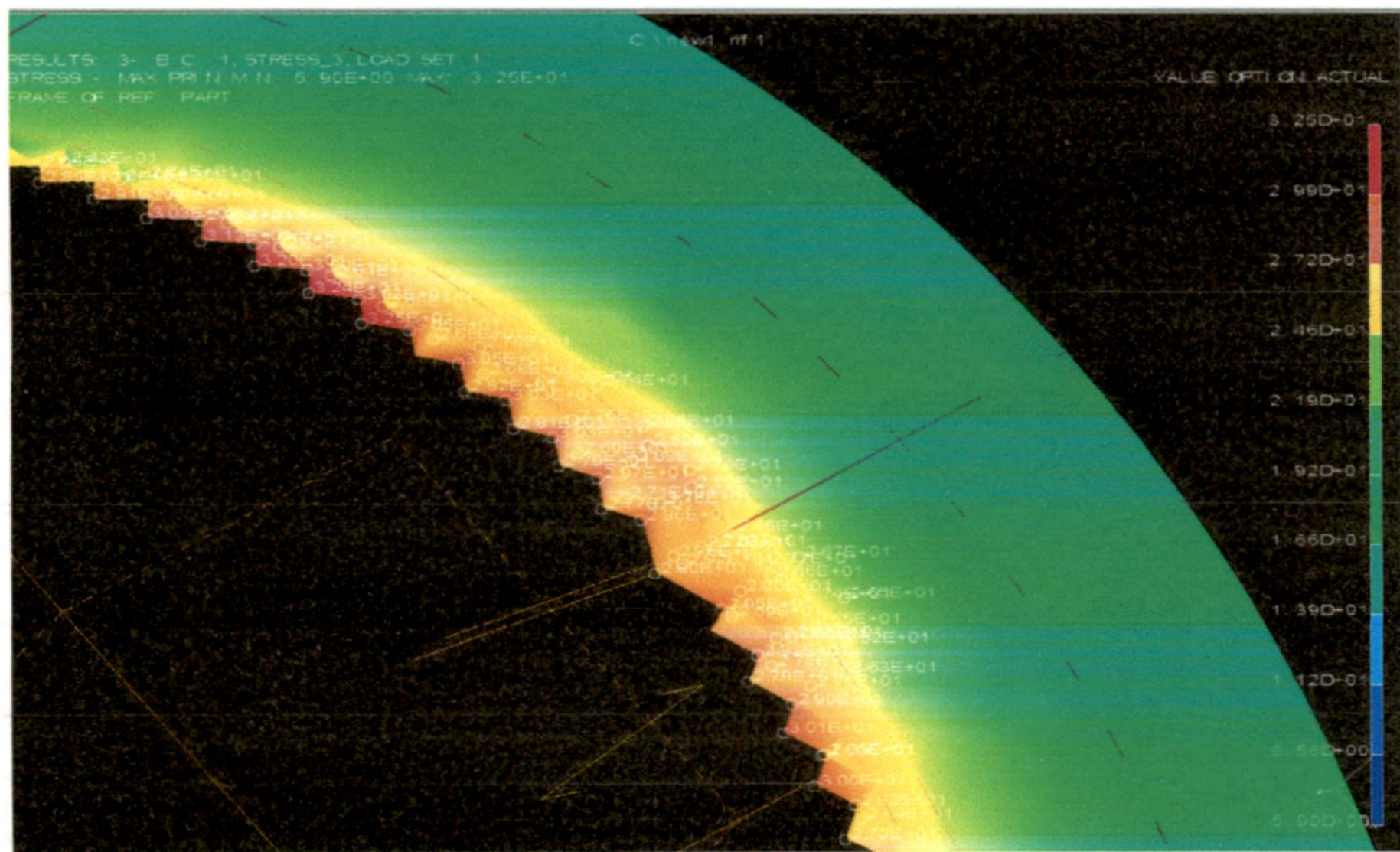
Fig.4.14: Maximum Principal Stresses showing Higher Order Values at the Selected Position at Bend-2

The maximum principal stresses at bend-2 showing higher order values are given in Table 4.2 is as below:

Table 4.2: Maximum Principal Stress at Bend-2

S. No.	Node No.	Stress Kg/cm^2	S. No.	Node No.	Stress Kg/cm^2	S. No.	Node No.	Stress Kg/cm^2
1	16551	3254.32	41	10130	2959.00	81	10199	2902.10
2	18480	2677.03	42	1318	2758.12	82	9175	2715.74
3	10124	3033.88	43	1196	2800.90	83	1166	2949.40
4	18481	2643.18	44	51	2920.16	84	51	2920.16
5	16464	3242.21	45	1166	2949.40	85	940	2694.24
6	10123	3003.67	46	1349	2801.74	86	1348	2780.73
7	17911	2600.82	47	51	2920.16	87	1347	2761.40
8	17481	3201.76	48	57	2723.93	88	1347	2761.40
9	10122	2951.28	49	1318	2758.12	89	8921	2634.68
10	18682	2555.22	50	1167	2920.18	90	9173	2819.31
11	17480	3131.53	51	6279	2787.23	91	9174	2743.17
12	10121	2903.64	52	1168	2895.32	92	8923	2664.09
13	18681	2576.24	53	6259	3007.05	93	1348	2780.73
14	17205	3031.46	54	7347	2694.15	94	1167	2920.18
15	10120	2799.51	55	1169	2845.63	95	940	2694.24
16	10141	2603.28	56	7347	2694.15	96	1349	2801.74
17	10362	2710.28	57	1169	2845.63	97	1166	2949.40
18	18680	2492.05	58	6025	3001.54	98	10130	2959.00
19	17476	2905.02	59	1170	2816.58	99	1318	2758.12
20	10119	2750.46	60	7348	2643.95	100	1196	2800.90
21	18979	2425.59	61	6582	2701.49	101	10130	2959.00
22	17211	2850.86	62	1171	2768.91	102	57	2723.93
23	10118	2651.99	63	1318	2758.12	103	9175	2715.74
24	18464	2678.62	64	10131	2784.83	104	9172	2668.47
25	10125	3046.84	65	10130	2959.00	105	9170	2651.27
26	18464	2678.62	66	1318	2758.12	106	8922	2654.27
27	10135	2778.32	67	51	2920.16	107	8829	2852.44
28	10126	3050.13	68	57	2723.93	108	938	2748.27
29	17952	2678.09	69	8671	2833.23	109	1347	2761.40
30	16847	2815.09	70	8672	2652.59	110	938	2748.27
31	10127	3032.51	71	10230	2823.31	111	1167	2920.18
32	16964	2805.30	72	19637	2758.30	112	940	2694.24
33	10133	2763.11	73	10231	2802.32			
34	10128	3027.35	74	10131	2784.83			
35	18216	2686.09	75	19637	2758.30			
36	16503	2789.94	76	10231	2802.32			
37	10129	2971.60	77	10197	2883.82			
38	17954	2707.80	78	19637	2758.30			
39	16506	2767.22	79	19635	2861.78			
40	10129	2971.60	80	19639	2736.72			
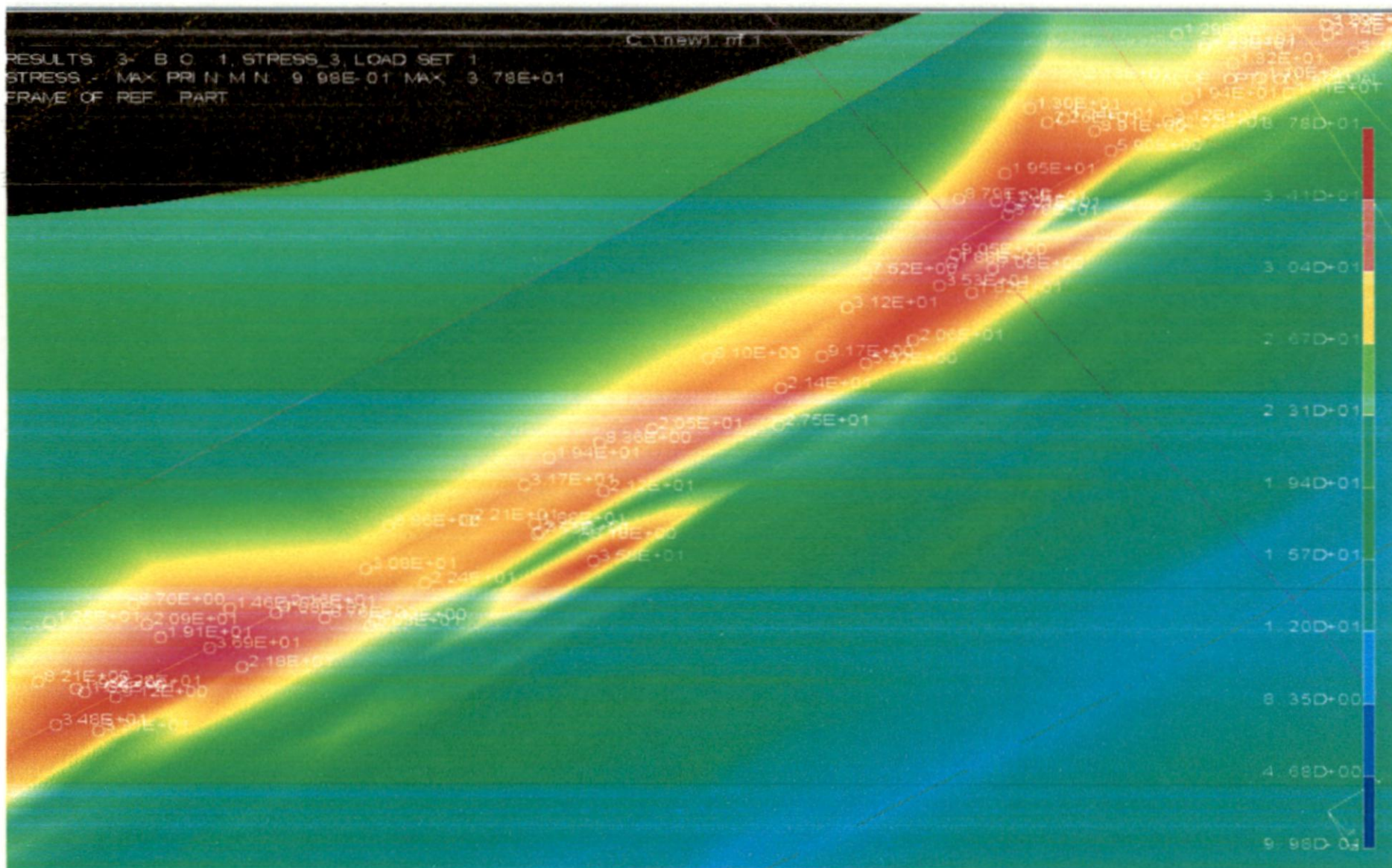
Fig.4.15: Maximum Principal Stresses showing Higher Order Values at the Selected Position at Sickle Plate
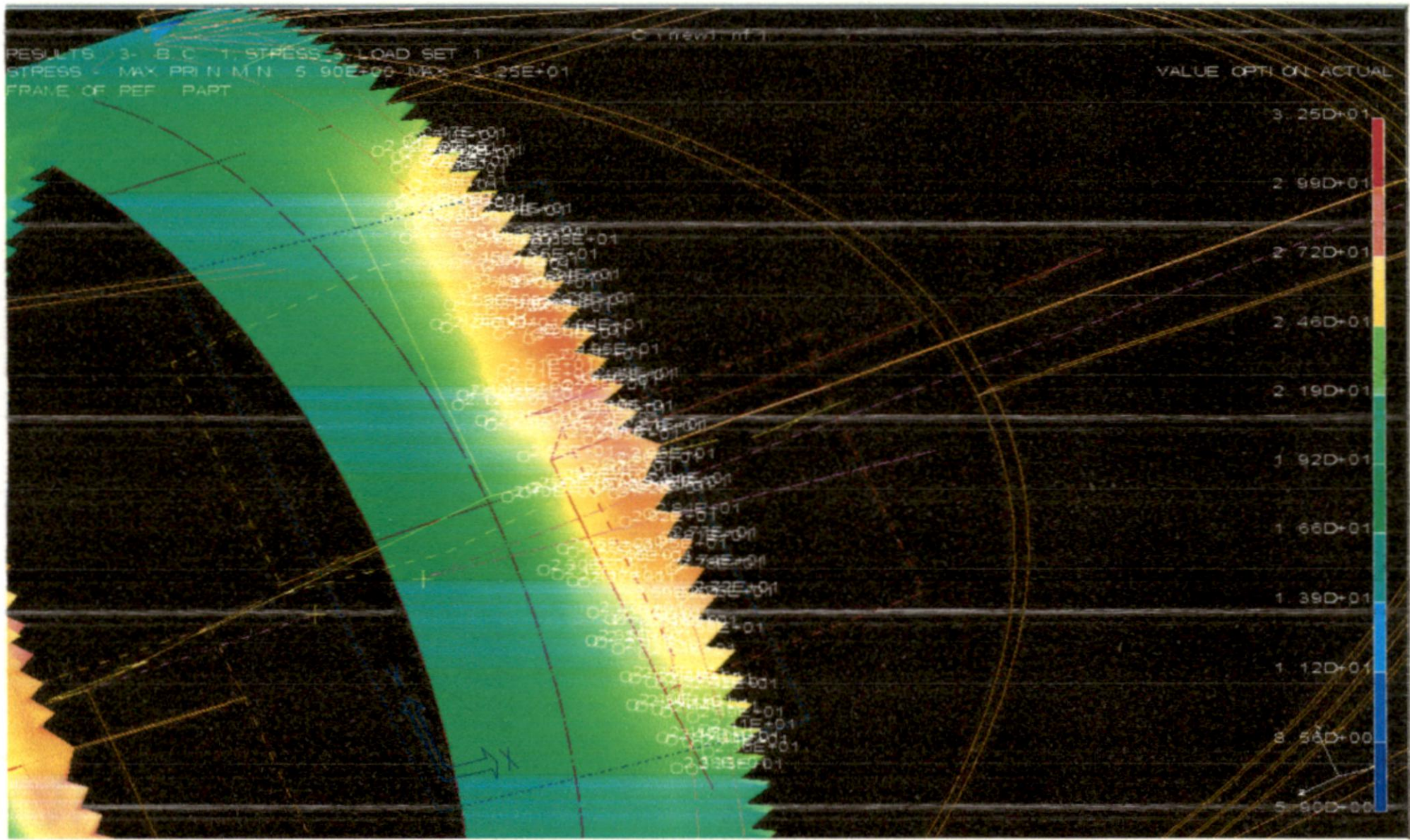
The maximum principal stresses at sickle plate showing higher order values are given in Table 4.3 is as below:

Table 4.3: Maximum Principal Stresses at Sickle Plate

S. No.	Node No.	Stress Kg/cm2	S. No.	Node No.	Stress Kg/cm2	S. No.	Node No.	Stress Kg/cm2
1	1760	3214.08	41	11969	878.84	81	11969	878.84
2	119	3078.95	42	11966	904.83	82	11966	904.83
3	1760	3214.08	43	12434	1879.19	83	12434	1879.19
4	119	3078.95	44	12249	3532.94	84	12249	3532.94
5	1760	3214.08	45	14098	1822.43	85	14098	1822.43
6	943	1861.22	46	11960	707.58	86	11960	707.58
7	1110	2099.02	47	14098	1822.43	87	14098	1822.43
8	943	1861.22	48	12249	3532.94	88	12249	3532.94
9	1493	839.64	49	12434	1879.19	89	12434	1879.19
10	1465	1037.86	50	11965	751.67	90	11965	751.67
11	12441	1894.11	51	10947	3121.06	91	10947	3121.06
12	1755	3194.98	52	12435	2064.63	92	12435	2064.63
13	117	3201.61	53	11947	551.88	93	11947	551.88
14	12441	1894.11	54	11948	916.73	94	11948	916.73

15	14111	2140.10	55	10947	3121.06	95	10947	3121.06
16	469	1113.92	56	12422	2142.04	96	12422	2142.04
17	467	1097.58	57	12247	2749.58	97	12247	2749.58
18	463	1234.82	58	11950	810.15	98	11950	810.15
19	465	1322.32	59	12494	046.65	99	12494	2046.65
20	14109	2226.03	60	11931	835.69	100	11931	835.69
21	461	1291.78	61	12503	2118.59	101	12503	2118.59
22	463	1234.82	62	14184	1937.40	102	14184	1937.40
23	12432	2130.35	63	10943	3167.05	103	10943	3167.05
24	12442	1939.71	64	12290	3284.95	104	12290	3284.95
25	21	3120.67	65	11918	754.98	105	11918	754.98
26	14108	2023.91	66	14186	1881.72	106	14186	1881.72
27	21	3120.67	67	12502	2212.21	107	12502	2212.21
28	11968	891.03	68	11921	886.05	108	11921	886.05
29	11971	1236.97	69	12509	2242.59	109	12509	2242.59
30	14100	2257.87	70	12173	3033.87	110	12173	3033.87
31	11878	1248.17	71	11884	842.34	111	11884	842.34
32	11963	589.80	72	11883	876.49	112	11883	876.49
33	14100	2257.87	73	12184	3583.67	113	12184	3583.67
34	11971	1236.97	74	11917	810.45	114	11917	810.45
35	11963	589.80	75	11882	1075.44	115	11882	1075.44
36	14100	2257.87	76	12510	2157.23	116	12510	2157.23
37	10949	3777.06	77	11881	1458.87	117	11881	1458.87
38	11969	878.84	78	11879	870.22	118	11879	870.22
39	11964	1235.16	79	12511	2094.63	119	12511	2094.63
40	11969	878.84	80	11878	1248.17			

4.3 PHYSICAL MODEL STUDIES USING STRAIN GAUGE TECHNOLOGY

To verify the structural design adequacy of penstock bifurcation physical model studies were conducted.

4.3.1 Fabrication of Model, Installation of Strain Gauges and Data Recording

In order to conduct physical model studies of penstock bifurcation, a geometrically similar model to a suitable scale[7, 19] was designed and fabricated using acrylic plastic/ Perspex sheet of suitable thickness. 3 mm thick perspex sheet was chosen for geometric similar model. All structural features such as sickle plate, conical bifurcation, etc of the penstock bifurcation were incorporated in the model. Perspex used for model construction has the elastic ratio with steel as 1:70 and the same Poisson' ratio, μ =0.33. The modulus of elasticity (E) and Poisson' ratio (μ) of the model material and prototype material are taken into account for calculation of prototype stresses, as the elastic ratio is constant and the elastic curve is linear in nature[5,15].

Model Component before Assembly
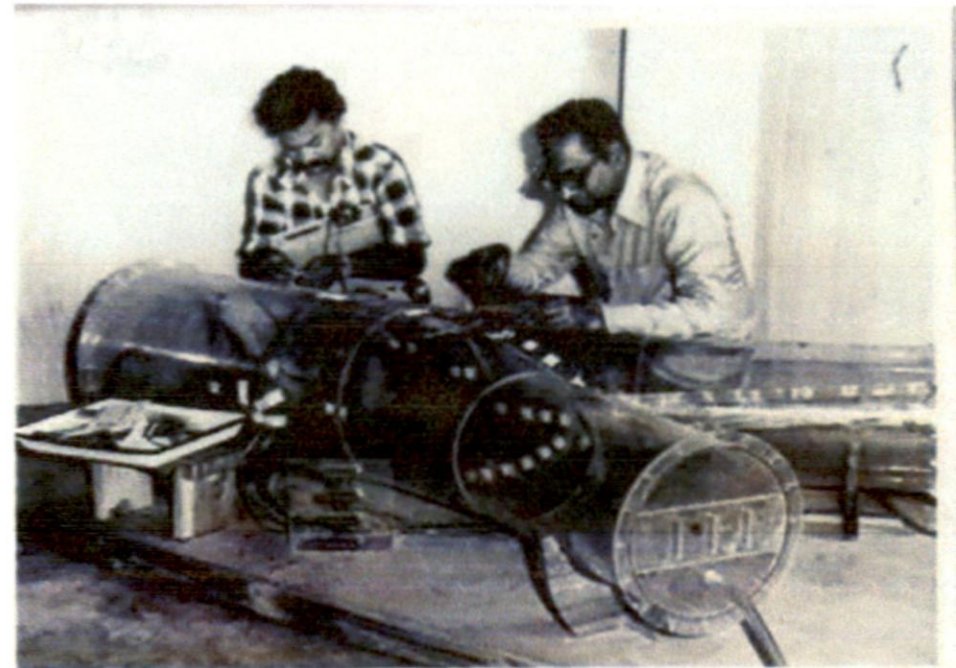
Installation of Strain Gauges on Model

Experimental Set up

Experiment in Progress

Photo 4.1: View of Experimental Setup and Data Recording for Physical Model Study of Penstock Bifurcation

(In this case geometric scale 1:10, Elastic ratio 1:70, for perspex E=30,000 kg/cm² and μ=0.33, for prototype E=2.1×10⁶ kg/cm²). The photo 4.1 shows the experimental set and data recording procedures for physical model study of penstock bifurcation.

Liquid chloroform is used as jointing material for model. Wooden form works are fabricated and perspex sheets are moulded at an elevated temperature 80°C and the plastic moulds were then annealed for removal of thermal stressed locked in during moulding. The various parts of the model were joined by using chloroform and acrylic cement. The joints are further sealed externally using celotapes to insure prevention of possible leakage through joints and instantaneous failure of model as experiences during the initial study. The required number of electrical resistance strain gauges are bonded/ installed on the model at selected / critical locations i.e., at the splitter plate, in the vicinity of intersection, on the shell of the bifurcation etc. to monitor the behavior of model subjected to internal pressure. Rosettes, biaxial or linear gauges are employed at the selected locations. Lead wires are connected to the gauges which are further connected to scanning box of multichannel data logger. The readings are taken manually by using strain meter or data is acquired by data logger.

The model is closed at the outlets sufficiently away from zone influence of the intersection by flat plates making model fully airtight. The model is subjected internal pressure pneumatically. Monometer tube is used to read the pressure accurately. In this model study, the model was loaded for internal pressures of 0.07 kg/cm², 0.14 kg/cm², 0.21 kg/cm² considering the bond strength of chloroform and acrylic at the joints. Strains were recorded using strain meter. The model strains thus recorded were converted in to equivalent prototype strains and stresses for the design pressure of 55 kg/cm².

4.3.2 Calculation of Strains and Stresses to Prototype

The recorded strains are converted in to prototype values using following relation[11]:

$$\frac{\varepsilon_p}{\varepsilon_m} = \frac{p_p}{p_m} \times \frac{E_p}{E_m}$$

ε_p = strain in prototype

p_p = pressure in prototype

ε_m = strain in model

p_m = pressure in model

E_p = modulus of elasticity of prototype material

E_m = modulus of elasticity of model material

The stresses are computed using following standard equations [13]:

Uniaxial or Single-element strain gauge

$$\sigma_1 = E.\,\varepsilon_1$$

Biaxial strain gauges or two-element rectangular rosette

$$\sigma_1 = \frac{E\left(\varepsilon_1 + \mu\,\varepsilon_2\right)}{1 - \mu^2}$$

$$\sigma_{2_1} = \frac{E\left(\varepsilon_{2_1} + \mu\,\varepsilon_1\right)}{1 - \mu^2}$$

Three strain gauges or three-element rosette

$$\varepsilon_1 = \frac{1}{2}\left(\varepsilon_A + \varepsilon_C\right) + \frac{1}{2}\sqrt{\left(\varepsilon_A - \varepsilon_C\right)^2 + \left(2\varepsilon_B - \varepsilon_A - \varepsilon_C\right)^2}$$

$$\varepsilon_2 = \frac{1}{2}\left(\varepsilon_A + \varepsilon_C\right) - \frac{1}{2}\sqrt{\left(\varepsilon_A - \varepsilon_C\right)^2 + \left(2\varepsilon_B - \varepsilon_A - \varepsilon_C\right)^2}$$

$$\sigma_1 = E\left[\frac{\left(\varepsilon_A + \varepsilon_C\right)}{2(1 - \mu)} + \frac{1}{2(1 + \mu)}\sqrt{\left(\varepsilon_A - \varepsilon_C\right)^2 + \left(2\varepsilon_B - \varepsilon_A - \varepsilon_C\right)^2}\right]$$

$$\sigma_2 = E\left[\frac{\left(\varepsilon_A + \varepsilon_C\right)}{2(1 - \mu)} - \frac{1}{2(1 + \mu)}\sqrt{\left(\varepsilon_A - \varepsilon_C\right)^2 + \left(2\varepsilon_B - \varepsilon_A - \varepsilon_C\right)^2}\right]$$

Where,

ε_A, ε_B and ε_C are measured strains along three directions at any rosette strain gauge location.

σ_1, σ_2 = principal stresses

ε_1, ε_2 = principal strains

μ = Poisson' ratio of steel

4.3.3 RESULTS OF PHYSICAL MODEL STUDY [7]

In case of physical model study, the maximum design pressure applied equivalent to prototype is 55 kg/cm² and the stresses developed are in different parts of penstock are within the permissible limit. The hoop stress developed in the shell near the junction of the sickle plate with the shell is shown in Fig.4.16 at section – AA varying from 2063 kg/cm² to 1169 kg/cm² (37.5 p_o to 21.26 p_o) and at the bend area of the order of 1595 kg/cm² (29 p_o). The peak

value of 37.5 p_o = 2063 kg/cm^2 is below the design value of hoop stress 2200 kg/cm^2 (40 p_o)

The vertical stress in the sickle plate varies from 2822 kg/cm^2 to 1794 kg/cm^2 [7]
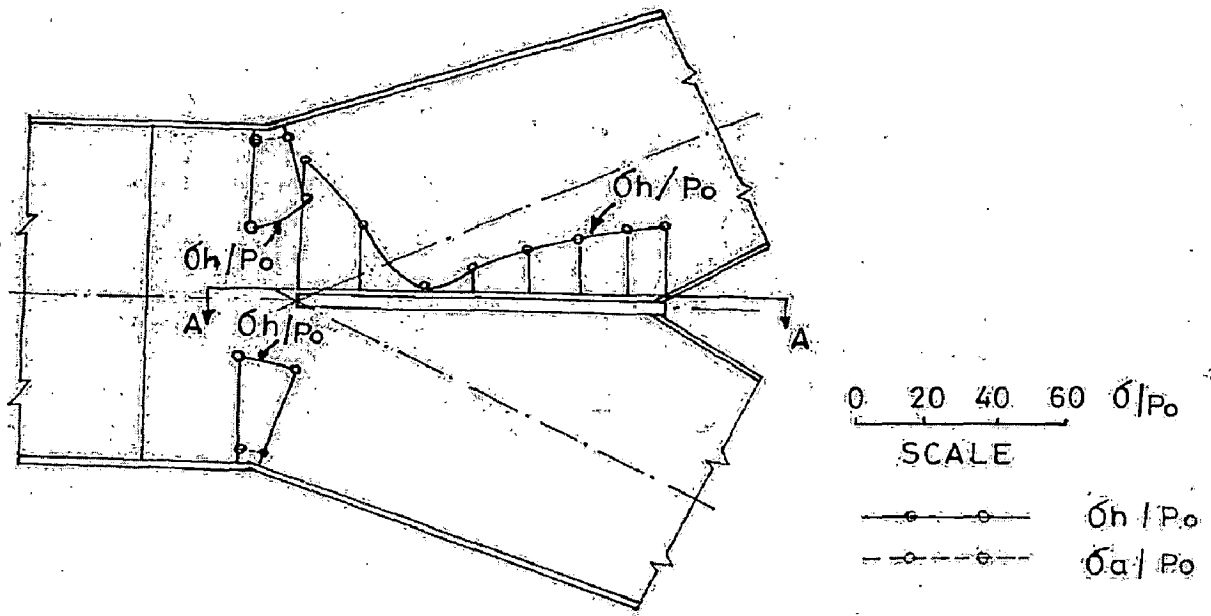
Fig. 4.16: Hoop Stresses at Bend and Section A-A

Table 4.4: Hoop Stress at Bend as shown in Fig .4.16

S No.	Locations	Hoop Stress σh/po	Hoop Stress at 50 kg/cm^2 internal pressure	Hoop Stress at 55 kg/cm^2 internal pressure
1	Upper point 1	29.5	1475	1623
2	Upper point 2	23	1150	1265
3	Lower point 1	31	1550	1705
4	Lower point 2	29	1450	1595

Table 4.5: Hoop Stress at Section A-A (External) as shown in Fig. 4.16

S No.	Locations	Hoop Stress σh/po	Hoop Stress at 50 kg/cm^2 internal pressure	Hoop Stress at 55 kg/cm^2 internal pressure
1	1	38	1900	2090
2	2	20	1000	1100
3	3	2	100	110
4	4	6.5	325	356
5	5	12	600	660

6	6	15	750	825
7	7	18	900	990
8	8	19.4	970	1067
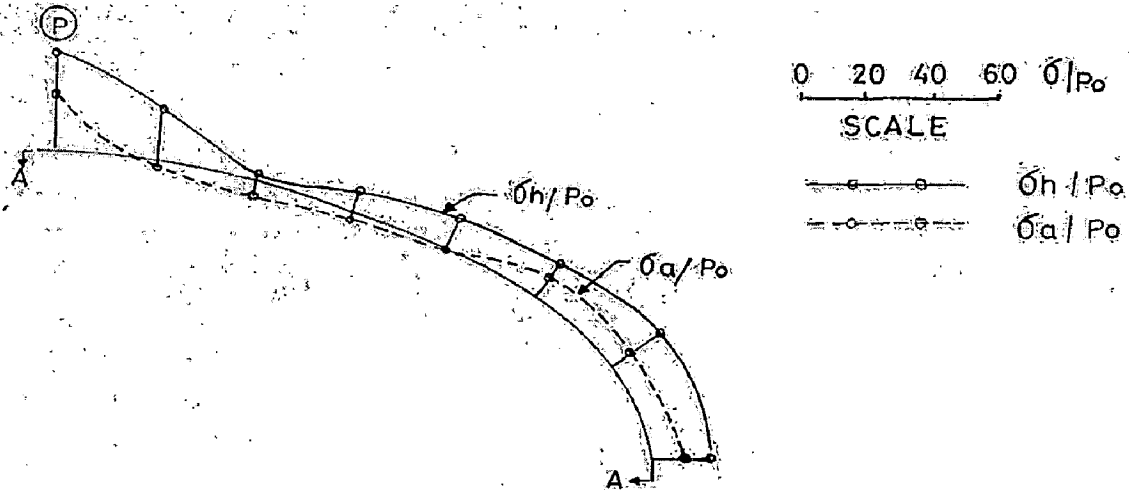
Fig. 4.17: Hoop Stress and Axial Stress at Section A-A (External) Outer Profile

Table 4.6: Hoop Stress at Section A-A (External) Outer Profile as shown in Fig.4.17

S No.	Locations	Hoop Stress $\sigma h/po$	Hoop Stress at 50 kg/cm^2 internal pressure	Hoop Stress at 55 kg/cm^2 internal pressure
1	P 1	36	1800	1980
2	2	18	900	990
3	3	8	400	440
4	4	8	400	440
5	5	12	600	660
6	6	12	600	660
7	7	20	1000	1100
8	8	19.5	975	1073

Table 4.7: Axial Stress at Section A-A (External) Outer Profile as shown in Fig.4.17

S No.	Location	Axial Stress $\sigma h/po$	Axial Stress at 50 kg/cm^2 internal pressure	Axial Stress at 55 kg/cm^2 internal pressure
1	P 1	18	1250	1375
2	2	-2	-100	-110

69

3	3	-6	-300	-330
4	4	-2	-100	-110
5	5	0	0	0
6	6	7	350	385
7	7	7	350	385
8	8	10	500	550
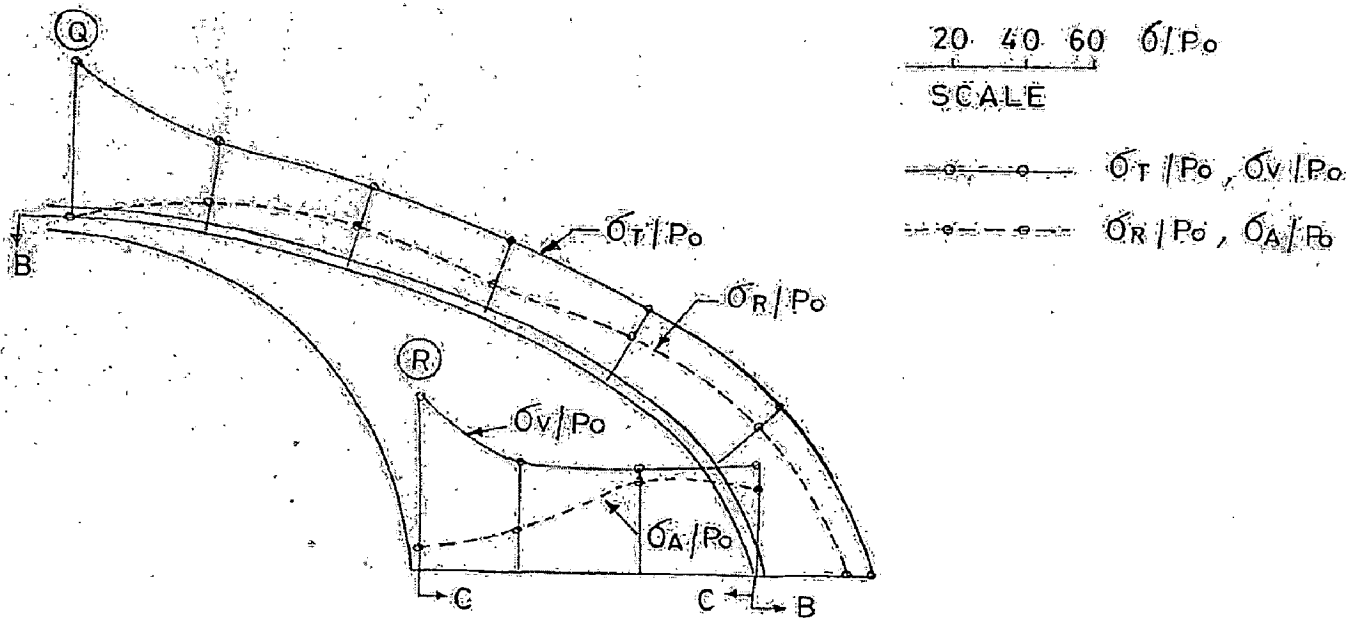
Fig. 4.18: Tangential and Radial Stresses on Section B-B & Vertical and Axial Stresses on Section C-C in Sickle Plate

Table 4.8: Tangential Stresses on Section B-B in Sickle Plate in Fig.4.18

S No.	Location	Tangential Stress $\sigma h/po$	Tangential Stress at 50 kg/cm^2 internal pressure	Tangential Stress at 55 kg/cm^2 internal pressure
1	Q 1	47	2350	2585
2	2	26	1300	1430
3	3	24	1200	1320
4	4	24	1200	1320
5	5	24	1200	1320
6	6	28	1400	1540
7	7	32	1600	1760

70

Table 4.9: Radial Stresses on Section B-B in Sickle Plate in Fig.4.18

S No.	Location	Radial Stress $\sigma h/po$	Radial Stress at 50 kg/cm^2 internal pressure	Radial Stress at 55 kg/cm^2 internal pressure
1	Q 1	0	0	2585
2	2	6	1300	1430
3	3	12	1200	1320
4	4	10	1200	1320
5	5	14	1200	1320
6	6	20	1400	1540
7	7	26	1600	1760

Table 4.10: Vertical Stresses on Section C-C in Sickle Plate in Fig.4.18

S No.	Location	Vertical Stress $\sigma h/po$	Vertical Stress at 50 kg/cm^2 internal pressure	Vertical Stress at 55 kg/cm^2 internal pressure
1	R 1	51	2550	2805
2	2	32	1600	1760
3	3	29	1450	1595
4	4	32	1600	1760

Table 4.11: Axial Stresses on Section C-C in Sickle Plate in Fig.4.18

S No.	Location	Axial Stress $\sigma h/po$	Axial Stress at 50 kg/cm^2 internal pressure	Axial Stress at 55 kg/cm^2 internal pressure
1	R 1	6	300	330
2	2	12	600	660
3	3	25	1250	1375
4	4	25	1250	1375

4.4 HYDROSTATIC TEST OF PROTOTYPE OF PENSTOCK BIFURCATION

Hydrostatic test is considered most reliable for performance assessment and identification of defects, if any, in welded components in the post fabrication stage. The above objective can achieve by conducting Hydrostatic test on prototype (at site or at the fabricator's workshop) prior to putting into service.

4.4.1 Fabrication of Penstock Bifurcation

The penstock bifurcation was fabricated by welding ASTM-A 537 grade II steel sheets as per following details as considered in the design:

Gross Head	: 475.4 m
Internal diameter of header pipe	: 4000mm
Internal diameter of branch pipe	: 3000mm
Thickness of cylindrical portion	: 50mm
Thickness of sickle plate	: 100 mm
Steel used for fabrication	: ASTM-A-537 class II
Minimum yield strength	: 4219 kg/ cm^2
Ultimate tensile strength	: 5625-7031kg/cm^2.

The allowable stress as per design criteria reported in agreement between KPCL and IHP is considered as 0.5 times of yield strength i.e. 2110 kg/ cm^2.

The penstock bifurcation was supported using three saddle supports. Free movement of the penstock bifurcation was ensured by applying grease lubricant to saddle supports in contact with bifurcation. The three ends of the bifurcation were closed by welding bulkheads.

4.4.2 Inspection Tests on Penstock Bifurcation

Before conducting hydrostatic test, the following inspections / tests are to be carried out for welds / cracks

4.4.2.1 Radiographic Examination

Radiographic examination is used for inspection of any flaws in welding such as pores, slag inclusion, lack of fusion and cracks. It is carried by X-rays or Gamma rays depending

upon the source of radiation to indicate any flaws in welding. Its records can be maintained permanently [4,22,24].

Recommendations:

➢ All the longitudinal joints shall be radiographed for 100 percent length.

➢ The circumferential joints shall be spot radiographed for 10 percent length of each joint.

➢ All the T-junctions between longitudinal and circumferential joints shall be radiographed.

➢ Any defects shown during radiography shall be repaired and subjected to re-examination.

4.4.2.2 Ultrasonic Examination

Ultrasonic examination enables faults to be located more accurately and access the necessity for repairs. It is carried out by electronic equipment and requires highly qualified operator. Its records can not be maintained permanently. The joints such as girth of linear in a tunnel or shaft with backing strips, which are difficult to radiographed or in accessible to radiographic examination may be subjected to ultrasonic examination in lieu of radiographic examination.

4.3.2.3 Magnetic Particle Method and Dye Penetration Method

Magnetic particle method and Dye penetration method are non-destructive tests and used to detect the surface cracks. These two methods may be adopted for inspection of field welds in case of a difficult weld and the intermediate runs of weld.

4.4.3   Installation of Electrical Resistance Strain Gauges

Structurally important and critical locations were selected on sickle plate and surface of the penstock bifurcation where electric resistance strain gauges were to be installed. The selected locations were rubbed by sand paper and thoroughly cleaned with the help cotton waste and acetone liquid. The prepared surfaces are coated with mixture of araldite and hardener. After drying the surfaces are to be smoothened for pasting the strain gauges. Then electric resistance strain gauges are pasted on each location with help of mixture of araldite and hardener and left for drying at least 24 hours. Rosettes, biaxial or linear gauges are employed at the selected locations as per requirement of stresses and their nature or pattern. Lead wires are connected to the strain gauges which are further connected to scanning box of data logger/

strain meter. The locations of strain gauges on the top, at the bottom and at the sickle plate are shown in Fig. 4.19, Fig. 4.20, and Fig. 4.21 respectively. The photo 4.2 explains the installation of strain gauges and other procedures of hydrostatic tests.

4.4.4 Experimental Procedures and Data Recording

After recording initial observations of all the strain gauges with the penstock bifurcation empty, the penstock bifurcation was completely filled with water using hydraulic pump. After filling the penstock bifurcation, small internal pressure was applied and air vent valve was operated to allow entrapped air to escape from pipe and pressure was brought down to zero. The pressure shall be applied three times successively increasing and decreasing at uniform rate. The pressure was gradually raised to test pressure. The test pressure shall be held stationary for such a time as is considered sufficient for inspection of all plates, joints and connections to detect leakage and signs of failure.

Accordingly, the cycle was repeated 3 times to completely remove entrapped air from pipe and then strain gauge readings were recorded at zero applied internal pressure. The internal pressure was applied in steps of 5 kg/ cm^2 upto 40 kg/ cm^2 and thereafter in steps of 2 kg/ cm^2 [8]. At each step, the applied internal pressure was held constant for at least 10 minutes and strain observations were recorded. At internal pressure equal to 44 kg/cm^2, the hoop stress of the order of 2814 kg/ cm^2 was found to be developed ($\approx$ 50% of minimum UTS of the steel) at strain gauge location B2. However, after discussions with design engineers, KPCL officers and IHP officials, it was decided to carry on the hydrostatic test up to 75% of yield point of the steel without endangering the safety of the structure. Accordingly, internal pressure was applied further in steps of 2 kg/ cm^2 upto 50 kg/ cm^2 internal pressure which resulted hoop stress of 3164 kg/ cm^2 (equal to 75% of yield point) at strain gauge location B2. This pressure was held constant for 15 minutes and the entire length of penstock bifurcation including weld joints was monitored minutely for leakage and sweating of joints Considering the criteria viz., lesser of 50% minimum ultimate tensile strength and 75% of yield point of the steel used in fabrication of penstock bifurcation, the internal pressure was not increased further in consultation with design engineers and project officials.

The pressure in the pipe was reduced gradually from 50 kg/cm^2 in steps of 2 kg/cm^2 up to 40 kg/ cm^2 thereafter in steps of 5 kg/cm^2. The strain gauge observations were recorded at each step during depressurising also. During the entire test, no leakages or sweating of joints were noticed. The stresses calculated for the penstock bifurcation for different location of strain gauges are given in Table 4.12, Table 4.13a, Table 4.13b, and Table 4.14. The variation

of hoop stresses with respect to applied pressure in header pipe is shown in Fig. 4.22 and the variation of major principal stresses with respect to applied pressure in sickle plate is shown in Fig. 4.23.

As per test criteria (agreement between IHP and KPCL) the test pressure is the pressure which produces a hoop stress in penstock bifurcation at any point equal to 50% of the minimum ultimate tensile strength (UTS) or 75% of yield point of the steel used in the fabrication of penstock bifurcation whichever is less.

According to CWC manual, in general, test pressure is equal to 1.5 times of design pressure or to a pressure which will develop a stress equal to 0.8 times yield point whichever is earlier[6].

4.4.5 Calculation and Plotting of Stresses

The hoop (circumferential) and axial stresses computed from measured strains in circular portion of the pipe were compared with theoretical hoop and longitudinal stresses calculated using standard formulae for thin cylindrical shell as follows[32]:

Tensile Hoop Stress, $\qquad \sigma_h = p.r \, / \, t$

Axial Stress, $\qquad \sigma_a = p.r \, / \, 2t$

Also, the principal stresses developed in header pipe, conical reducer and sickle plate are calculated from the measured strain by installed rosette strain gauges using the following standard formulae[11,32];

Uniaxial or Single-element strain gauge

$\sigma_1 = E. \, \varepsilon_1$

ε_1

————————————— x

Biaxial strain gauges or two-element rectangular rosette

$$\sigma_1 = \frac{E\left(\varepsilon_1 + \mu\,\varepsilon_2\right)}{1 - \mu^2}$$

$$\sigma_{2_1} = \frac{E\left(\varepsilon_{2_1} + \mu\,\varepsilon_1\right)}{1 - \mu^2}$$

y

ε_2

ε_1

x

Three strain gauges or three-element rosette

$$\varepsilon_1 = \frac{1}{2}(\varepsilon_A + \varepsilon_C) + \frac{1}{2}\sqrt{(\varepsilon_A - \varepsilon_C)^2 + (2\varepsilon_B - \varepsilon_A - \varepsilon_C)^2}$$

$$\varepsilon_2 = \frac{1}{2}(\varepsilon_A + \varepsilon_C) - \frac{1}{2}\sqrt{(\varepsilon_A - \varepsilon_C)^2 + (2\varepsilon_B - \varepsilon_A - \varepsilon_C)^2}$$

$$\sigma_1 = E\left[\frac{(\varepsilon_A + \varepsilon_C)}{2(1-\mu)} + \frac{1}{2(1+\mu)}\sqrt{(\varepsilon_A - \varepsilon_C)^2 + (2\varepsilon_B - \varepsilon_A - \varepsilon_C)^2}\right]$$

$$\sigma_2 = E\left[\frac{(\varepsilon_A + \varepsilon_C)}{2(1-\mu)} - \frac{1}{2(1+\mu)}\sqrt{(\varepsilon_A - \varepsilon_C)^2 + (2\varepsilon_B - \varepsilon_A - \varepsilon_C)^2}\right]$$

Where;

σ_1, σ_2 = principal stresses

ε_1, ε_2 = principal strains

μ = Poisson' ratio of steel

p = internal pressure in the circular pipe

r = internal radius of circular pipe

t = thickness of pipe shell

E = Young's modulus of elasticity of steel

ε_A, ε_B and ε_C are measured strains along three directions at any rosette strain gauge location.

The recorded strain gauge observations for biaxial and uniaxial strain gauges were also used to calculate hoop, axial strains, which were in turn converted to hoop and axial stresses by as follows:

$\sigma = \varepsilon.\ E$

No leakages or sweating of weld joints should noticed during hydrostatic test at designed internal pressure. The maximum hoop stress / longitudinal stress developed due to the applied internal pressure gives the indication of local stress at that location, should not be more than 75% of yield strength. All the fabricated sections, straight pipe, bends, expansion joints, wyes etc. shall be subjected to hydrostatic test [1,4].

Front View of Bifurcation

Cleaning of surface area of size 100mm x 100mm

Application of araldite for proper bonding
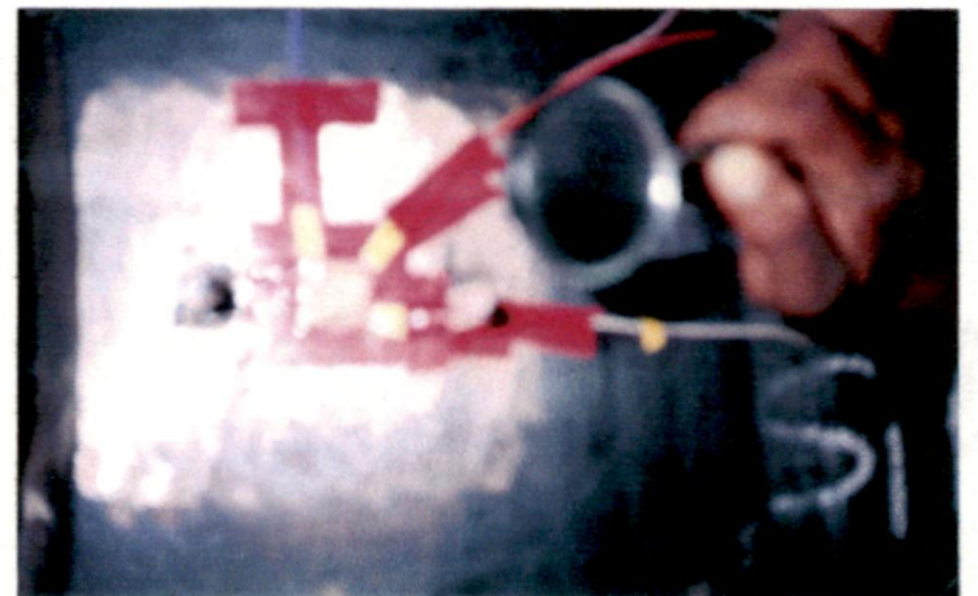
A rosette gauge after pasting on sickle plate

Cable routing through pipe bend for internal gauges

Pipe bend was filled with epoxy

Photo: 4.2 View of Hydrostatic Test of Penstock bifurcation

4.4.6   RESULTS OF HYDROSTATIC TEST ON PROTOTYPE [8]

(A) Stresses in main pipe

The hoop stress at 50 kg/cm^2 internal pressure in header pipe varies from 2086.6 kg/cm^2 to 2360.6 Kg/cm^2 along the diameter of the pipe

(B) Stresses at the junction of main pipe and branch pipe

The hoop stress at 50 kg/cm^2 internal pressure in branch pipe varies from 328.4 kg/cm^2 to 3162.6 Kg/cm^2 along the diameter of the pipe

(C) Stresses in sickle plate

The major principal stress at 50 kg/ cm^2 internal pressure varies from 985.5 kg/cm^2 to 1008.8 Kg/cm^2 at the centerline of the sickle plate.

The maximum stress of the order of 3164 kg/cm^2 was found to develop at an internal pressure of 50 kg/cm^2 on location B2 at half diameter point near the intersection of header and conical pipes which works out to be 75% of minimum yield strength of steel making the bifurcation.
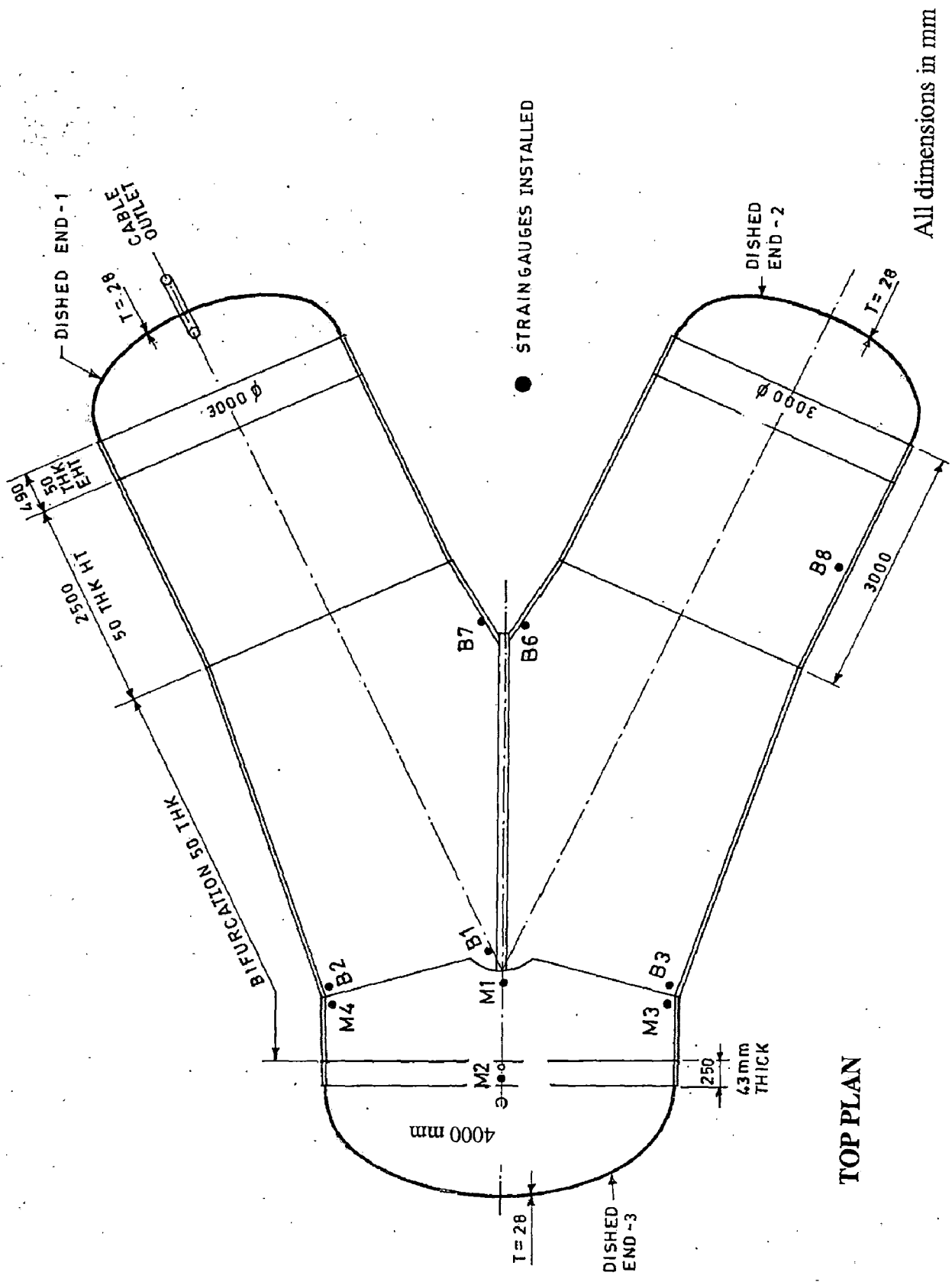
All dimensions in mm

Fig 4.19: Strain Gauge Locations on Top Surface of Penstock Bifurcation

79
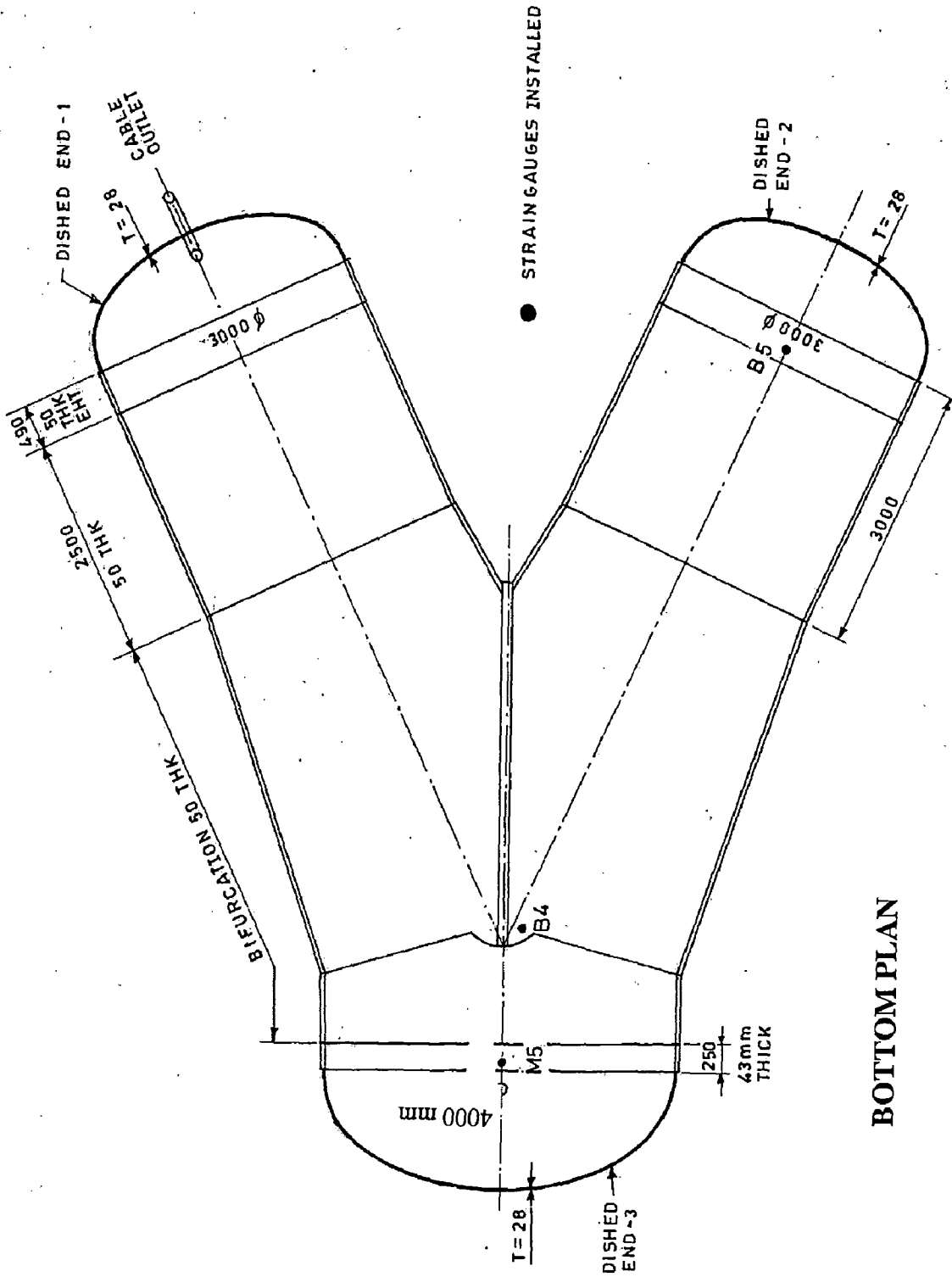
Fig 4.20: Strain Gauge Locations on Bottom Surface of Penstock Bifurcation

All dimensions in mm

80

SECTIONAL ELEVATION
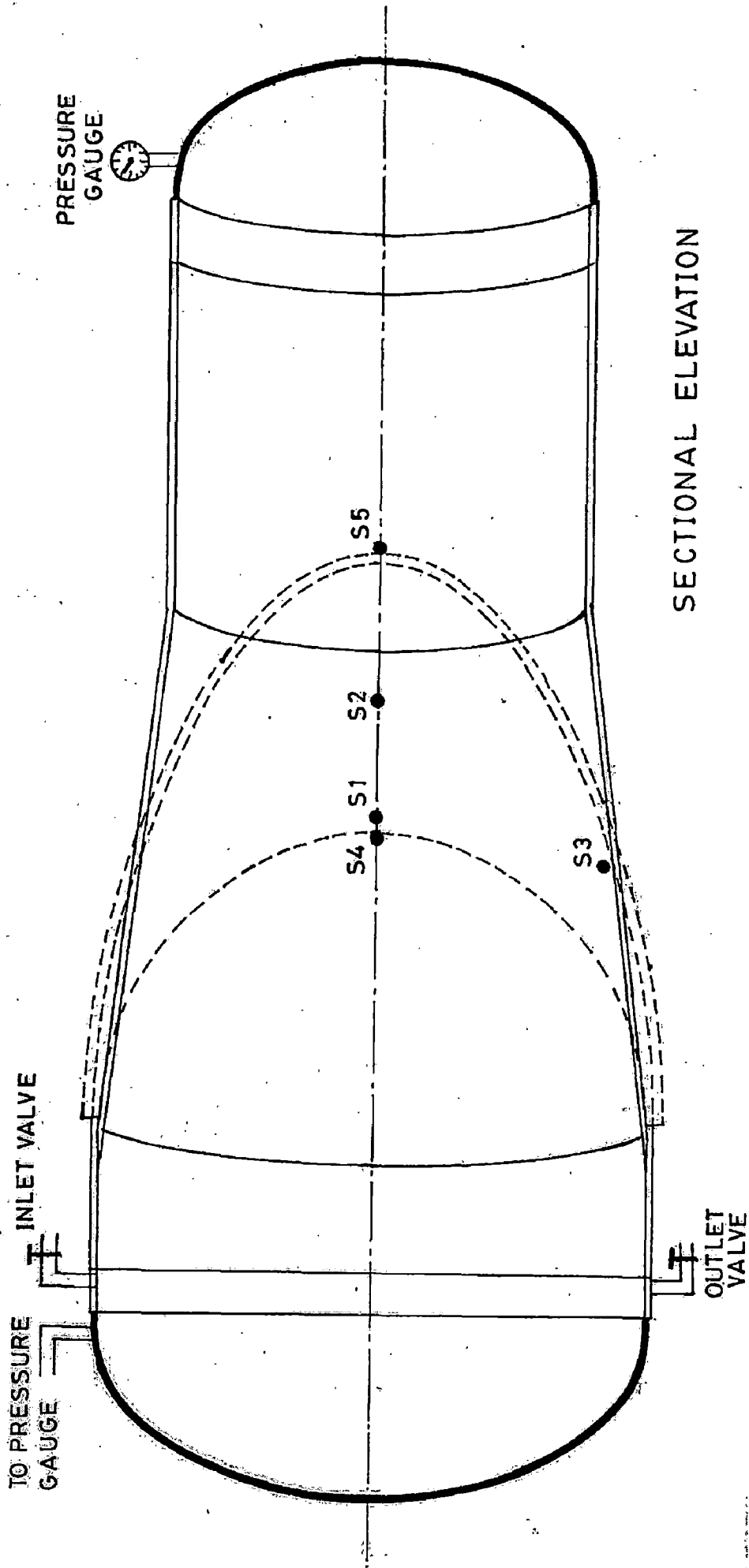
Fig 4.21: Strain Gauge Locations on Surface of Splitter Plate

81
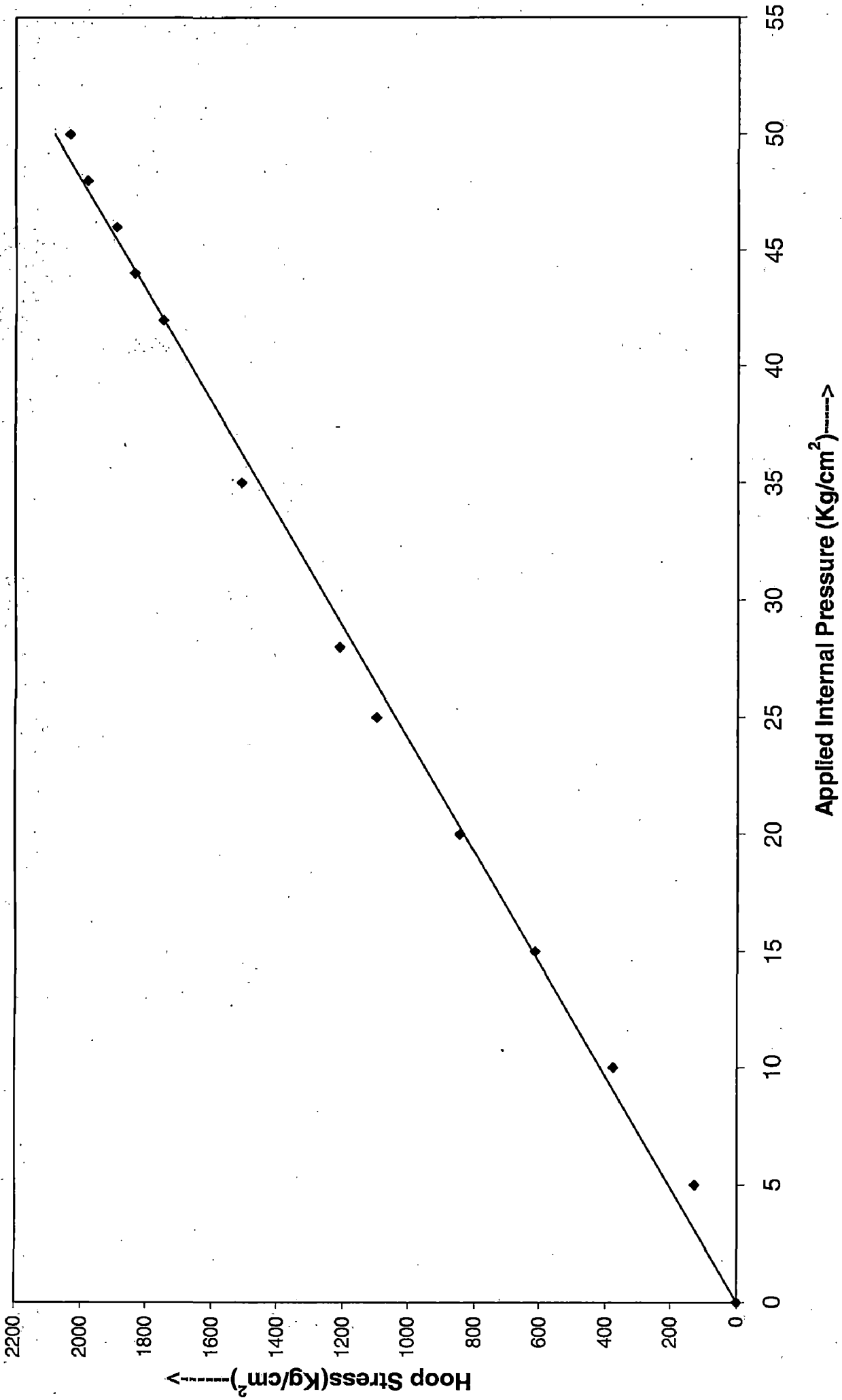
Fig.4.22 Variation of Hoop Stress due to Internal Pressure on Header Pipe at Strain Gauge Location M1
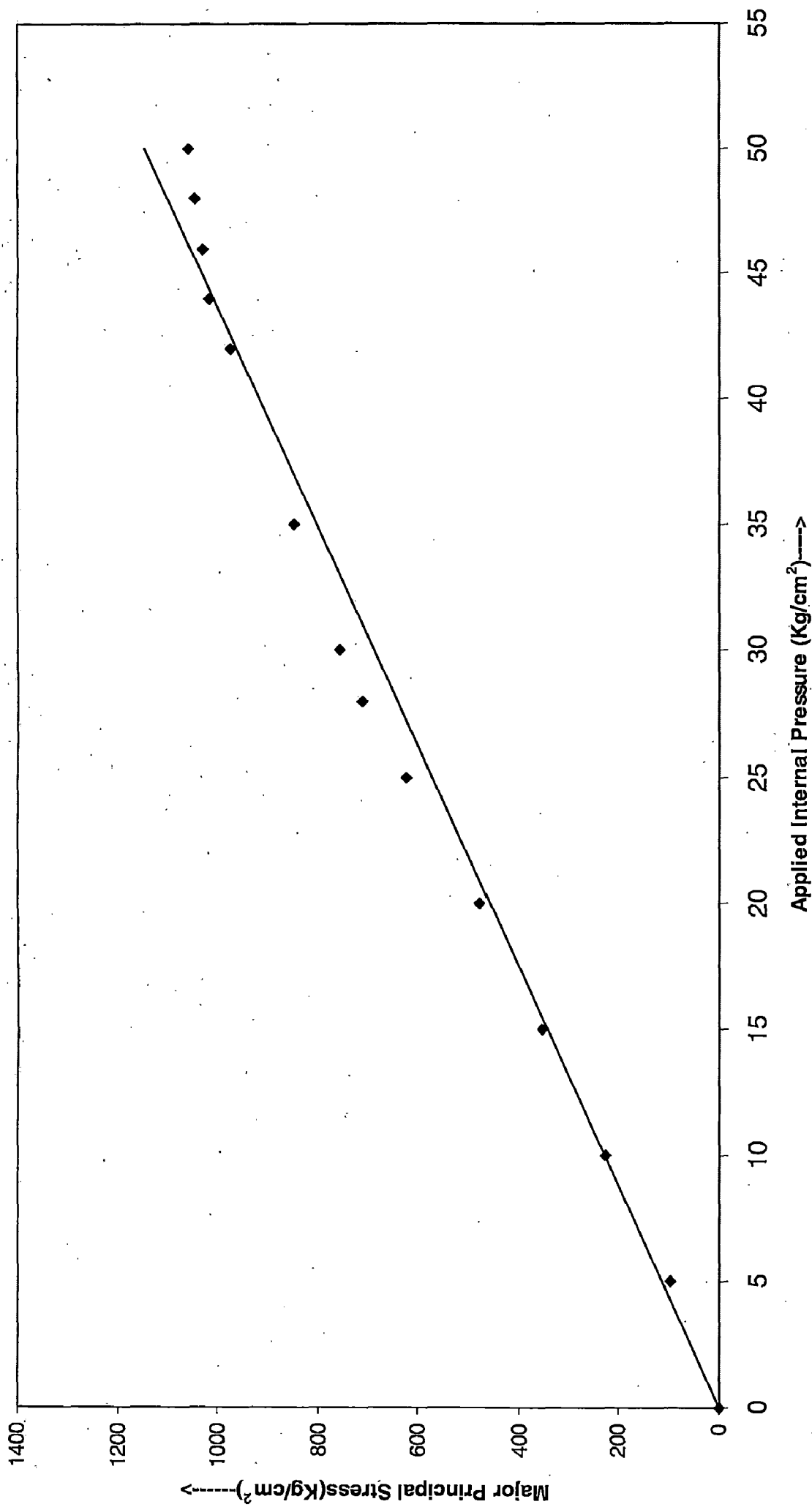
Fig.4.23 Variation of Major Principal Stress due to Internal Pressure in Sickle Plate at Strain Gauge Location S2

83

Table 4.12: Prototype Hoop & Axial Stresses in Header Pipe of Penstock Bifurcation during Hydrostatic Test

Location	M1		M2	M3		M4		M5
Internal Pressure (kg/cm²)	Hoop Stresses (kg/cm²)	Axial Stresses (kg/cm²)	Axial Stresses (kg/cm²)	Hoop Stresses (kg/cm²)	Axial Stresses (kg/cm²)	Hoop Stresses (kg/cm²)	Axial Stresses (kg/cm²)	Axial Stresses (kg/cm²)
0	0.0	0.0	0.0	0.0	0.0	0.0	0.0	0.0
5	208.7	81.3	126.2	191.6	75.9	193.2	58.3	124.2
10	417.3	162.6	263.3	412.8	165.7	413.2	127.0	245.6
15	626.0	243.9	407.9	655.9	265.5	653.2	203.1	364.5
20	834.6	325.2	556.5	923.4	371.9	907.4	283.5	481.3
25	1043.3	406.5	705.7	1178.0	481.1	1168.8	365.2	596.3
30	1250.0	487.8	851.9	1442.0	589.3	1431.1	445.4	710.0
35	1460.6	569.1	991.8	1698.0	693.0	1687.9	520.8	822.7
40	1669.3	650.4	1122.0	1938.5	788.5	1932.7	588.7	934.7
42	1752.7	683.0	1170.5	2028.6	823.6	2025.8	613.0	979.5
44	1836.2	715.5	1216.7	2114.6	856.5	2115.6	635.4	1024.2
46	1919.7	748.0	1260.3	2196.0	887.1	2201.6	655.8	1068.9
48	2003.1	780.5	1301.2	2272.9	915.0	2283.4	673.9	1113.7
50	**2086.6**	813.1	**1339.1**	**2342.9**	970.1	**2360.6**	689.5	**1158.5**
% of σy at 5o	**49.5**	19.3	31.7	**55.5**	22.3	**56.0**	16.3	27.5

(+)→ Tension   (-)→Compression   σy =yield strength of steel used for the fabrication of penstock bifurcation

84

Table 4.13a: Prototype Hoop & Axial Stresses in Branch Pipe of Penstock Bifurcation during Hydrostatic Test

Location	B1		B2		B3		B4	
Internal Pressure (kg/cm²)	Hoop Stresses (kg/cm²)	Axial Stresses (kg/cm²)	Hoop Stresses (kg/cm²)	Axial Stresses (kg/cm²)	Hoop Stresses (kg/cm²)	Axial Stresses (kg/cm²)	Hoop Stresses (kg/cm²)	Axial Stresses (kg/cm²)
0	0.0	0.0	0.0	0.0	0.0	0.0	0.0	0.0
5	99.8	46.6	316.4	69.4	121.1	27.9	29.5	2.2
10	199.7	93.2	632.8	138.4	242.2	55.8	59.0	4.3
15	299.5	139.7	949.2	208.1	363.3	83.7	88.5	6.5
20	399.3	186.3	126.6	277.5	464.4	111.6	118.0	8.7
25	499.1	232.9	1582.0	346.9	605.5	139.5	147.5	10.9
28	559.0	260.9	1771.8	388.5	678.2	156.3	165.2	12.2
30	599.0	279.5	1898.4	416.3	726.6	167.5	177.0	13.0
35	698.8	326.1	2214.8	485.7	847.7	195.4	206.5	15.2
40	798.6	372.7	2531.2	555.0	968.8	223.3	236.0	17.4
42	838.5	392.3	2657.7	582.8	1017.3	234.4	247.8	18.2
44	878.5	409.9	2784.3	610.5	1065.7	245.6	259.6	19.1
46	918.4	428.5	2910.8	638.3	1114.2	256.8	271.4	20.0
48	958.3	447.2	3037.4	666.0	1162.6	267.9	283.2	20.8
50	998.3	465.8	3164.0	693.8	1211.1	279.1	295.0	21.7
% of σ_y at 50	23.7	11.0	75.0	16.4	28.7	6.6	7.0	0.5

(+)→ Tension (-)→Compression σ_y =yield strength of steel used for the fabrication of penstock bifurcation

Table 4.13b: Prototype Hoop & Axial Stresses in Branch Pipe of Penstock Bifurcation during Hydrostatic Test

Location	B5		B6		B7		B8	
Internal Pressure (kg/cm^2)	Hoop Stresses (kg/cm^2)	Axial Stresses (kg/cm^2)	Hoop Stresses (kg/cm^2)	Axial Stresses (kg/cm^2)	Hoop Stresses (kg/cm^2)	Axial Stresses (kg/cm^2)	Hoop Stresses (kg/cm^2)	Axial Stresses (kg/cm^2)
0	0.0	0.0	0.0	0.0	0.0	0.0	0.0	0.0
5	-3.4	116.9	103.7	75.2	109.0	61.7	125.5	22.6
10	-6.8	233.8	207.4	150.4	218.0	123.4	251.1	45.3
15	-10.2	350.7	311.1	225.6	327.0	185.1	376.6	67.9
20	-13.6	467.6	414.8	300.8	435.9	246.8	502.1	90.6
25	-17.0	584.5	518.5	376.1	544.9	308.6	627.7	113.2
28	-19.1	654.6	580.7	421.2	610.3	34506	703.0	126.8
30	-20.4	701.4	622.2	451.3	653.9	370.3	753.2	135.9
35	-23.8	818.3	725.9	526.5	762.9	432.0	878.7	158.5
40	-27.3	935.2	829.6	601.7	871.9	493.7	1004.3	181.2
42	-28.6	981.9	871.1	631.8	915.5	518.4	1054.5	190.2
44	-30.0	1028.7	912.6	661.8	959.1	543.0	1104.7	199.3
46	-31.3	1075.4	954.0	691.9	1002.7	567.7	1154.9	208.3
48	-32.7	1122.2	995.5	722.0	1046.3	592.4	1205.1	217.4
50	-34.1	1169.0	1037.0	752.1	1089.9	617.1	1255.4	226.4
% of σ_y at 5o	-0.8	87.7	24.6	17.8	25.8	14.6	29.8	5.4

(+)→ Tension (-)→Compression σ_y =yield strength of steel used for the fabrication of penstock bifurcation

86

Table 4.14: Prototype Major & Minor Principal Stresses in Sickle Plate of Penstock Bifurcation during Hydrostatic Test

Location	S1		S2	
Internal Pressure (kg/cm^2)	Major Principal Stresses (kg/cm^2)	Minor Principal Stresses (kg/cm^2)	Major Principal Stresses (kg/cm^2)	Minor Principal Stresses (kg/cm^2)
0	0.0	0.0	0.0	0.0
5	97.3	108.1	104.5	31.5
10	239.5	199.4	225.4	75.3
15	396.8	269.5	365.3	128.0
20	546.7	316.7	490.6	186.0
25	674.4	342.4	622.0	245.5
28	737.0	349.3	696.7	280.5
30	772.6	351.2	744.0	303.1
35	841.4	350.3	850.1	355.1
40	888.4	350.3	933.9	397.9
42	904.3	353.5	959.7	414.7
44	920.4	359.8	980.5	423.1
46	938.1	370.5	995.9	432.1
48	959.2	386.7	1005.5	438.4
50	**985.5**	409.5	**1008.8**	441.6
% of σ$_y$ at 5o	23.4	9.7	23.9	10.5

(+)→ Tension   (-)→Compression σ$_y$ =yield strength of steel used for the fabrication of penstock bifurcation

ANALYSIS OF RESULTS AND DISCUSSION

The results obtained through four type studies are as follows:

5.1   ANALYSIS OF RESULTS

5.1.1   ANALYTICAL APPROACH:

Actual shell thickness =   50 mm

As per calculation, Shell thickness = 49.12 mm (form article 5.3)

Hoop stress developed in thin cylindrical section theoretically,

$$\text{Hoop stress} = p.r/t \quad = \frac{50 \times 200}{5} = 2000 \text{ kg/cm}^2$$

$$\text{Axial stress} = p.r/2t \ = \frac{50 \times 200}{2 \times 5} = 1000 \text{ kg/cm}^2$$

In sickle plate:

If the walls of pipe are assumed to be thin membranes having no resistance against bending so that they inflict only tractive and shearing force on the strengthening collar, when subjected to internal pressure 'p' then the forces per unit length in cylindrical membrane are:

    i) In circumferential direction, $p.\ r$

    ii) In axial direction, $(1/2)\,p.\ r$

In circumferential direction, σ_c= resultant of circumferential stress along the junction of shell and sickle plate vares from 4289.01kg/cm^2 at 0^0 to 378.81 or up to 0 kg/cm^2 at 90^0

In axial direction, σ_a = resultant of circumferential stress along the junction of shell and sickle plate varies from 1570.80 kg/cm^2 at 90^0 to 87.28 or up to 0 kg/cm^2 at 0^0

Vertical forces, V= vary from 4289.01kg/cm^2 at 90^0 to 378.81 or up to 0 kg/cm^2 at 0^0

Horizontal forces, H = vary from 906.31 kg/cm^2 at 45^0 to 157.38 or up to 0 kg/cm^2 at 0^0 or 90^0

Resultant forces, R = varies from 0.0 kg/cm^2 at 0^0 to 4298. 01 kg/cm^2 at 90^0

5.1.2   PHYSICAL MODEL STUDY [7]

In case of physical model study the maximum design pressure applied equivalent to prototype is 55 kg/cm^2 and the stresses developed are in different parts of penstock are within the permissible limit[7].

1. The hoop stress developed in the shell near the junction of the sickle plate with the shell is shown in Fig.4.16 at section–AA varying from 2063 kg/cm^2 to 1169 kg/cm^2 (37.5 p_o to 21.26 p_o) and at the bend area of the order of 1595 kg/cm^2 (29 p_o).

2. The peak value of 37.5 p_o = 2063 kg/cm^2 is below the design value of hoop stress 2200 kg/cm^2 (40 p_o) The vertical stress in the sickle plate varies from 2822 kg/cm^2 to 1794 kg/cm^2

3. The vertical stress distribution on the section-CC of the sickle plate of Fig.4.18 is varying from stress value 2822 kg/cm^2 to 1794 kg/cm^2 (51.3 p_o to 32.62 p_o)

4. Radial stress on parabolic section-BB of the sickle plate of Fig.4.18 is varying from stress value 2530 kg/cm^2 to 1760 kg/cm^2 (46.0 p_o to 32.0 p_o)

5.1.3   HYDROSTATIC TEST ON PROTOTYPE [8]

(A) Stresses in main pipe

The hoop stress at 50 kg/cm^2 internal pressure in header pipe varies from 2086.6 kg/cm^2 to 2360.6 Kg/cm^2 along the diameter of the pipe

(B) Stresses at the junction of main pipe and branch pipe

The hoop stress at 50 kg/cm^2 internal pressure in branch pipe varies from 328.4 kg/cm^2 to 3164.0 Kg/cm^2 along the diameter of the pipe

(C) Stresses in sickle plate

The major principal stress at 50 kg/ cm^2 internal pressure varies from 985.5 kg/cm^2 to 1008.8 Kg/cm^2 at the centerline of the sickle plate.

The maximum stress of the order of 3164 kg/cm² was found to develop at an internal pressure of 50 kg/cm² on location B2 at half diameter point near the intersection of header and conical pipes which works out to be 75% of minimum yield strength of steel making the bifurcation.

5.1.4 FINITE ELEMENT ANALYSIS

I-DEAS software is used for the analysis of stresses in penstock bifurcation. The internal pressure of 50 kg/cm² is applied in the finite element model.

(A) Stresses Evaluated at Bend Area near the Junction of Main Pipe and Branch Pipe

The stress found in finite element analysis is of higher order 3250 kg/cm² at the bend region of penstock where the cylindrical pipe and conical pipe meet. Higher stress values at some nodes of Bend-B1 and Bend-B2 near the junction of main pipe and branch pipe are shown in the Table4.1 and Table4.2 respectively. The counter of higher stresses is indicated in the Fig.5.1.
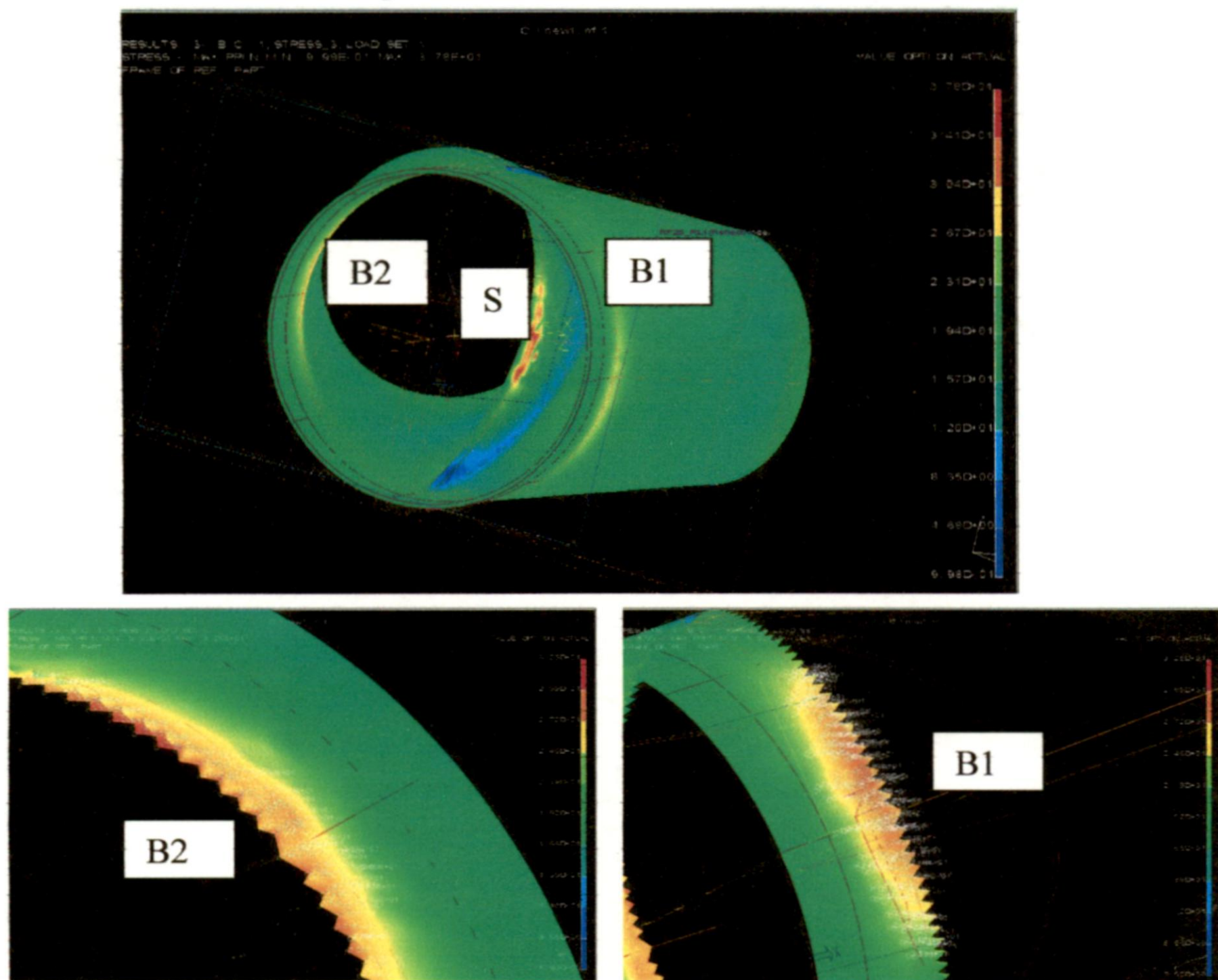

Fig.5.1: Higher Stresses indicated as at Bend B1and B2near the Junction of Main Pipe and Branch Pipe in Table4.1 and Table4.2 respectively.

90

(B) Stresses Evaluated at Sickle plate area

The stresses found in finite element analysis using I-DEAS software is of higher order 3840 kg/cm^2 and is within the permissible limit. It is seen that the higher order of stresses is found in the sickle plate and bends at the junction of header pipe and branch pipes, which is expected as per design .
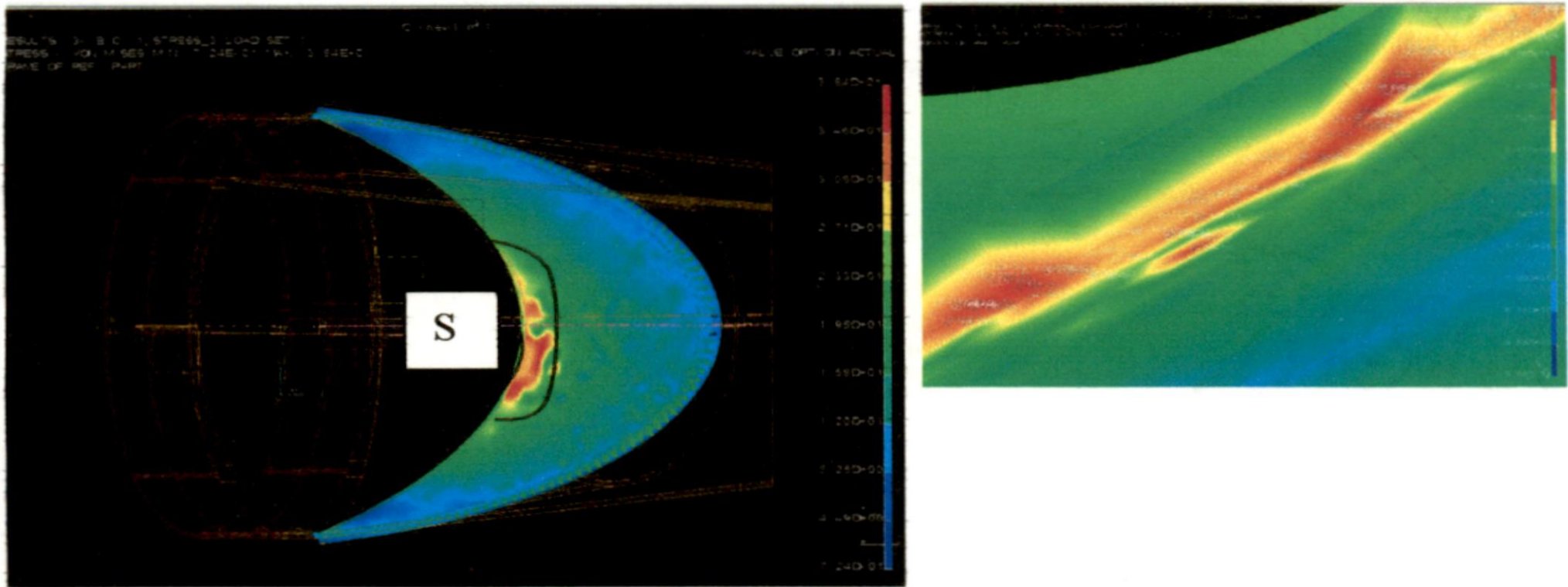

Fig.5.2: Higher Stresses indicated in Sickle Plate

5.2 DISCUSSION

In case of physical model study, the stresses found in the region of bends where the main pipe and branch pipe meet, are quite less in comparison of FEM analysis and hydrostatic test on prototype. This may be due to the different materials used for model and prototype as well as their weld efficiencies because the model is pressurized in taking consideration of the bond strength of liquid chloroform and acrylic cement.

In case of hydrostatic test on prototype, the stresses found the sickle plate is less in comparison to FEM analysis and physical model study. The reason behind it may be the un-sustainability of electric resistance strain gauges against very high pressure of water.

The FEM analysis results matches with the analytical analysis results by conventional methods having many assumptions and simplification.

The stresses developed in the region bends at junction of cylindrical and conical pipes are in permissible limit and well match with the hydrostatic test on prototype results.

The stresses evaluated by finite element method in the sickle plate are in permissible limit and well match with the physical model studies results.

The stresses in sickle plate are of higher order 3840 of kg/cm^2 at the central curve portion of sickle facing the water flow and are within the permissible limit.

It is seen that the higher order of stresses is found in the sickle plate and bends at the junction of header pipe and branch pipes, which is expected as per design and analysis.

The results compared among the four types of studies at internal pressure 50 kg/cm^2 are given tabular form as below:

5.3 COMPARISON OF RESULTS

The results of all the four studies are compared in Table 5.1

Table 5.1: Comparison of Results of Four Types of Studies

Location	Conventional Methods	Physical Model Study on Perspex Model	Hydrostatic Test on prototype	FEM
Maximum Stress at Junction of main and branch pipe	2242.46 Kg/cm^2	1900 Kg/cm^2	3164 Kg/cm^2	3250 kg/cm^2
Maximum Stress in Sickle plate	4289.01Kg/cm^2	2565 Kg/cm^2	1009 Kg/cm^2	3840 kg/cm^2

CONCLUSIONS AND RECOMENDATIONS

6.1 CONCLUSIONS:

1. The maximum stresses calculated by analytical analysis or conventional methods are approximate as there are many assumptions and simplifications made in the formula due to complex geometry of penstock bifurcation. The stresses calculated by this method in the sickle plate are having value of higher order as compared to physical model studies and hydrostatic test on prototype.

2. The maximum stresses evaluated near the junction of header and branch pipes by physical model study are somewhat lower in comparison to FEM analysis and hydrostatic test on prototype. The reason may be that the material used for model study is of Perspex having different engineering properties and also difference in weld efficiency.

3. The stresses evaluated in the sickle plate by hydrostatic test on prototype are much less than FEM analysis and physical model study. The reason behind it may be the un-sustainability of electric resistance strain gauge against very high pressure of water.

6.2 RECOMMENDATIONS:

1. The results may be further improved by precise finite element analysis by proper selection of element, type of boundaries etc.

2. The stresses evaluated by analytical method must be verified by other methods such as prototype testing, physical model studies and finite element analysis.

3. Above all, the hydrostatic test on prototype penstock bifurcation should be carried out for design verification, performance, assessment and identification of defects like leakage or sweating on penstock surface and joint efficiency at high water pressure.

4. Various combinations of reinforcement should be tried better improvement of design.

5. Physical model study should be conducted carefully by fabricating elastic models.

REFERENCES

1. American Iron and Steel Institute 'Steel Plates Engineering Data –Volume 4 for Steel Penstock and Tunnel Liners (A manual on materials, Design and construction with simple design Computations), 1982.

2. American Iron and Steel Institute Steel Plate Engineering Data-Volume 3 for Welded Steel Pipe (Merits, Designs Standard, Technical data and references) ,1983

3. Arthur, H.G. and Walker, J.J., New Design Criteria for Penstock, Journal of Power Division, ASCE , Jan 1970.

4. American water works Association, AWWA-C –203, 'Standard for Coal- tar Enamel protective Coatings for Steel Water –pipe, 1984'.

5. ASCE List of sources of information on pipeline design. Jl. of the Pipeline Division. Proc ASCE, vol. 93, PL2, Paper No. 53-55, July 1967, pp. 103-139.

6. Central Water and Power Commission, New Delhi: Manual on 'Design, Fabrication, Erection and Maintenance of Steel Penstock' Prepared by E. Divatia, A.S. Chelvaraj and G.N. Murthy,1998.

7. Central Water & Power Research Station Khadakwasla, Pune, Technical Report No. 2137/Aug. 1983: Conducting Model Studies on Varahi Penstock Bifurcation Varahi H. E. Project, Karnataka.

8. Central Water & Power Research Station Khadakwasla, Pune, Technical Report No. 4467/Jul. 2007: Monitoring of Stresses using Strain gauges on Penstock Bifurcation during Hydrostatic Test-Varahi H. E. Project, Karnataka.

9. Central Water &Power Research station, Khadakwasla, Pune. Gates and Valves Division. Reports on hydraulic model studies for penstock branches of Idikki and pong plants.

10. Chirst, Dr. A Research on head losses in Escher wyes type distribution pipes. Escher wyes news, vol. 39 No. 2, 1966, pp. 36-40

11. Creager, W.P.: Justin, J.D. Hydroelectric Handbook, 1927, John Wiley & Sons

12. Dutta, O.P., Bifurcation for steel penstocks. Indian Jl. of Power & River Valley Development , vol. XXII, No. 8, Aug. 1972, pp. 329-332.

13. Dally, W James: Riley, F. Williem. Experimental Stress Analysis, McGraw-Hill Book Company, 1978.

14. Dolder, G., Escher wyss distribution pipes with internal reinforcement free from bending stresses. Escher wyss News, vol. 39, 1969, No. 2, pp 26-35.

15. Engineering Monograph No.3 (US dept.of interior BR): Weld Steel Penstocks, 1967

16. Engineering Monograph No.32 (US dept. of interior BR): 'Stress Analysis of wye branches' by Roud F.O. 1964.

17. Fessier, H.; lewin, B.H., Stresses in branched pipes under internal pressure, Proc. of the Institution of Mechanical Engineers , vol.176, No. 29, 1962 pp 771-788.

18. Guthrie Brown, J., Hydro Electric Engineering Parctice, vol. I, II, III, Blackie & Son, Ltd., London, 1966.

19. Glenn Murphy. Similitude in Engineering. The Ronald press Company, New York, 1950.

20. Gopal Chauhan, Penstock Wyes, Lecture Notes-2007, Water Resources Development Training Centre, University of Roorkee.

21. Ghanekar, G.S. Specifications of steel plates for high- head welded penstocks in Hydro Projects Indian Jr. of power and River Valley Development,1963 .

22. Herold G, Arthure; John J. Walker. New Design criteria for USBR penstocks. Jl. of power Division, proc. ASCE, vol. 96, No., pol paper No. 7034, Jan. 1970, pp.129-143

23. Indian Standard, IS: 11639 (part- I)- 1986 Criteria for Structural Design of Penstocks (Surface Penstocks)

24. Indian Standard, IS: 11639 (part- II)-1995, Structural Design of Penstocks Criteria (Buried/ Embedded penstocks in Rock)

25. Indian Standard IS: 11639 (part- III)-1996, Criteria for Structural Design of Penstocks.(Specials for penstocks)

26. Indian Standard IS: 11625, 1986, Criteria for Hydraulic Design of Penstocks.

27. Indian Standard Institute IS: 2825-1969 'Code for Unfired Pressure Vessels'.

28. Indian Standard Institute IS: 814, Code for classification and coding of covered Electrodes for Metal Arc Welding for Structural Steel'.

29. I-DEAS manual for modelling, meshing, solving and post processing.

30. Indian standards Institution. IS: 1182-1967, Recommended Practice for raiographic examination of fusion welded butt joints in steel plates.

31. Junnarkar S.B. 'Mechanics of Structure Volume I', 1966, Vivek Publication.

32. Krishnamurthy, C.S, Finite Element Analysis, 1994, Tata McGraw Hill, Delhi

33. Kenneth E. Sorensen, M. ASCE, Reinforcing Steel for Penstock Wye Branch, Jr. of the Power Division, Proceeding of the ASCE Oct.1969

34. Miller, W. Stratmann, H. Friction losses in penstocks. Jl. of Power Div. Proc. ASCE, vol. 95, Pol paper 6456, March 1969. pp 35-53.

35. Makkapati Sivaji, 'Study on penstock branching', Dissertation for master of engineering Degree submitted at water Resources Development Training centre, University of Roorkee, Roorkee, 1975.

36. R. Swarup, The Geometry of Wyepieces, Indian Journal of Power and River Valley Development, 1989.

37. Swanson, H.S., Chapton, H.J., Wilkinson, W.J., King, C.L., Nelson, E.D,; Design of Wye Branch for Steel Pipe,Journal of American Water Works Association ,Vol 47, No.6,June 1955

38. Timeshenko S. and Gleason H. maccullough 'Elements of strength of materials' D Van Nostrand, 1968.

39. Timoshenko S. and Goodier J.N. 'Theory of Elasticity ', Thied edition 1970 Mc-GrawHill New York.1951.

40. Willamson V. James; Rhone J. Thomas. Dividing flow in branches and wyes. Jl. of Hyd. Div., Proc. of ASCE, vol. 99 No. HY5, Paper 9729,

41. Zhou Y., Bryant R. H., The Optimal Design for an Internal Stiffener Plate in a Penstock Bifurcation, ASME, Journal of Pressure Vessel Technology, May 1992, Vol.114/193.

42. Zienkiewicz, O.C., Taylor, R.L. and Zhu, J.Z, The Finite Element Method: its Basic and Fundamental. Volume-1 Elsevier, Butterworth-Heinemann Burlington, 6th Edition Reprinted -2006

43. Zienkiewicz, O.C. and Taylor R. L, The Finite Element Method: for Solid and Structural Mechanics. Volume-2 Elsevier, Butterworth-Heinemann, Burlington, 6th Edition Reprinted -2006